

**IDENTIFICATION AND FUNCTIONAL ANALYSIS OF SIALIC ACID
METABOLISM IN *VIBRIO VULNIFICUS***

by

Jean-Bernard Lubin

A dissertation submitted to the Faculty of the University of Delaware in partial fulfillment of the requirements for the degree of Doctor of Philosophy in Biological Sciences

Summer 2014

© 2014 Jean-Bernard Lubin
All Rights Reserved

UMI Number: 3642334

All rights reserved

INFORMATION TO ALL USERS

The quality of this reproduction is dependent upon the quality of the copy submitted.

In the unlikely event that the author did not send a complete manuscript and there are missing pages, these will be noted. Also, if material had to be removed, a note will indicate the deletion.



UMI 3642334

Published by ProQuest LLC (2014). Copyright in the Dissertation held by the Author.

Microform Edition © ProQuest LLC.

All rights reserved. This work is protected against unauthorized copying under Title 17, United States Code



ProQuest LLC.
789 East Eisenhower Parkway
P.O. Box 1346
Ann Arbor, MI 48106 - 1346

IDENTIFICATION AND FUNCTIONAL ANALYSIS OF SIALIC ACID

METABOLISM IN *VIBRIO VULNIFICUS*

by

Jean-Bernard Lubin

Approved:

Randall L. Duncan, Ph.D.
Chair of the Department of Biological Sciences

Approved:

George H. Watson, Ph.D.
Dean of the College of Arts and Sciences

Approved:

James G. Richards, Ph.D.
Vice Provost for Graduate and Professional Education

I certify that I have read this dissertation and that in my opinion it meets the academic and professional standard required by the University as a dissertation for the degree of Doctor of Philosophy.

Signed:

E. Fidelma Boyd, Ph.D.
Professor in charge of dissertation

I certify that I have read this dissertation and that in my opinion it meets the academic and professional standard required by the University as a dissertation for the degree of Doctor of Philosophy.

Signed:

Thomas E. Hanson, Ph.D.
Member of dissertation committee

I certify that I have read this dissertation and that in my opinion it meets the academic and professional standard required by the University as a dissertation for the degree of Doctor of Philosophy.

Signed:

John H. McDonald, Ph.D.
Member of dissertation committee

I certify that I have read this dissertation and that in my opinion it meets the academic and professional standard required by the University as a dissertation for the degree of Doctor of Philosophy.

Signed:

Michelle A. Parent, Ph.D.
Member of dissertation committee

I certify that I have read this dissertation and that in my opinion it meets the academic and professional standard required by the University as a dissertation for the degree of Doctor of Philosophy.

Signed:

Daniel Simmons, Ph.D.
Member of dissertation committee

ACKNOWLEDGMENTS

I would like to express my gratitude to Dr. E. Fidelma Boyd for giving me this project. It was thorough her excellent mentorship and extraordinary patience that have come to be well prepared for the scientific challenges that lay ahead. I would also like to thank all my committee members for their time and guidance into deepening my knowledge base and asking the relevant questions.

I would like to thank the Boyd lab for all their help and camaraderie throughout my time in graduate school. I could not ask for a better working environment and colleagues whom with to share it. In particular, I would like to thank Dr. Salvador Almagro-Moreno for my training when I first entered the lab as a fledgling researcher. I would also like to thank Dr. Seth Blumerman and Dr. W. Brian Whitaker for furthering my technical knowledge and ability.

I would also like to express my gratitude to my collaborator Dr. Amanda Lewis, Dr. Warren Lewis and the entire Lewis lab. With their help, I greatly increased my knowledge of biochemistry and facilitated my project to an incredible degree.

Finally, I would like to thank my close friends in the department as well my family. My friends provided great support and insight to navigating the waters of graduate school as smoothly as possible. My girlfriend Senem, in particular, was instrumental in keeping me sane the last few months. In addition to support, my family, particularly my mother Mirmose and my aunt Marieline, provided something greater. They were vital in nurturing my curiosity and love of science at an early age,

and enabled me to stay the course towards my goal. Without them it is certain I would not be where I am today.

TABLE OF CONTENTS

| | |
|-----------------------|------|
| LIST OF TABLES | x |
| LIST OF FIGURES | xi |
| ABSTRACT | xiii |

Chapter

| | | |
|---|--|----|
| 1 | INTRODUCTION | 1 |
| | <i>Vibrio vulnificus</i> | 1 |
| | Sialic Acids | 4 |
| | Sialic Acid Catabolism in Bacteria | 6 |
| | Sialic Acid Biosynthesis in Bacteria | 8 |
| | Dissertation Work | 12 |
| 2 | SIALIC ACID CATABOLISM AND TRANSPORT GENE CLUSTERS ARE LINEAGE SPECIFIC IN <i>VIBRIO VULNIFICUS</i> | 21 |
| | Introduction | 21 |
| | Materials and Methods | 26 |
| | Bacterial strains | 26 |
| | Molecular analysis | 26 |
| | Bioinformatic analysis of sialic acid catabolism and transporter genes among Vibrionaceae | 27 |
| | Growth analysis in minimal media supplemented with sialic acid. | 27 |
| | Mutant construction | 28 |
| | cDNA synthesis and reverse transcriptase PCR (RT-PCR). | 29 |
| | Results and Discussion | 30 |
| | <i>Vibrio vulnificus</i> sialic acid catabolism (SAC) and transport (SAT) region is predominately lineage I specific | 30 |
| | <i>Vibrio vulnificus</i> SAC and SAT positive strains can utilize sialic acid as a sole carbon and energy source. | 32 |
| | <i>Vibrio vulnificus</i> SiaPQM (VV2_0731-VV2_0733) TRAP transporter is essential for growth on sialic acid as a sole carbon source. | 33 |
| | Sialic acid induces expression of SAC and SAT genes. | 35 |

| | | |
|---|---|----|
| 3 | GENOMIC AND METABOLIC PROFILING OF NONULOSONIC ACIDS IN VIBRIONACEAE REVEAL BIOCHEMICAL PHENOTYPES OF ALLELIC DIVERGENCE IN <i>VIBRIO VULNIFICUS</i> | 47 |
| | Introduction | 47 |
| | Materials and Methods | 50 |
| | Abbreviations used. | 50 |
| | Bacterial strains and culture conditions..... | 50 |
| | Molecular analysis..... | 50 |
| | Bioinformatic and phylogenetic analysis of <i>nab</i> genes..... | 51 |
| | Nucleotide sequence accession numbers..... | 51 |
| | Release of NulOs by mild acid hydrolysis. | 53 |
| | Thiobarbituic acid assays. | 53 |
| | DMB derivatization and high performance liquid chromatography. | 54 |
| | Electrospray mass spectrometry..... | 55 |
| | Results | 55 |
| | Frequency of <i>nab</i> gene clusters in Vibrionaceae..... | 55 |
| | Evolution of NulO biosynthesis in Vibrionaceae..... | 56 |
| | Gene cluster organization matches phylogenetic signatures of Nab1 and Nab2 in Vibrionaceae..... | 57 |
| | Biochemical analyses of Vibrionaceae isolates confirm that many species express NulOs..... | 58 |
| | Distribution of <i>nab</i> alleles among diverse <i>V. vulnificus</i> isolates..... | 59 |
| | NulOs are expressed at higher levels in lineage I clinical isolates with CMCP6-like alleles..... | 60 |
| | Discussion..... | 61 |
| 4 | SIALIC ACID-LIKE MOLECULES EXPRESSED ON <i>VIBRIO VULNIFICUS</i> LIPOPOLYSACCHARIDE ARE ESSENTIAL FOR BLOODSTREAM SURVIVAL IN A MURINE MODEL OF SEPTICEMIA..... | 76 |
| | Introduction | 76 |
| | Materials and Methods | 79 |
| | Strains and culture conditions | 79 |
| | Allelic exchange mutagenesis in <i>V. vulnificus</i> | 80 |
| | HPLC analysis | 81 |
| | Lipopolysaccharide analysis..... | 82 |
| | Antibiotic sensitivity | 82 |

| | |
|--|-----|
| Preparation of flagellin monomers for NulO analysis..... | 83 |
| <i>V. vulnificus</i> motility | 84 |
| Electron microscopy of <i>V. vulnificus</i> flagellation | 84 |
| Biofilm assay | 84 |
| Mouse infection model..... | 85 |
| Results | 86 |
| HPLC analysis establishes the genetic basis of nonulosonic acid biosynthesis in <i>V. vulnificus</i> | 86 |
| <i>V. vulnificus</i> LPS is modified with NulO residues, which contribute to the natural resistance of <i>V. vulnificus</i> to the LPS-binding antibiotic polymyxin-B..... | 87 |
| NulO synthesis is essential for full motility in <i>V. vulnificus</i> | 89 |
| <i>V. vulnificus</i> NulO residues play a role in biofilm formation..... | 90 |
| Discussion..... | 92 |
| 5 PERSPECTIVES AND FUTURE DIRECTIONS..... | 106 |
| Origins of sialic acid catabolism and transport diversity | 107 |
| Structural diversity and environmental role of sialic acid biosynthesis | 109 |
| REFERENCES | 113 |
| Appendix | |
| A IACUC PROTOCOL APPROVAL | 134 |
| B Strains and plasmids used in <i>V. vulnificus nab1</i> studies | 135 |
| C Primers used in <i>V. vulnificus nab1</i> studies | 137 |
| D Functional analysis of CMCP6 $\Delta nab1$ | 138 |
| E Functional analysis of YJ016 $\Delta nab1$ | 140 |
| F Macrophage activation assay of <i>V. vulnificus nab</i> mutants..... | 142 |
| G Acknowledgement of previously published chapters..... | 143 |

LIST OF TABLES

| | | |
|---------|--|-----|
| Table 1 | Bacterial strains and plasmids used in this study | 44 |
| Table 2 | Primers used in this study | 45 |
| Table 3 | Species and strains examined in this study..... | 71 |
| Table 4 | <i>V. vulnificus</i> strains used in this study and their <i>nab</i> alleles | 72 |
| Table 5 | Primers used for PCR assays in this study | 75 |
| Table 6 | Bacterial strains and plasmids used in this study | 104 |
| Table 7 | Primers used in this study..... | 105 |

LIST OF FIGURES

| | | |
|-----------|---|----|
| Figure 1 | Structural configurations of the sialic acid family.. .. | 17 |
| Figure 2 | Representative schematic of sialic acid catabolism in bacteria. | 18 |
| Figure 3 | Representative schematic of bacterial sialic acid synthesis. | 19 |
| Figure 4 | Structural configurations of bacterial-specific sialic-acid like molecules, Legionaminic, and Pseudaminic acids. | 20 |
| Figure 5 | Genome context and arrangement of sialic acid catabolism (SAC) and transporter (SAT) gene clusters among <i>Vibrio</i> species. | 38 |
| Figure 6 | Distribution of <i>nanA</i> within the <i>V. vulnificus</i> phylogeny.. .. | 39 |
| Figure 7 | PCR analysis of <i>V. vulnificus nanA</i> -negative strains. PCR analysis of <i>V. vulnificus nanA</i> -negative strains. | 40 |
| Figure 8 | Growth analysis of <i>V. vulnificus</i> in M9 minimal medium supplemented with glucose..... | 41 |
| Figure 9 | Growth analysis of <i>V. vulnificus</i> wild-type strain CMCP6 and its nonpolar <i>siaM</i> deletion mutant strain JJK0731 in M9 minimal medium supplemented with glucose or <i>N</i> -acetylglucosamine (NAG) (A) or <i>N</i> -acetylneuraminic acid (sialic acid) (B). ***, P < 0.001. | 42 |
| Figure 10 | Expression analysis of sialic acid catabolism (e.g., <i>nanA</i> , <i>nanE</i>) and transporter (e.g., <i>siaQ</i>) genes, and a reference (housekeeping) gene (<i>mdh</i>) in <i>V. vulnificus</i> strain CMCP6 in the presence of glucose (G) or sialic acid (S).. .. | 43 |
| Figure 11 | Genetic structure of the nab gene cluster among sequenced Vibrionaceae species.. .. | 64 |
| Figure 12 | Distribution of nab genes among sequenced members of the family Vibrionaceae..... | 65 |

| | | |
|-----------|--|-----|
| Figure 13 | Correlation of phylogenetic branching patterns and analysis of Nab1 and Nab2 among Vibrionaceae species. Evolutionary relationships of Nab1 (A) and Nab2 (B) amino a | 66 |
| Figure 14 | Analysis of putative NulOs in Vibrionaceae. | 67 |
| Figure 15 | Mass spectrometry reveals masses of DMB-derivatized di- <i>N</i> -acetylated NulOs in Vibrionaceae. | 68 |
| Figure 16 | Distribution of <i>nab1</i> and <i>nab2</i> allele types among <i>V. vulnificus</i> | 69 |
| Figure 17 | CMCP6-like nab alleles are associated with high levels of NulO expression in mostly clinical strains..... | 70 |
| Figure 18 | <i>V. vulnificus nab2</i> is essential for NulO expression.. | 96 |
| Figure 19 | <i>V. vulnificus LPS</i> is modified with NulO. | 97 |
| Figure 20 | Functional analysis of <i>V. vulnificus</i> YJ016 <i>nab2</i> | 98 |
| Figure 21 | SDS-PAGE of <i>V. vulnificus</i> flagellin. | 99 |
| Figure 22 | HPLC analysis of aflagellar, non-motile Δ <i>flhF</i> shows no decrease in NulO levels..... | 100 |
| Figure 23 | Impairment of NulO Biosynthesis leads to a defect in Motility. (A, | 101 |
| Figure 24 | Elaboration of NulO is required for <i>V. vulnificus</i> bacteremia. | 102 |
| Figure 25 | Biofilm assay and in vivo competition assays of WT CMCP6 versus the Δ <i>flhF</i> flagellum mutant..... | 103 |

ABSTRACT

Vibrio vulnificus is a Gram-negative, rod shaped, Gammaproteobacteria, found in estuarine and coastal waters throughout the world. *V. vulnificus* is a disease causing agent in fish and humans. It causes a severe and rapid septicemia, contracted primarily through raw oyster consumption, with a mortality rate of over 50% in susceptible individuals. The mechanisms by which *V. vulnificus* colonizes the host gastrointestinal tract and survives and proliferates in the host bloodstream are poorly understood

Sialic acids (neuraminic acids) also known as nonulosonic acids, are a diverse family of nine carbon amino sugars, the most common and widely studied being *N*-acetylneuraminic acid, or Neu5Ac. Crucial to cell to cell communication and self-recognition in metazoans, sialic acids are typically positioned at the terminal end of glycoconjugates allowing them to interact with the external environment. The self-recognition function of sialic acid has been shown to be crucial as a modulator of immune function. Sialic acid is also a major component of mucin and thus is found throughout the mucosal layer of the gastrointestinal tract of mammalian species.

Bacteria have the ability to catabolize sialic acids as a sole carbon, nitrogen and energy source. This ability is overwhelmingly confined to commensal and pathogen species, where it has been shown to confer a competitive advantage in the host environment. Within bacteria, the ability to synthesize sialic acid has been demonstrated in a number of human pathogens and is phylogenetically widespread through diverse lineages. In addition to the canonical Neu5Ac, bacterial specific sialic acid-like molecules, legionaminic acid, and pseudaminic acid, are known. Several

organisms relevant in human disease have been shown to decorate their surfaces with sialic acid to aid in host colonization and avoidance of immune responses. Preliminary investigations revealed that *V. vulnificus* could catabolize sialic acid and that disruption in this pathway lead to defects in intestinal colonization. It was also determined that *V. vulnificus* contained a putative sialic acid biosynthetic gene cluster. We hypothesized that sialic acid catabolism in *V. vulnificus* plays an important role in this organism's pathogenicity. We also believed that *V. vulnificus* utilizes sialic acid biosynthesis to decorate its cell surface, promoting survival in the host bloodstream.

Initial genomic analysis of *V. vulnificus* clinical strains found the sialic acid catabolism (SAC) and transport (SAT) cluster present on chromosome II, and unlike *Vibrio cholerae*, is not associated with a pathogenicity island. However, the region was present predominantly among lineage I of *V. vulnificus*, which is comprised mainly of clinical isolates. We demonstrated that the isolates that contain this region can catabolize sialic acid as a sole carbon source and that the tripartite ATP-independent periplasmic (TRAP) transporter SiaPQM is essential for sialic acid uptake. Expression analysis of the SAT and SAC genes indicates that sialic acid is an inducer of expression. Overall, our study demonstrates that the ability to catabolize and transport sialic acid is predominately lineage specific in *V. vulnificus*, found predominantly in genotypically clinical isolates.

Next we investigated the distribution, diversity and function of sialic acid biosynthesis in *V. vulnificus*. We found that 44% of the Vibrionaceae species examined contained sialic acid biosynthetic (*nab*) clusters. Evidence of duplication, divergence, horizontal transfer, and recombination was widespread in this region and biochemical analyses confirmed production of di-*N*-acetylated sialic acid-like sugars.

V. vulnificus clinical isolates CMCP6 and YJ016, were found to contain two highly divergent clusters. PCR genotyping found the CMCP6-like cluster to be found overwhelmingly in the clinical, lineage I, isolates. Isolates containing the CMCP6-like alleles produced 40-fold higher levels of sialic acids than YJ016-like alleles associated with environmental isolates. Studies into the functional significance of biosynthesis in *V. vulnificus* found the LPS to be decorated with sialic acid residues. Expression of sialic acid was found to be is required for optimal motility, flagellar formation and biofilm formation. Competition experiments in a mouse model of septicemia reveal a significant 300-fold decrease in survival of the sialic acid synthase (*nab2*) mutant strain versus the CMCP6 wild type. Competition experiments conducted in the YJ016 background, which produces less sialic acid, revealed significantly less attenuation in the mutant strain when compared to CMCP6. In summary, these data demonstrate a key biological function of sialic acid molecules in *V. vulnificus* and provides insight on how this species survives in the host bloodstream.

Chapter 1

INTRODUCTION

Vibrio vulnificus

Vibrio vulnificus is a Gram-negative, rod shaped, Gammaproteobacteria. It is a member of the family Vibrionaceae and is found in estuarine and coastal waters throughout the world. It has been isolated in open water and sediment, as well as associated with varied marine life, including shrimps, crabs, fish, mollusks, and zooplankton (Oliver et al., 1983; Kaysner et al., 1987). Members of the genus *Vibrio*, including *V. vulnificus*, play an important role in the marine environment through the degradation of chitin (Wortman et al., 1986; Hunt et al., 2008). With an estimated 1×10^{12} tons of chitin produced annually in marine environments (Li and Roseman, 2004), chitinase producing bacteria contribute to nitrogen and carbon cycling in the environment, freeing up nutrients which would otherwise be unavailable to higher organisms.

In addition to its environmental role, *V. vulnificus* is a disease causing agent in fish and humans. In humans, it causes severe septicemia, and is contracted primarily through raw oyster consumption, as *V. vulnificus* is a persistent member of the oyster microbiota (Oliver et al., 1983; Tamplin and Capers, 1992). This infection has a mortality rate of over 50% and death usually occurs within 48 hours (Jones and Oliver, 2009). *V. vulnificus* also causes wound infections, which account for roughly 27% of cases, which lead to necrotizing fasciitis. *Vibrio vulnificus* is an opportunistic pathogen with a majority of cases in males over the age of 50, or those with liver

diseases, or are immunocompromised (Tacket et al., 1984; Oliver, 2005). However infections have been steadily climbing and it is the most common cause of seafood related death in the United States (Frerk, 2000). This has been attributed to climate change and the warming waters of the gulf coast where danger of exposure is at its highest in the United States. In fact, risk of infection is highest in the warm summer months and *V. vulnificus* is barely detected in oyster derived samples in the winter (Motes et al., 1998).

Little is confirmed about the factors that contribute to *V. vulnificus* pathogenicity, as there is no gene or gene cluster found to be exclusively unique to clinical isolates. The presence of the capsule appears to be crucial in the organism's pathogenesis, with an opaque colony morphology indicative of an encapsulated strain and virulence, whereas a translucent colony appears to be avirulent (Simpson et al., 1987). The mechanisms of iron acquisition also appear to play an important role in *V. vulnificus* pathogenicity. Ferric uptake regulator (Fur) and siderophore production have been implicated as virulence factors, with the former shown to interact with the quorum sensing regulator SmcR to express further virulence factors (Litwin et al., 1996; Kim et al., 2013). Other genetic factors that have been associated with *V. vulnificus* pathogenicity are motility, pili, and RtxA1, a cytolytic haemolysin (Paranjpye and Strom, 2005; Kim et al., 2006; Lee et al., 2007).

Vibrio vulnificus contains a 3.4 Mbp chromosome and a smaller 1.9 Mbp; two chromosome genomes being characteristic of the Vibrionaceae family. This allows for multiple events of interchromosomal rearrangement, and it was found that the small chromosome is less conserved among *Vibrio* spp. (Chen et al., 2003). The *V. vulnificus* genome in particular was found to be highly plastic, as evidenced by more

frequent duplication and transposition events than its close relative *V. cholerae* (Chen et al., 2003). This plasticity leads to isolates of *V. vulnificus* harboring strain specific DNA (Quirke et al., 2006). In fact, the ability of *V. vulnificus* to infect and cause disease is strain specific, with environmental isolates being shown to require up to a 350 fold higher dosage to elicit the same disease state as clinical isolates (Starks et al, 2000). This characteristic of the organism makes it challenging to genetically define isolates as virulent or clinical, or avirulent environmental. Several genetic markers have been utilized to define *V. vulnificus* isolates as clinical or environmental. Warner and Oliver utilized randomly amplified polymorphic DNA PCR that was able to genotypically distinguish between environmental (E) and clinical (C) isolates (1999). With the use of 16s RNA sequences, it was discovered that most environmental isolates had a distinct genotype, designated as A, and clinical isolates were designated as B (Nilsson et al., 2003). Despite this, it has never been shown that a specific virulence gene or genomic island identified associates solely with clinical isolates; therefore it's not well understood what makes the clinical isolates more virulent. Our group developed a multi locus sequence typing system based on the phylogeny of six concatenated housekeeping genes (*gyrB*, *mdh*, *rpoD*, *groEL1*, *groEL2*, and *pyrC*), which formed three distinct clades in *V. vulnificus* (Cohen et al., 2007). The Lineage I clade contained primarily clinical (B/C) isolates and Lineage II contained primarily environmental isolates (A/E). The much smaller Lineage III was composed of strains isolated from an outbreak of *V. vulnificus* in Israel, which is restricted to that region of the world.

Sialic Acids

Sialic acids (neuraminic acids) also known as nonulosonic acids, are a family of nine carbon amino sugars, the most common and widely studied being *N*-acetylneuraminic acid (5-acetylamino-3,5-dideoxy-*D*-glycero- α -*D*-galacto-nonulosonic acid), or Neu5Ac (**Fig. 1A**) (Angata and Varki, 2002). The Neu5Ac structure is typified by a 6-carbon carboxylic acid ring structure with a glycerol tail, an acetamido at the C-5 position and hydroxyl groups present on C-4, C-7, C-8, and C-9. Modifications occur primarily on the hydroxyl groups, and this enables the nine carbon backbone to exhibit rich structural diversity with over 60 known naturally occurring derivatives (Angata and Varki, 2002). O-acetylation is the most common alteration, and substitutions have been shown to occur after the completion of the core structure (Butor et al., 1993). Other modifications such as O-methylation, O-lactylation and O-sulfation add to the diversity of this molecule in vivo, and similar modifications are made to their core structure (Angata and Varki, 2002).

Two structurally similar sialic acids also occur in nature: *N*-glycolylneuraminic acid (Neu5Gc), and 2-keto-3-deoxy -*D*-glycero-*D*-galacto-nonulosonic acid (KDN). Neu5Gc which differs from Neu5Ac by the presence of a hydroxyl group on the *N*-5 acetyl moiety, and 2-keto-3-deoxy -*D*-glycero-*D*-galacto-nonulosonic acid (KDN), a deaminated form of Neu5Ac (**Fig. 1B**). These three sugars form the basis of the sialic acid family due to retention of the same stereochemical configuration of the 9-carbon backbone.

Among metazoans, sialic acid is primarily limited to members of the deuterostome lineage of the phyla Chordata and Echinodermata. Neu5Gc is commonly utilized on mammalian cells, but due to loss of the hydroxylase gene required for its formation, it is absent in humans (Varki, 2001). KDN was once thought to be

exclusive to lower order vertebrates such as fish and amphibians, but recent studies have found it to be present in humans in an unbound form. Its presence in the gametes of fish as well as human ovarian cells and fetal serum may indicate that KDN plays a role in development (Inoue and Kitajima, 2006). Sialic acids in eukaryotes are typically positioned at the terminal end of glycoconjugates allowing them to interact with the external environment and play a role in cell to cell communication as well as self-recognition. The self-recognition function of sialic acid has been shown to be crucial as a modulator of immune function. An example of this would include the signaling molecule, Factor H, which preferentially binds to complement factor on cell surfaces containing sialic acid glycoconjugates, preventing the binding of Factor B and halting the alternative complement cascade (Kazatchkine et al., 1979). Sialic acids also bind to a family of cell surface proteins known as sialic acid-binding immunoglobulin-like lectins (Siglecs). This interaction between sialic acid glycoconjugates and Siglecs has been reported to dampen immune function in macrophages, natural killer cells, neutrophils, and B-cells (Bennett and Schmid, 1980; Cameron and Churchill, 1982; Ozkan and Ninnemann, 1985; Lanoue et al., 2002). The brain and central nervous system (CNS) utilize sialic acids, and is the origin of the name, neuraminic acid (neurons). Within the brain and CNS, polysialic acid chains are associated with the neural cell adhesion molecules of neurons, glial cells and ganglions (Rutishauser, 2008; Wang, 2012). Lastly, a major reservoir of sialic acids is located on mucosal surfaces. Sialic acid's common name is derived from the Greek word sialon, meaning saliva, as it was first isolated in bovine submaxillary mucin (Blix, 1936), and has subsequently been found to be present in the mucin generated in various parts of the body (Culling et al., 1974; Scudder and Chantler, 1982; Thornton

et al., 1996). In particular, sialic acid is a principal component of intestinal mucin with over 65% of glycans containing sialic acid residues (Robbe et al., 2004). The addition of sialic acid on mucin glycans is thought to play a role in protecting the underlying peptides from proteolysis, and it has also been implicated in playing a role in mucin mediated bacterial aggregation and hydroxyl radical scavenging (Ho et al., 1995; Slomiany et al., 1996; Ogasawara et al., 2007).

Sialic Acid Catabolism in Bacteria

Bacteria have been found to possess the ability to catabolize sialic acids as a sole carbon, nitrogen and energy source (Vimr et al., 2004). Sialic acid catabolism is overwhelmingly confined to commensal and pathogen species (Almagro-Moreno and Boyd, 2009). Bacteria acquire sialic acid from their eukaryotic hosts either through the synthesis of a sialidase, a glycoside hydrolase, which cleaves terminal Neu5Ac residues from host glycoconjugates or by scavenging free Neu5Ac released by other bacterial species (Lewis et al., 2013). Uptake of sialic acid uses specialized transport systems: a major facilitator superfamily (MFS) permease designated as NanT, a tripartite ATP-independent periplasmic (TRAP) transporter SiaPQM, a sodium solute symporter (SSS) SiaT, or an ATP-binding cassette (ABC) transport system SatABCD (Vimr and Troy, 1985; Martinez et al., 1995; Allen et al., 2005; Post et al., 2005; Severi et al., 2005; Severi et al., 2007; Almagro-Moreno and Boyd, 2009; Mulligan et al., 2009; Severi et al., 2010). In Gram-negative bacteria, uptake of sialic acids requires transport across the outer membrane by either a general porin such as OmpC/F or a sialic acid specific porin such as NanC (Condemine et al., 2005). Once inside the bacterial cell, Neu5Ac is broken down by *N*-acetylneuraminic acid lyase

(NanA), *N*-acetylmannosamine kinase (NanK), and *N*-acetylmannosamine epimerase (NanE) to GlcNAc-6-P (**Fig. 2**) (Almagro-Moreno and Boyd, 2009).

Possessing Neu5Ac catabolic capabilities becomes significant due to the fierce competition for nutrients within eukaryotic hosts. As previously mentioned, mucosal layers are a rich food source for sialic acid catabolizers due to the sialylation of the mucin proteins. This has been shown in pathogenic organisms, such as *Treponema denticola*, that colonize the oral cavity leading to periodontitis (Kurniyati et al., 2013). Recently, sialic acid catabolism in *Gardnerella vaginalis*, a causative agent of bacterial vaginosis, has been shown to be important in host vaginal colonization (Lewis et al., 2013). Furthermore, pathogenic organisms of the mucus rich regions of the respiratory and intestinal tract also use sialic acid catabolism to confer a competitive advantage in host colonization (Sakarya et al., 2010; Marion et al., 2011; Bertin et al., 2013).

Members of the family Vibrionaceae, including the noteworthy pathogens *Vibrio cholerae* and *V. vulnificus*, were found to cluster with members of Shewanellaceae, Psychromonadaceae and Pseudoaltermonadaceae, by NanA phylogenetic analysis (Almagro-Moreno and Boyd, 2009). This lineage is distinct to that of enteric γ -Proteobacteria, and forms a closer relationship with eukaryotic NanA representatives. *Vibrio* species were found to preferentially utilize the Tripartite ATP-independent periplasmic transporter (TRAP) as the means of up taking sialic acid into the cell, instead of the NanT permease found enteric γ -Proteobacteria. In *Vibrio cholerae*, the sialic acid catabolism cluster is located on a pathogenicity island, VPI-2, and has been shown to convey a competitive advantage in the early stage of infection in the infant mouse model and is present in all toxigenic O1 serogroup isolates and is

missing in non-toxigenic strains (Jermyn and Boyd, 2002; Almagro-Moreno and Boyd, 2009b). A *V. vulnificus* mutant deficient in sialic acid catabolism, *nanA* exhibited a decreased growth rate and adherence on the epithelial INT-407 cell line as well as a decreased ability to colonize the mouse intestinal tract and subsequently a higher LD50 (Jeong et al., 2009).

Sialic Acid Biosynthesis in Bacteria

Bacteria can also biosynthesize sialic acids and this ability was originally thought to be present in a handful of bacteria, primarily commensals and pathogenic species. However, recent phylogenetic analysis indicated that this ability is highly prevalent across a large number of diverse bacterial lineages (Lewis et al., 2009). The sialic acids biosynthesis pathway begins with UDP *N*-acetylglucosamine (UDP-GlcNAc), which can be converted to *N*-acetylmannosamine (ManNAc) through the function of UDP *N*-acetylglucosamine 2-epimerase (Nab3/NeuC) (**Fig. 3**) (Vann et al., 1987; Vann et al., 2004). Nab3/NeuC hydrolyzes the UDP moiety, as well as forming the isomer from the substrate. This enzyme appears to be well conserved, as *E. coli* mutants deficient in Nab3 can be complemented by a homolog from the Gram-positive bacterium *Streptococcus agalactiae* (Vann et al., 2004). *Neisseria meningitidis* Nab3, known as SiaA in this organism, catalyzes the isomerization of GlcNAc-6-P to ManNAc-6-P (Petersen et al., 2000). This is unique in that the canonical epimerase acts on nonphosphorylated GlcNAc and the phosphatase activity that generates the final product of UDP-ManNAc is unknown. *N*-acetylneuraminate synthase (Nab2/NeuB) converts ManNAc, with the addition of pyruvate to Neu5Ac (Vann et al., 1997). The final step is carried out by *N*-acetylneuraminate cytidyltransferase (Nab1/NeuA), which activates Neu5Ac by adding a cytidine monophosphate (CMP)

moiety to the hydroxyl group on Carbon 2 of the molecule (Vann et al., 1987). This step is required for the Neu5Ac to be recognized by sialyltransferases. The lesser studied acetyltransferase (Nab4/NeuD) protein was found in *E. coli* not to be directly involved in synthesis of sialic acid, as mutants lacking Nab4 accumulated sialic acid in the cells, but were unable to form sialic acid polymers (Annunziato et al., 1995). In *S. agalactiae*, Nab4 was shown to function as an acetyltransferase on Neu5Ac, and this type of acetyltransferase appears to be unique to prokaryotes (Lewis et al., 2006). While Neu5Ac is found in eukaryotes and some prokaryotes, two 9 carbon amino sugars bearing a strong resemblance to Neu5Ac have been found exclusively in bacteria. 5,7-diamino-3,5,7,9-tetraoxy-D-glycero-D-galacto-nonulosonic acid, also known as legionaminic acid, was discovered in and named after *Legionella pneumophila* (**Fig. 4A**) (Knirel et al., 1994). A GlcNAc derivative called diacetylbacillosamine is the precursor for legionaminic acid, and homologs of Nab3 catalyze it to 2,4-diacetamido-2,4,6-trideoxymannose, and Nab2 homologs convert it to legionaminic acid (Glaze et al., 2008). Legionaminic acid has been isolated in 3 three structurally distinct forms: the aforementioned D-glycero-D-galacto configuration, as well as epimers, D-glycero-D-talo (4-epi- Legionaminic acid), and D-glycero-L-galacto (8-epi-Legionaminic acid) (**Fig. 4A**) (Tsvetkov et al, 2001, Thibault et al, 2001). A stereoisomer of legionaminic acid, 5,7-diacetamido-3,5,7,9-tetraoxy-L-glycero-L-manno-nonulosonic acid, is known as pseudaminic acid (Pse), due to its discovery in *Pseudomonas aeruginosa* (**Fig. 4B**) (Knirel et al., 1984). Structurally, they differ from Neu5Ac by the addition of an amide group at carbon 7 and the removal of a hydroxyl group on carbon 9 (**Fig. 4**). Between each other, the

primary difference is an amide group on carbon 5 in the equatorial position in legionaminic acid and in the axial position in pseudaminic acid.

In bacteria, sialic acid biosynthesis is used to decorate several cell surface structures implicated in pathogenesis. This was first discovered in *E. coli* in which certain strains possessed polysialic acid chains attached to their capsules (Barry, 1958; Kundig et al., 1971). Several strategies are used to acquire sialic acids for sialylation: *de novo* biosynthesis, or scavenging from host environments, by uptake of free Neu5Ac or CMP-activated Neu5Ac from the host (Severi et al., 2007). There are many examples of bacterial sialylation and the role it plays in survival and colonization of host systems. Capsular polysaccharide sialylation by polysialic acid, as previously mentioned, occurs in *E. coli* and *Neisseria meningitidis* (Kundig et al., 1971; Kasper et al., 1973). It has been shown that sialylated *N. meningitidis* capsule mimic mammalian polysialic acid chains of neuronal cells (Finne et al., 1983). Capsular polysaccharide sialylation of *S. agalactiae* allows interaction with sialic acid binding Ig-like lectins (Siglecs), expressed on the surface of neutrophils and monocytes, which can dampen immune responses (Carlin et al., 2007). The O-antigen of lipopolysaccharide is sialylated in *N. meningitidis*, *N. gonorrhoeae*, and *H. influenzae*, conferring resistance to serum-mediated killing (Parsons et al., 1988; Vogel et al., 1997; Jenkins et al., 2010). Terminal sialic acids on LPS are characteristic of its usage, enabling the sugar to interact with the host environment. Sialylation of flagella in *Campylobacter jejuni* was shown to increase colonization in the ferret diarrheal model system (Guerry et al., 2006). It is particularly interesting to note that in the absence of sialic acid modification, *C. jejuni* became non-motile, internalizing

flagellin monomers, suggesting that the sialylation of the flagellin plays a role in the assembly of the component.

Sialic acids were identified in several organisms in the *Vibrio* genus by phylogenetic analysis (Lewis et al., 2009) and biochemically (Edebrink et al., 1996; Hashii et al., 2003; Vinogradov et al., 2009; Post et al., 2012). Research into the phylogenetic relationship of *Vibrio* Nab-2 homologs to other sialic acid producing organisms found representatives of *V. fischeri*, *harveyi*, *parahaemolyticus*, *shilonii*, *Ex25*, *splendidus* and *vulnificus* to cluster with legionaminic acid producing organisms (Lewis et al., 2009). Investigations into the structure of the sialic acids present in *Vibrio* spp. yielded evidence to the diversity present in this metabolic pathway between closely related species. It was discovered that the lipooligosaccharide (LOS) of *V. parahaemolyticus* serogroups O2 and O3 contained a legionaminic acid isomer in the D-glycero D-galacto configuration (Hashii et al., 2003; Mazumder et al., 2008). The sialic acid was found to be α 2-6 linked to the LOS and on the terminal end of a branch off the main LOS chain. In contrast, a separate study concluded that *V. vulnificus* type strain 27562 contained a L-glycero L-manno configured pseudaminic acid residue in its LOS (Vinogradov et al., 2009). This was also found to be α 2-6 linked and terminally situated on a branched LOS chain. This would indicate that relying on phylogenetic clustering of *Vibrio* spp. with known legionaminic acid producers is not sufficient in determining the final product of its cluster. The LPS of *V. fischeri* ES114 was found to be unlike the other *Vibrio* spp. studied, as it contained a legionaminic isomer in its core connected to a *N*-acetylgalactosamine by an α 1-8 linkage (Post et al., 2012). Despite investigations into the structure and genetics of sialic acid biosynthesis in *Vibrio* spp., very little is known of the functional

significance of sialylation in these organisms. The sole example of the role it could play potentially in this family was found when the loss of sialic acid containing LPS of *V. fischeri* reduced the initial colonization of the light organ of its symbiont, *Euprymna scolopes* (Post et al., 2012). But since the entire O-antigen was deleted, it is impossible to determine whether the sialic acid residues are the primary factor in this colonization defect. Nonetheless, considering that juvenile *E. scolopes* produce a Neu5Ac rich mucus essential for the colonization of *V. fischeri* (Nyholm et al., 2000), the unique sialic acids present in the microorganism could play a role in this interaction.

Dissertation Work

The role of sialic acid biosynthesis has been elucidated only in a few organisms, predominately human pathogens or species predominantly associated with vertebrate hosts, leaving several unanswered questions. For example, bacteria that produce the eukaryotic associated sialic acid, Neu5Ac, have been the most studied, and little is known whether the structurally similar Leg and Pse acids have the same ability to interact with mammalian host immune cells and cause immunosuppressive effects. Furthermore, genetic diversity among the genes that control sialic acid biosynthesis is poorly understood and it is unknown if this diversity can have an effect on what is sialylated and to what degree. Lastly, due to the recently discovered prevalence of sialic acid biosynthesis amongst many divergent lineages of bacteria, it can be surmised that sialic acid would play a role in more than pathogenic or commensal host interactions. The role that sialic acids play independent of pathogenesis is largely unknown. They could play a key role in structural integrity of surface exposed components, as seen in flagella assembly in *C. jejuni*, or the

promotion of biofilm formation, which is a key ability in environmental as well as host settings. The ability of the predominately marine dwelling *V. vulnificus* to catabolize and biosynthesize sialic acids makes an excellent model to study the implications of sialic acid metabolism at greater depth. We hypothesized that sialic acid metabolism in *V. vulnificus* plays a role in the acquisition of scarce nutrients in the intestinal tract upon infection and a structural role that confers an advantage in survival and fitness. Interestingly, preliminary studies of two fully sequenced clinical isolates, CMCP6 and YJ016, found the putative sialic acid biosynthesis genes to be highly divergent; two strains that commonly share upwards of 99% identity outside of this region on chromosome I. This led us to also explore whether the divergence in the putative genes responsible for sialic acid biosynthesis correlated to differences in structure or utilization of the final product.

In Chapter 2, we first investigated the distribution and functionality of the sialic acid catabolism cluster in *V. vulnificus*. We found that among the three sequenced *V. vulnificus* clinical strains, the sialic acid catabolism genes were present on chromosome II and are not associated with a pathogenicity island. This is incongruous with *V. cholerae* which contains these genes on *Vibrio* pathogenicity island-2 on chromosome I, which is confined to pathogenic isolates. To determine whether the genes responsible for transport and catabolism of sialic acid is ubiquitous within *V. vulnificus*, we examined 67 natural isolates which we previously able to phylogenetically cluster as either Lineage I composed of primarily clinical isolates or Lineage II consisting of primarily environmental isolates. We found that the region was present predominantly among the clinical isolates lineage I clade of *V. vulnificus*. Furthermore, we confirmed that isolates that contain this region can utilize sialic acid

as a sole carbon source. We found two putative transporters are genetically linked to the region in *V. vulnificus*, the tripartite ATP-independent periplasmic (TRAP) transporter SiaPQM and a component of an ATP-binding cassette (ABC) transporter. An in-frame deletion mutation in *siaM*, the large subunit of the TRAP transporter, demonstrated that this transporter is the sole route of sialic acid uptake in this species. We were also able to show the inability to catabolize sialic acid was the result of the absence of the entire 12 kb region encoding the catabolism and transport genes, and not due to point mutations rendering *nanA* nonfunctional. Finally, we showed that up-regulation of sialic acid catabolism genes were induced by sialic acid in the environment. Overall, our study demonstrated that the ability to catabolize and transport sialic acid is predominately lineage specific in *V. vulnificus*, largely found in clinical isolates. This would indicate that sialic acid catabolism plays an important role in the pathogenesis of this organism. We also confirmed that the TRAP transporter is essential for sialic acid uptake.

In Chapter 3, we examined the phylogenetic relationships, distribution, and function of the diverse sialic acid biosynthesis pathways of the family Vibrionaceae, with an emphasis on *V. vulnificus*. We found that roughly half the sequenced species of Vibrionaceae contained putative synthesis genes. The synthesis capability of these species was confirmed by biochemical analyses, and it was discovered that *Vibrio* species do in fact produce the bacterial specific sialic acids, and not Neu5Ac. Duplication, divergence, horizontal transfer, and recombination of *nab* gene clusters was prevalent amongst Vibrionaceae. This was typified by *V. vulnificus* CMCP6 and YJ016 being located in highly divergent clades. We used our collection of 67 different isolates of *V. vulnificus* to assess the distribution of the CMCP6 and YJ016 alleles.

Our analysis showed that the CMCP6-like alleles overwhelmingly mapped to the clinical lineage I isolates and that this genotype produced upwards of 40-fold higher levels of sialic acids than the environmental lineage II isolates. Furthermore, biochemical analysis discovered a potential third cluster in *V. vulnificus*, producing sialic acids at a level intermediate to CMCP6 and YJ016. These results would suggest that Vibrionaceae is a “hot spot” of sialic acid evolution and suggest that these molecules may play a role in environmental fitness. Lastly, we sought to establish the functional significance of sialic acid biosynthesis in *V. vulnificus*.

In Chapter 4, we confirmed the genetic basis of sialic acid biosynthesis in *V. vulnificus* by an isogenic in-frame deletion of the putative sialic acid synthase gene *nab2* ($\Delta nab2$) in the CMCP6 and YJ016 background. Abolishing sialic acid synthesis led to a shift in the molecular weight of *V. vulnificus* LOS fragments indicating that the LPS is modified with sialic acid. The removal of sialic acid from *V. vulnificus* LPS caused a significant increase in sensitivity to the LPS-associated polymyxin-B antibiotic. We also determined that synthesis was required for optimal biofilm formation, motility, and flagellar construction and function. Competition experiments in a mouse model of septicemia revealed a significant 300-fold survival advantage of the wild type CMCP6 strain versus the $\Delta nab2$ strain. YJ016 also exhibited a survival advantage when competed against $\Delta nab2$ strain, but at a significantly less level than CMCP6. This was the first phenotypic difference that could be attributed to a greater amount of sialic acid production in CMCP6. In summary, we were able to demonstrate key biological functions of sialic acid molecules in *V. vulnificus*, which include protection from cationic antibiotics, structural integrity of the flagellum and promotion of biofilm formation. Critically, we were able to show that a bacterial specific sialic

acid protects *V. vulnificus* from immune responses in a host bloodstream. To our knowledge, this is the first time it has been proven.

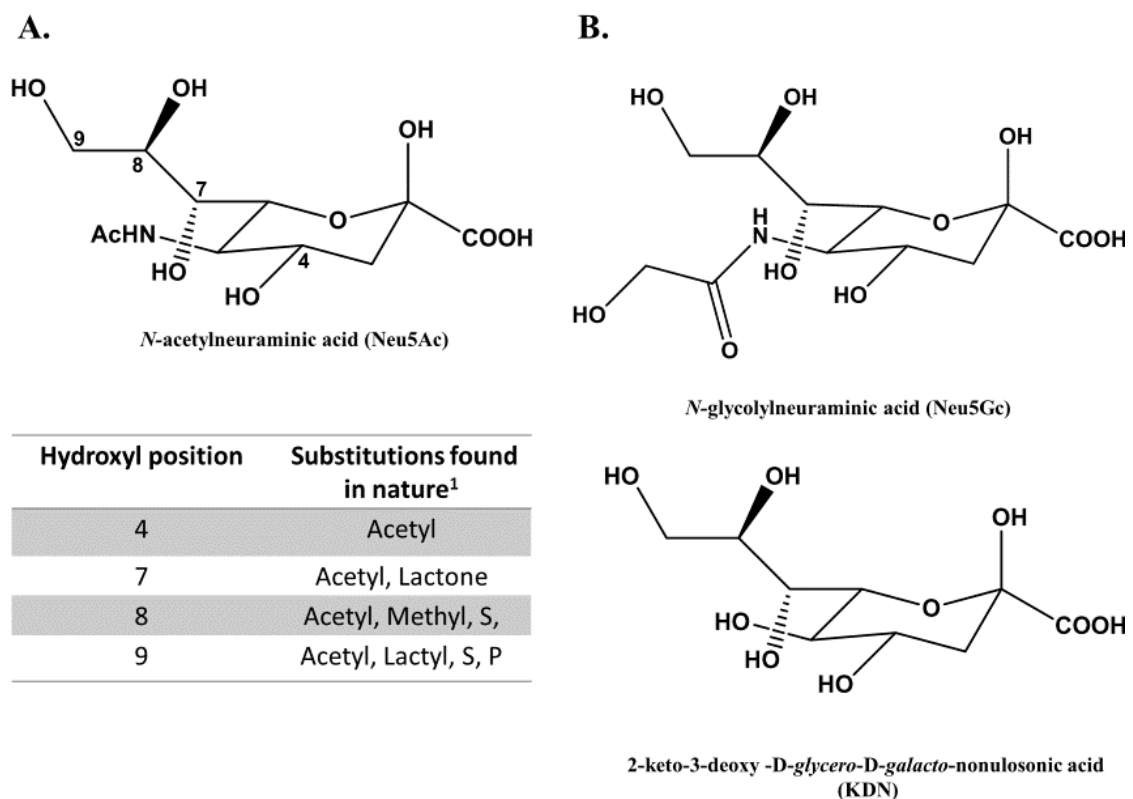


Figure 1 Structural configurations of the sialic acid family. A. Structure of *N*-acetylneuraminic acid with the commonly modified hydroxyl groups on C-4, C-7, C-8, and C-9 labeled. Naturally occurring modifications of each hydroxyl site are presented and reviewed in Angata and Varki, 2002. (B) Structurally similar sialic acids *N*-glycolylneuraminic acid (Neu5Gc), and 2-keto-3-deoxy -D-glycero-D-galacto-nonulosonic acid (KDN).

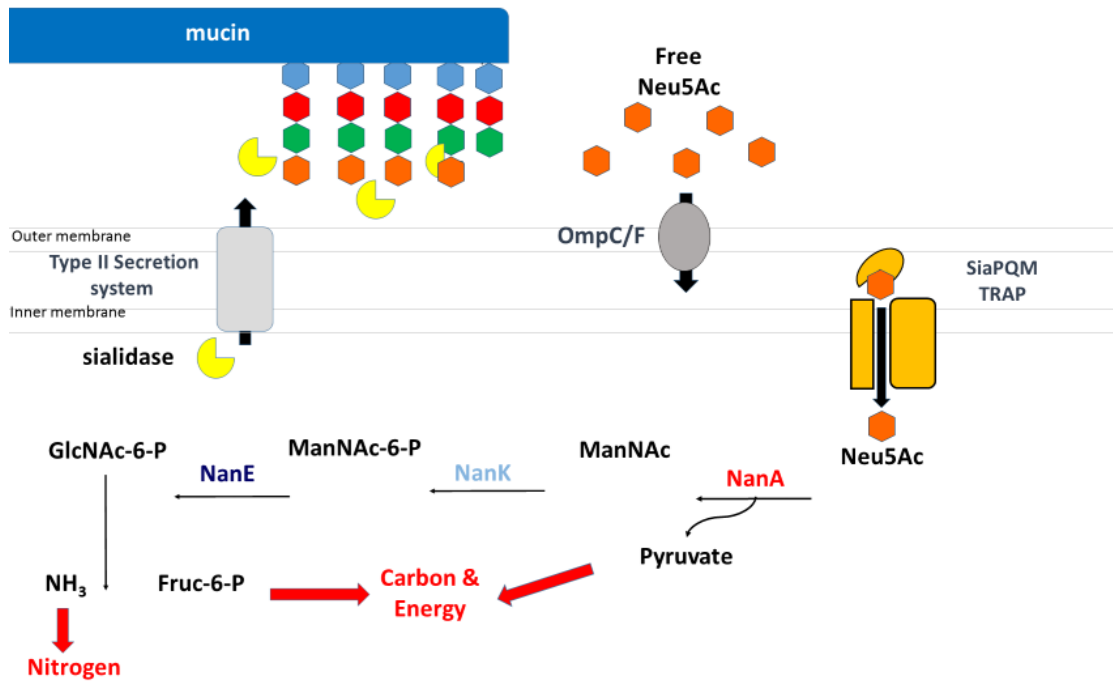


Figure 2 Representative schematic of sialic acid catabolism in bacteria. In *nanA*+ *V. cholerae* strains, sialidase is excreted to the external environment by a Type II secretion system. Outermembrane proteins C (OmpC) and or F (OmpF) enable free Neu5Ac to enter periplasm of Gram negative species. *Vibrio* SiaPQM TRAP system, is used as representative sialic acid specific transporter. Abbreviations: GlcNAc – *N*-acetylglucosamine, ManNAc – *N*-acetylmannosamine, Fruc-6-P – Fructose 6-phosphate. NanA – *N*-acteylneuraminic acid lyase NanK- *N*-acetylmannosamine kinase NanE – *N*-acetylmannosamine -6-P epimerase

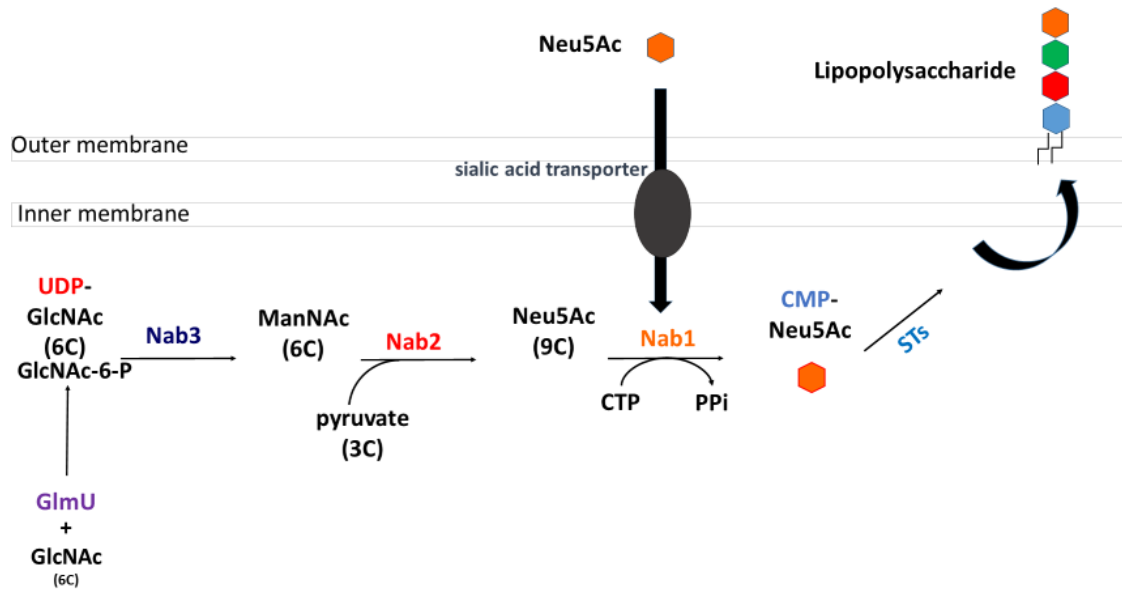


Figure 3 Representative schematic of bacterial sialic acid synthesis. *N*-acetylglucosamine (GlcNAc) is a principal metabolite found in the bacterial cytosol. Abbreviations: GlcNAc – *N*-acetylglucosamine, ManNAc – *N*-acetylmannosamine, CTP – Cytosine triphosphate, PPi – pyrophosphate, CMP-Neu5Ac – Cytosine monophosphate linked Neu5Ac. Enzymes: GlmU - *N*-acetylglucosamine-1-phosphate uridylyltransferase, Nab3- *N*-acetylmannosamine -6-P epimerase, Nab2 - *N*-acteylneuraminic acid lyase, Nab1 - *N*-acetylmannosamine kinase, ST - Sialyltransferase

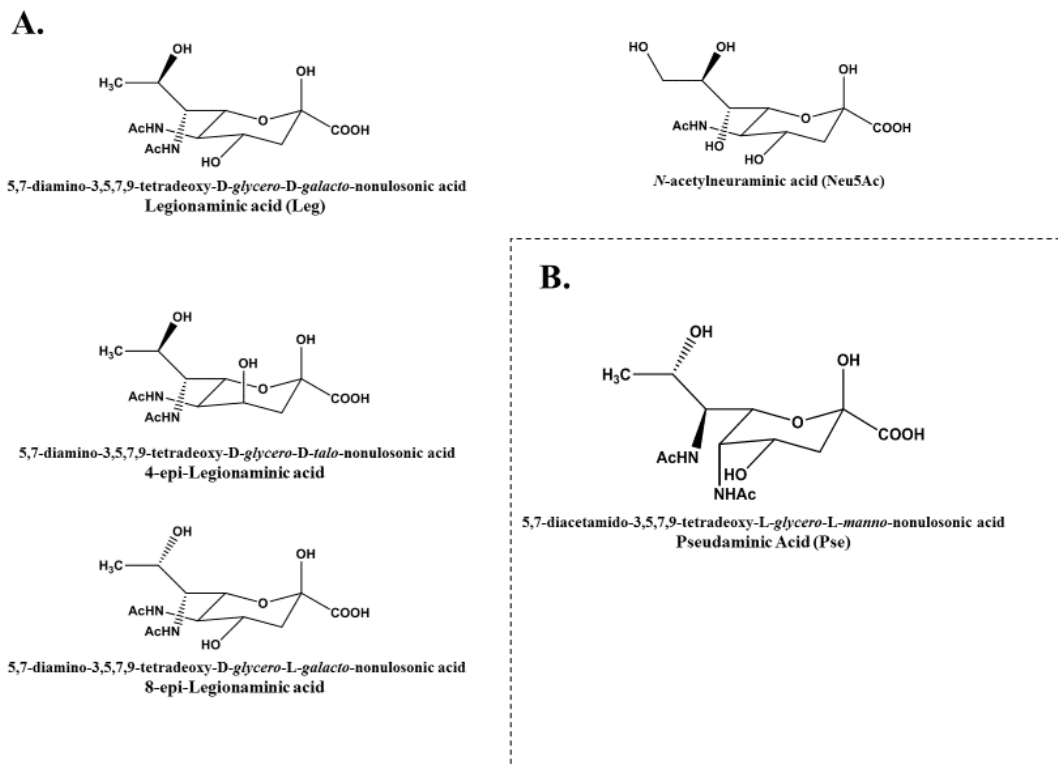


Figure 4 Structural configurations of bacterial-specific sialic-acid like molecules, Legionaminic, and Pseudaminic acids. (A) Structural comparison of *N*-acetylneuraminic acid and Legionaminic acid containing di-*N*-acetylation, and a loss of hydroxyl groups on C-7 and C-9. Isomeric forms of legionaminic acid, *D*-glycero-*D*-talo, 4-epi-Legionaminic, and *and D*-glycero-*L*-galacto, 8-epi-Legionaminic are presented. (B) Pseudaminic acid, a *L*-glycero-*L*-manno stereoisomer of legionaminic acid. Dotted line to emphasis pseudaminic acid difference in stereo-configuration, which is identical in Neu5Ac and legionaminic acid.

Chapter 2

SIALIC ACID CATABOLISM AND TRANSPORT GENE CLUSTERS ARE LINEAGE SPECIFIC IN *VIBRIO VULNIFICUS*

Introduction

Sialic acids, also known as neuraminic or nonulosonic acids, are a family of nine-carbon alpha keto-sugars. Sialic acids are widely distributed in deuterostomes where they perform a number of functions such as cell-cell interactions, stabilizing glycoconjugates and cell membranes, and acting as chemical messengers (Varki, 1992; 2008). Sialic acids are utilized by commensal and pathogenic bacteria in a number of ways, for example, several pathogenic species of bacteria have been shown to decorate their cell surfaces with sialic acid to avoid recognition by the host immune system (Varki, 1992; Vimr and Lichtensteiger, 2002; Vimr et al., 2004; Varki, 2008). Bacteria can also utilize sialic acid as a sole carbon source, which was first shown in *Clostridium perfringens* (Nees et al., 1976). The enzymatic pathway to catabolize *N*-acetylneuraminic acid (Neu5Ac), the most common sialic acid, was shown by Vimr and colleagues in *Escherichia coli* to require three key enzymes (Vimr and Troy, 1985; Vimr et al., 2004). First, Neu5Ac is broken down into *N*-acetylmannosamine (ManNAc) and phosphoenolpyruvate (PEP) by a lyase/aldolase (NanA). ManNAc kinase (NanK) adds a phosphate group to generate *N*-acetylmannosamine-6-phosphate (ManNAc-6-P), which ManNAc-6-P epimerase (NanE) acts on to convert into *N*-acetylglucosamine-6-P (GlcNAc-6-P). In bacteria, the genes for the first three enzymes (NanA, NanK, and NanE) in the catabolism pathways are usually found clustered together in the genome (Almagro-Moreno and Boyd, 2009a). Recently, a novel epimerase was identified in *Bacteroides fragilis* and *Tannerella forsythia* that

has no requirement for a phosphorylated substrate (Brigham et al., 2009; Roy et al., 2010). Finally, GlcNAc-6-P deacetylase (encoded by *nagA*) and glucosamine-6-P deaminase (encoded by *nagB*) then converts GlcNAc-6-P into fructose-6-P (Fru-6-P), which is a substrate in the glycolysis pathway.

Of the bacteria that encode a sialic acid catabolism (SAC) gene cluster, most are species known to colonize the animal intestine as pathogens or commensals (Nees et al., 1976; Vimr and Troy, 1985; Severi et al., 2005; Steenbergen et al., 2005; Almagro-Moreno and Boyd, 2009a; Brigham et al., 2009). In *V. cholerae* the causative agent of cholera, the SAC genes are present on chromosome I within the 57 kb *Vibrio* Pathogenicity Island-2 (VPI-2) region, which is confined to pathogenic strains (Jermyn and Boyd, 2002; 2005). By using an infant mouse model of infection, it was shown that the ability to catabolize sialic acid conveys a significant competitive advantage in the early stage of infection for *V. cholerae* (Almagro-Moreno and Boyd, 2009b). Genetically linked to the SAC cluster in *V. cholerae* are homologues of *siaPQM*, which encode a substrate-binding protein (SBP) dependent secondary transporter belonging to the Tripartite ATP-independent periplasmic (TRAP) transporter family (Severi et al., Almagro-Moreno and Boyd, 2009a; b; Fischer et al., 2010; Mulligan et al., 2011). The homologous TRAP transporter associated with the SAC cluster in *H. influenzae* was shown to be highly efficient in the uptake of sialic acid (Severi et al., 2005; Fischer et al., 2010; Mulligan et al., 2011). And it has been more recently demonstrated in *V. cholerae* that the SBP of the TRAP transporter SiaPQM (VC1777-VC1779) is a Na⁺-dependent high affinity secondary transporter for sialic acid also (Fischer et al., 2010; Mulligan et al., 2011a; Mulligan et al., 2011b; Thomas and Boyd, 2011).

There are at least four diverse families of solute transporters that are genetically linked with the SAC cluster among bacteria (Severi et al., 2007; Almagro-Moreno and Boyd, 2009a; Fischer et al., 2010; Severi et al., 2010; Mulligan et al., 2011), the above mentioned TRAP transporter from *V. cholerae* and *H. influenzae*, the major facilitator superfamily (MFS) NanT found in *E. coli*, an ABC-type transporter from *H. ducreyi*, and the sodium solute symporter (SSS) first identified in *Photobacterium profundum* (Severi et al., 2007 ; Almagro-Moreno and Boyd, 2009a; Fischer et al., 2010; Severi et al., 2010; Mulligan et al., 2011). Among Enterobacteriaceae, NanT is the most prevalent transporter associated with the SAC cluster whereas in the Pasteurellaceae and the Vibrionaceae, the TRAP transporter is the predominant type found (Almagro-Moreno and Boyd, 2009a; Fischer et al., 2010; Severi et al., 2010). Among the Firmicutes, the predominant transporters associated with the SAC cluster belong to the SSS, ABC, or Sodium/proline (Sym) family of transporters (Severi et al., 2007 ; Almagro-Moreno and Boyd, 2009a; Fischer et al., 2010; Severi et al., 2010#532). Recent *in silico* and *in vitro* analyses of sialic acid transporters revealed the presence of two functional systems in *Salmonella enterica*, an MFS type and an SSS type (Severi et al., 2010).

Vibrio vulnificus is an inhabitant of the marine ecosystem and an opportunistic pathogen of humans where it can cause severe and rapid septicemia (Oliver et al., 1982; Wright et al., 1996; Gulig et al., 2005; Blackwell and Oliver, 2008; Jones and Oliver, 2009). *Vibrio vulnificus* is commonly isolated from the water column and is also isolated in high numbers from oysters and other filter-feeding shellfish and infections occur after the consumption of raw or improperly cooked shellfish (Depaola et al., 2003; Harwood et al., 2004; Gulig et al., 2005; Jones and Oliver, 2009).

Mortality associated with *V. vulnificus* infection is very high (>50%), making this bacterium the leading cause of death in the United States associated with the consumption of seafood (Strom and Paranjpye, 2000; Harwood et al., 2004; Gulig et al., 2005; Jones and Oliver, 2009). A number of different typing schemes have been developed to separate *V. vulnificus* isolates into groups based on whether they are pathogenic or non-pathogenic by using biochemical, serological, or genetic methods (Morris et al., 1987; Hayat et al., 1993; Amaro and Biosca, 1996; Biosca et al., 1997; Depaola et al., 2003; Nilsson et al., 2003; Bisharat et al., 2005; Rosche et al., 2005; Chatzidaki-Livanis et al., 2006; Cohen et al., 2007; Sanjuan and Amaro, 2007; Vickery et al., 2007; Sanjuan et al., 2009). Thus, 3 biotypes are recognized among isolates based on phenotypic characteristics and host range criteria (Bisharat et al., 2005; Cohen et al., 2007; Sanjuan et al., 2010; Kwak et al., 2011). Based on 16S rRNA genotyping, Nilsson and workers found most environmental isolates had a distinct 16S rRNA genotype named genotype A and most clinical isolates had a distinct genotype designated genotype B (2003). Phylogenetic analysis divides *V. vulnificus* strains into two major groupings designated lineage I and lineage II (Bisharat et al., 2005; Cohen et al., 2007; Sanjuan et al., 2010; Kwak et al., 2011). Lineage I is comprised almost entirely of strains that cause disease in humans and encompasses predominantly biotype 1 strains and are designated C-type strains in some typing schemes (Roche et al., 2005). Lineage 2 is comprised mainly of environmental or fish isolates encompassing biotypes 1 and 2 and are designated as E-type strains (Roche et al., 2005). A third lineage is comprised of strains that are biotype 3 human pathogens (Bisharat et al., 2005; Cohen et al., 2007; Sanjuan et al., 2010). A recent *in vivo* study using a subcutaneously inoculated iron dextran-treated

mouse model indicates that genotype is correlated with virulence of *V. vulnificus* biotype 1 strains (Thiaville et al., 2011).

Bioinformatic analysis demonstrated the presence of sialic acid catabolism and transporter gene clusters in the genome sequence of two *V. vulnificus* clinical isolates YJ016 and CMCP6 (Almagro-Moreno and Boyd, 2009a). Using SOLiD sequencing analysis of four *V. vulnificus* strains, Gulig and colleagues, demonstrated that three of these strains encoded genetically linked sialic acid catabolism and transport genes (Gulig et al., 2010). In another study, it was demonstrated that a clinical strain of *V. vulnificus* had the ability to catabolize sialic acid, which was shown to be important for *in vivo* survival using a mouse model (Jeong et al., 2009). Jeong and co-workers speculated that unlike *V. cholerae*, *V. vulnificus* has a NanT homologue for sialic acid transport (Jeong et al., 2009).

In this study, we examined the genome arrangement of the SAC gene cluster within *V. vulnificus* and *Vibrio* species in general to determine the type of transporter associated with the cluster. Next, we examined a collection of *V. vulnificus* isolates, whose phylogenetic relationships are known, for the presence of the SAC gene cluster. To determine whether the presence of the SAC region is lineage specific, we mapped the distribution of *nanA*, which encodes aldolase required in the first step of sialic acid catabolism, onto the phylogeny of the *V. vulnificus* isolates. Then, we investigated whether *V. vulnificus* isolates that encode the SAC region can catabolize sialic acid as a sole carbon source. Although *V. vulnificus* sequenced isolates appear to have two transporters associated with the SAC genes, the predominant transporter system found among *Vibrio* species is the TRAP system. We created a deletion mutation in TRAP system to examine whether it is essential for sialic acid transporter in this species.

Materials and Methods

Bacterial strains

Strains and plasmids used in this study are listed in **Table 1**. A total of 67 *V. vulnificus* natural isolates whose phylogenetic relationships are known were examined in this study (Cohen et al., 2007). These isolates represent all three biotypes found in *V. vulnificus*. The isolates were collected between 1980-2005, from Asia, USA, Europe, and India, with 27 isolates recovered from clinical sources, and 40 from environmental (clams, mussels, fish, oysters, seawater, sediment) (Cohen et al., 2007). All strains were grown aerobically (250 rpm) at 37°C in Luria-Bertani broth (Fisher Scientific, Fair Lawn, NJ) with a final NaCl concentration of 2% (Fisher Scientific) and stored at -80 °C in LB broth with 20% (v/v) glycerol.

Molecular analysis

Chromosomal DNA was extracted from the 67 *V. vulnificus* isolates using the DNA isolation kit from Bio101 following the manufactures protocol (MP Biomedicals, Solon, OH). PCR primers for *nanA* were designed based on the sequence of *V. vulnificus* strain YJ016, VVA1199F- TTATCGCCGCTCCCCATACA and VVA1199R-GCAACGCCACCGTATTCAAC. PCR assays were performed in 25µl reactions with 2.5µM concentration of each primer, 2.5mM dNTP mix, 10x PCR buffer, and 1U of ChoiceTM Taq DNA polymerase (Denville Scientific, Metuchen, NJ, USA). The PCR cycle program consisted of an initial denaturation step at 94°C for one minute followed by 94°C for 30s, 55°C for 30s, 72°C for 1 min for 30 cycles. PCR products were visualized on 1.0% agarose gels. Long-range PCR primer pair VVA1194F and VVA1212R was designed from *V. vulnificus* strain YJ016 to encompass an 18 kb region spanning the SAC and SAT gene clusters from ORFs

VVA1194 to VVA1212. Primer VVA1194F (TTG GTG TGC TAT CGG GTA CA) was designed within the *napC* gene that encodes a periplasmic nitrate reductase, cytochrome C-type protein and primer VVA1212R (AAA GGC ATC GCT CAC AAA CT) was designed within *secF* that encodes a preprotein translocase subunit. The PCR assay was conducted using DyNAzyme™ EXT DNA polymerase (New England Biolabs, Ipswich, MA, USA), in 50 µl reactions. The program of an initial denaturation step at 94 °C for one minute followed by 94 °C for 30s, 60 °C for 30s, and 68 °C for 12 min for 10 cycles, followed by 94 °C for 30s, 60 °C for 30s, 68 °C for 18 min for 15 cycles, then a final extension at 70 °C for 5 min was used. The PCR products were visualized on 0.6% agarose gels.

Bioinformatic analysis of sialic acid catabolism and transporter genes among Vibrionaceae.

We performed BLAST searches (BLASTP) against the sequenced genome database (Altschul et al., 1997). We used as probes the sequences of proteins encoded by *nanA* (aldolase), *nanE* (epimerase) and *siaP* (periplasmic binding component of the TRAP transporter) from *V. vulnificus* YJ016. In addition, we examined the genes immediately upstream and downstream of the region encoding *siaPQM* and *nanA*, *nanEK* and *nagA* among all sequenced Vibrionaceae to investigate whether additional transporter genes were present.

Growth analysis in minimal media supplemented with sialic acid.

Two strains positive for the presence of *nanA*, YJ016 and CMCP6 and three strains negative for the presence of *nanA*, C7184, ss108A-3A and 98-640 DP B9, were examined for their ability to grow in sialic acid as a sole carbon source. Precultures of each strain were grown to stationary phase at 37°C in LB and a 100 µl aliquot of these

cultures was added to 5 mls of fresh M9 minimal media supplemented with *N*-acetylneuraminic acid (1 mg/ml) or D-glucose (1 mg/ml) (Sigma Aldrich, St. Louis, MO) of which a 200 μ l aliquot per well was added to a 96-well microtiter plate and incubated at 37°C with shaking. Optical densities at 595 nm (O.D.₅₉₅) were measured hourly for 24 h using a Genios microplate reader and Magellan plate reader software (TECAN US, Durham, NC, USA). Graphpad Prism software was used to construct graphs based on the data obtained. Growth assays were performed in triplicate at least two times.

Mutant construction.

An in-frame non-polar deletion mutant was constructed using the splicing by overlap extension (SOE) PCR and allelic exchange procedure (Horton et al., 1989). We used *V. vulnificus* CMCP6 genome sequence as a template to design primers, which were purchased from Integrated DNA Technologies (Coralville, IA), to perform SOE PCR and obtain an in-frame single knockout mutation for VV2_0731, which encodes the *siaM* gene (**Table 2**). A 774-bp deletion was created in VV2_0731 resulting in a 510 bp non-polar truncated version of the *siaM* gene (1284 bp), thus creating a non-functioning TRAP transporter. Briefly, the *siaM* AD PCR fragment was cloned into the suicide vector pDS132 (Philippe et al., 2004), which was designated as pDS Δ *siaMAD* and electroporated into the *Escherichia coli* strain DH5 α λ -pir. pDS Δ *siaMAD* was then plasmid purified and transformed into the *E. coli* strain β 2155, a diaminopimelic acid (DAP) auxotroph, and pDS Δ *siaMAD* was then conjugated into *V. vulnificus* CMCP6 via cross streaking on LB plates containing 0.3 mM DAP (Sigma Aldrich, St. Louis, MO). Growth from these plates was then transferred to LB 2% NaCl plates containing chloramphenicol (25 μ g/ml) to select for

V. vulnificus pDS Δ siaMAD only. Exconjugate colonies were cultured overnight in the absence of antibiotics and serial dilutions were plated on LB 2% NaCl containing 10% sucrose to select for cells that had lost pDSsiaMAD. Double-crossover deletion mutants were then screened by PCR using the SOEFLsiaQF and SOEFLnanAR primers and confirmed by sequencing.

cDNA synthesis and reverse transcriptase PCR (RT-PCR).

Prior to RNA isolation, *V. vulnificus* CMPC6 was cultured overnight in LB containing 2% NaCl at pH 7 and diluted in fresh M9 minimal media 2% NaCl at pH 7 supplemented with 1 mg/ml of sialic acid or glucose and grown to an OD₅₉₅ of 0.6 (log phase). Total RNA was extracted from *V. vulnificus* CMPC6 using RNAprotect Bacteria reagent (Qiagen, Valencia, CA) and an RNeasy mini kit (Qiagen) according to the manufacturer's protocols. RNA quantity was measured on a Nanodrop spectrophotometer (Thermo Scientific, Waltham, MA), and samples were then treated with DNase to remove genomic DNA (Turbo DNase, Invitrogen, Carlsbad, CA) as per the manufacturer's protocol. One μ g of each sample of RNA was assessed on a 1% agarose gel in 1 \times TBE buffer (Mediatech Inc, Herndon, VA) to ensure quality of the samples. cDNA was synthesized by using SuperScript II Reverse Transcriptase (Invitrogen) according to the manufacturer's protocol, with 500 ng of RNA as template and primed by 200 ng of random hexamers. cDNA samples were diluted 1:25 and 1:125 and used as templates for semi quantitative reverse transcription-PCR reactions using gene-specific primers designed using Primer3 software and are listed in **Table 2**.

Results and Discussion

Vibrio vulnificus sialic acid catabolism (SAC) and transport (SAT) region is predominately lineage I specific.

We performed a BLAST search against the three genomes of *V. vulnificus* strains YJ016, CMCP6 and MO6-24 in the NCBI genome database to identify homologues of sialic acid catabolism and transport genes from *V. cholerae* (Almagro-Moreno and Boyd, 2009a; b; Almagro-Moreno and Boyd, 2010). We identified the genes encoding enzymes in the sialic acid catabolic and transport pathways; *nanA* (VV2_0730), *nanK* (VV2_0735), *nanE* (VV2_0734), *nagA* (VV2_0736) and *siaPQM* (VV2_0731_ VV2_0733) in strain YJ016 (**Fig. 5**). The sequences of these genes among the three *V. vulnificus* strains YJ016, CMCP6 and MO6-24 was >99% identical suggesting a highly conserved region. The order and arrangement of the sialic acid catabolism (SAC) and transport (SAT) genes in all three strains of *V. vulnificus* was identical to those present in *V. cholerae* (**Fig. 5**). However, in *V. vulnificus* the SAC and SAT region was carried on chromosome II and was not associated with a pathogenicity island (**Fig. 5**). An additional difference between the two species is the absence of the *nanH* gene from *V. vulnificus* strains. In *V. cholerae*, the *nanH* gene encodes sialidase (neuraminidase), a glycohydrolase that cleaves sialic acid from high order gangliosides releasing free sialic acid.

The SiaM protein (VV2_0731) shared an overall sequence identity of 95% with *V. cholerae* SiaM (VC1777) and 57% with SiaM from *Haemophilus influenzae*, which was shown previously to be part of a high-affinity, Na (+)-dependent unidirectional secondary TRAP transporter for sialic acid (Severi et al., 2005). No homolog of NanT, a MFS transporter present in *E. coli* was identified in any of the genomes examined. Directly downstream of *nagA* in all three sequences was a

homologue of an ABC-type transporter component (**Fig. 5**). However, this periplasmic ABC component has domains associated with oligopeptide binding and not amino sugar or carbohydrate binding in general. It appears that *V. vulnificus* is genetically capable of sialic acid transport into the bacterial cell, which can then be catabolized as a carbon source.

Vibrio vulnificus strains YJ016, CMCP6 and MO6-24 are clinical isolates from Asia. We wanted to determine whether the SAC and SAT region is confined to clinical isolates of *V. vulnificus* similar to *V. cholerae*. To accomplish this, we examined a collection of 67 natural isolates, which is comprised of both clinical and environmental isolates, for the presence of *nanA*. The *nanA* gene encodes the aldolase required in the first step of sialic acid catabolism. Of the 27 clinical isolates examined for the presence of *nanA*, 21 were positive for the gene by our PCR assay, whereas of the 40 environmental isolates examined, 17 strains gave a positive PCR band indicating they contained *nanA*. To further investigate the distribution of *nanA* among *V. vulnificus* isolates, we mapped the presence or absence of *nanA* onto the phylogeny of these strains (**Fig. 6**). The phylogenetic tree was constructed based on the analysis of six housekeeping genes as previously described (Cohen et al., 2007) and contained two major lineages, lineage I was comprised primarily of clinical strains and lineage II was comprised predominately of environmental strains (Cohen et al., 2007). We found that 34 out of the 37 lineage I isolates were positive for the presence of *nanA*, whereas only 7 of the 26 lineage II isolates were positive for the presence of *nanA*. These data demonstrate a strong correlation between the presence of the SAC region and lineage I strains (**Fig. 6**). The three strains in lineage I that lacked *nanA* were clinical strains isolated in Japan and the USA and they did not cluster together on the tree suggesting

independent loss of the region. To determine whether the entire SAC and SAT region is missing in these strains and if a similar deletion event occurred in each strain, we used a long range PCR assay with a primer pair that encompassed the SAC and SAT gene clusters (**Fig. 7A**). We designed the primer pair within genes that are conserved among other *Vibrio* species (**Fig. 7A**). We examined four *nanA*-negative strains from divergent branches of the *V. vulnificus* phylogenetic tree. An expected 18-kb PCR band was obtained for YJ016, which contain the SAT and SAC gene clusters. Only an ~7 kb size PCR product was obtained for three of the *nanA*-negative strains, JY1701, E86 and L-180, which demonstrated that the SAC and SAT region was absent from these strains and the same deletion event occurred (**Fig. 7B**). Since no product was obtained for K2637, we speculate that a larger deletion event that involved either *vva1194* or *vva1212* or both genes occurred.

Vibrio vulnificus SAC and SAT positive strains can utilize sialic acid as a sole carbon and energy source.

In silico analysis showed that *V. vulnificus* lineage I isolates carry the genes required for the transport and catabolism of sialic acid. Our next step was to determine whether *V. vulnificus* is capable of growth on sialic acid as a sole carbon and energy source. We examined two *nanA*-positive isolates and three *nanA*-negative isolates for their ability to grow in M9 minimal media supplemented with glucose (M9+glucose) or sialic acid (M9+sialic acid) (**Fig. 8**). All *V. vulnificus* strains grew in M9+glucose, showing similar growth patterns, and reaching final O.D.₅₉₅ values between 0.44 and 0.5 (**Fig. 8A**). However, only *V. vulnificus nanA*-positive strains grew in M9+sialic acid, whereas the *nanA*-negative strains failed to do so (**Fig. 8B**). This finding demonstrates that *V. vulnificus nanA*-positive strains are able to uptake and utilize

sialic acid as a sole carbon and energy source. Our data adds to the growing list of bacterial species that have been shown to utilize sialic acid as a carbon and energy source (Severi et al., 2005; Steenbergen et al., 2005; Severi et al., 2007; Almagro-Moreno and Boyd, 2009a; b; Brigham et al., 2009; Jeong et al., 2009; Roy et al., 2010; Severi et al., 2010).

Vibrio vulnificus SiaPQM (VV2_0731-VV2_0733) TRAP transporter is essential for growth on sialic acid as a sole carbon source.

Bioinformatic analysis of sialic acid catabolism genes among Vibrionaceae indicates that the TRAP transporter system is the predominant type of transporter genetically linked to the catabolism genes within this group (**Table 3**). However, closer examination of the genes flanking SAC identified several species whose DNA encoded two types of transporters genetically linked to the catabolism genes (**Fig. 5**). In *V. orientalis* both a TRAP system and a Bcr/CflA transporter were adjacent to the sialic acid catabolism genes (**Fig. 5** and **Table 3**). In *P. profundum* strain SS9 both a TRAP and a SSS system were genetically linked to the SAC genes. In *V. vulnificus*, the TRAP *siaPQM* operon is linked to the catabolism genes as well as an ABC transporter component. Thus, we investigated whether the TRAP system was essential for sialic acid uptake in this species. We constructed an isogenic knockout strain of *V. vulnificus* CMCP6 with an in-frame non-polar truncated version of *siaM*. The *siaM* gene encodes a large permease containing 12 transmembrane helices, which is an essential component of the TRAP transporter system. The SiaPQM TRAP system was first characterized in *H. influenzae* and has recently been shown in *V. cholerae* *in vitro* experiments to be a high affinity sialic acid transporter (Severi et al., 2005; Steenbergen et al., 2005; Severi et al., 2007; Almagro-Moreno and Boyd, 2009a; b;

Brigham et al., 2009; Jeong et al., 2009; Roy et al., 2010; Severi et al., 2010). The wild-type CMCP6 and mutant strain JJK0731 were inoculated into LB or M9 supplemented with glucose, *N*-acetylglucosamine (NAG) or *N*-acetylneuraminic acid (sialic acid) as sole carbon sources. Both wild-type and mutant strains demonstrated similar growth patterns in LB (data not shown) indicating that there is not a general growth defect in these strains. In addition, the wild-type and the mutant strain JJK0731 grew similarly in M9 supplemented with glucose (**Fig. 9A**). However, strain JJK0731 did not grow in M9 supplemented with sialic acid as a sole carbon source whereas the wild-type strain showed growth when examined under the same growth conditions (**Fig. 9B**). Thus, these data demonstrate that SiaPQM is essential for growth on sialic acid as the sole carbon source in *V. vulnificus*. As expected both the wild-type and mutant strains grew similarly in M9 supplemented with NAG, which is one of the products of the sialic acid catabolism pathway and does not require SiaPQM for uptake into the bacterial cell (**Fig. 9A**).

A recent study in *V. cholerae* proposed that a different TRAP transporter unrelated to SiaPQM from *V. cholerae* and *V. vulnificus* was required for sialic acid transport (Sharma et al., 2011). Sharma and colleagues proposed that ORF VC1929, which encodes a C4-dicarboxylate-binding periplasmic protein named DctP, was part of a TRAP system (VC1927-VC1929) involved in sialic acid transport (Sharma et al., 2011). They argued that in an El Tor strain of *V. cholerae*, VC1929 was a mannose-sensitive haemagglutinin that was required for sialic acid utilization (Sharma et al., 2011). This was an unexpected finding since VC1929 shared high sequence homology with C4 dicarboxylate permeases that are involved in the transport of malate, fumarate, or succinate (Thomas and Boyd, 2011). A homologue of VC1929 is present

in *V. vulnificus*, VV1_0030, which shows 89% amino acid identity to DctP. However, at least in *V. vulnificus*, DctP (VV1_0030) does not appear to be involved in sialic acid transport given that our *siaM* (VV2_0731) mutant is no longer able to utilize sialic acid as a sole carbon source.

Sialic acid induces expression of SAC and SAT genes.

Next, we examined whether the catabolism and transporter genes are constitutively expressed or induced in the presence of sialic acid. We examined the expression of three genes; *siaQ*, *nanA*, and *nanE*. The *siaQ* gene encodes a small permease containing 4 transmembrane helices, which is a component of the TRAP transporter, *nanA* encodes *N*-acetylneuraminic acid aldolase, the first enzyme in the sialic acid catabolism pathway and *nanE* encodes ManNAc-6-P epimerase that catalyzes the last step in the pathway. We isolated RNA from cultures of *V. vulnificus* CMCP6 grown at 37°C with aeration in M9 supplemented with glucose or sialic acid. Semi-quantitative reverse transcriptase PCR (RT-PCR) was performed and the three genes showed no expression in M9 supplemented with glucose at 3 hr post-inoculation (**Fig. 10**). However, RT-PCR analysis of *V. vulnificus* strain CMCP6 cultured in M9 supplemented with sialic acid showed that all three genes were expressed (**Fig. 10**). Our results demonstrate that the level of expression of both the transporter and catabolism genes is induced in the presence of sialic acid in *V. vulnificus*. This is in agreement with what has been shown for *V. cholerae*, where both the catabolism and transporter genes were highly expressed in the presence of sialic acid (Almagro-Moreno and Boyd, 2009b). Kim and colleagues have recently demonstrated that the divergently transcribed *siaP* and *nanE* genes are under the control of the negative regulator *rpiR* (VV2_0730) in *V. vulnificus* (Kim et al., 2011). They showed that both

the catabolic and transport genes are induced in the presence of sialic acid. However, they also found that *N*-acetylmannosamine 6-phosphate specifically bound to RpiR (NanR) and functioned as the inducer of the *nan* genes (*nanEKnagA* and *siaPQM*) in nutrient rich LB media (Kim et al., 2011).

Overall our data show that the ability to catabolize and transport sialic acid is lineage specific in *V. vulnificus* and clinical isolates are capable of growth in sialic acid as a sole carbon and energy source. In addition, we have demonstrated that the *siaPQM* genes (VV2_0731-0733) genetically linked to the catabolism genes encode a TRAP transporter for sialic acid uptake. The linking of sialic acid catabolism genes with a high affinity transport system would certainly be advantageous to a species either in environments where nutrients are limited or in environments where competition for nutrients is high such as the animal gut. The presence of free glucose is highly limited in the animal intestine and gastrointestinal pathogens have evolved to take advantage of alternative carbon sources in this niche. Mucous membranes are ubiquitous within the intestinal tract and are made up of mucins, which are glycosylated glycoproteins and represent a potential nutrient source. Many different pathogenic and commensal species harbor genes that enable them to utilize glycosaminoglycans (GAGs) as carbon and nitrogen sources. Sialic acids are nine carbon amino sugars that are present at the termini of GAGs in many cell types. Commensals and pathogens can carry the gene for sialidases that cleave terminal sialic acids releasing them for uptake into the bacterial cells. Thus, the ability to uptake and utilize sialic acid as a sole carbon source should be advantageous to gastrointestinal pathogens. Indeed, it has been demonstrated that in both *V. cholerae* and *V. vulnificus*

the ability to use sialic acid as a sole carbon source increases their fitness *in vivo* (Almagro-Moreno and Boyd, 2009b; Jeong et al., 2009).

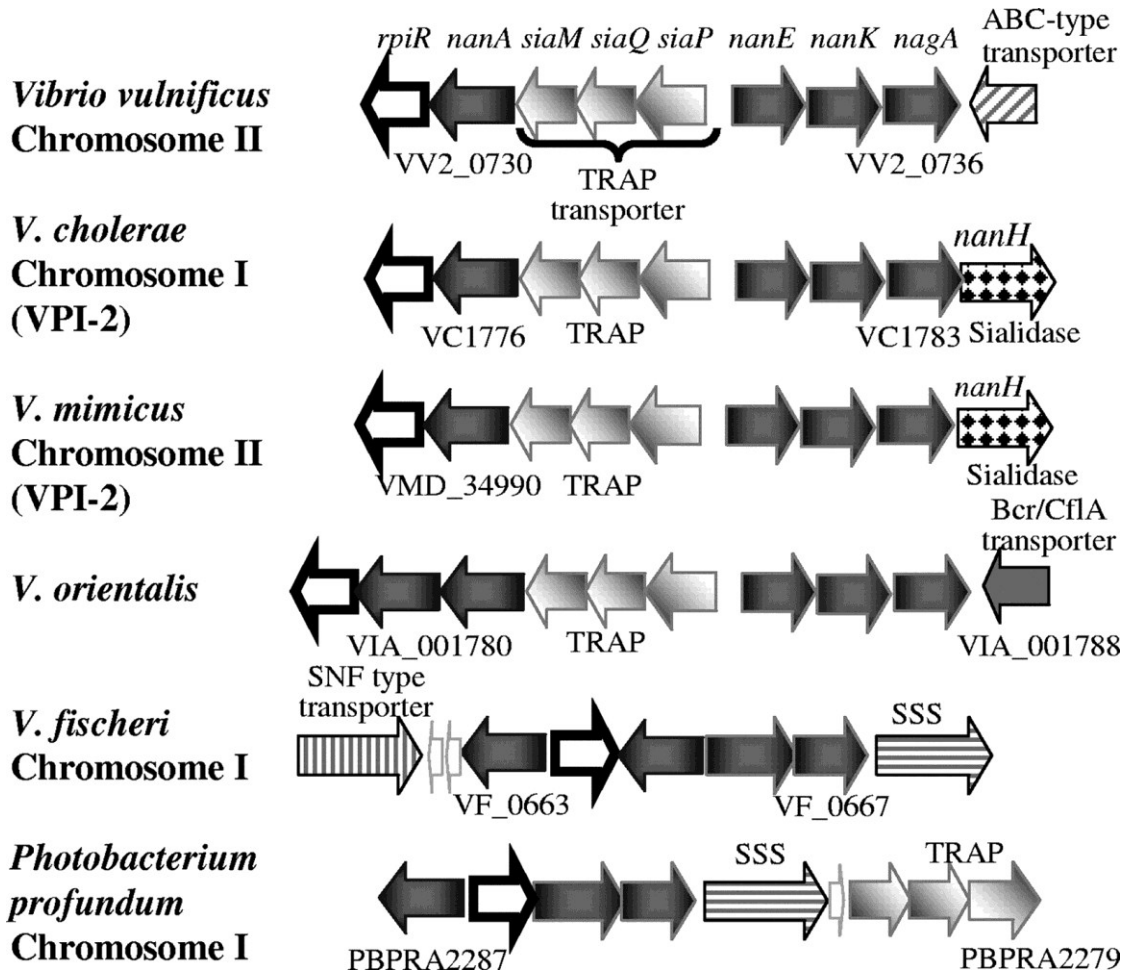


Figure 5 **Genome context and arrangement of sialic acid catabolism (SAC) and transporter (SAT) gene clusters among *Vibrio* species.** Open reading frames (ORFs) are indicated as arrows, the direction of which shows the direction of transcription. Numbers underneath ORFs represent locus tags. ORFs of similar shading represent homologous genes among the different species examined. The following annotated ORFs are shown: *rpiR*, transcriptional regulator; *nanA*, *N*-acetylneuraminic acid aldolase/lyase; *siaPQM*, TRAP transporter; *nanE*, *N*-acetylmannosamine-6-P epimerase; *nanK*, *N*-acetylmannosamine kinase; *nagA*, *N*-acetylglucosamine-6-phosphate deacetylase; ABC, ATP-binding cassette transporter; SSS, sodium solute symporter transporter.

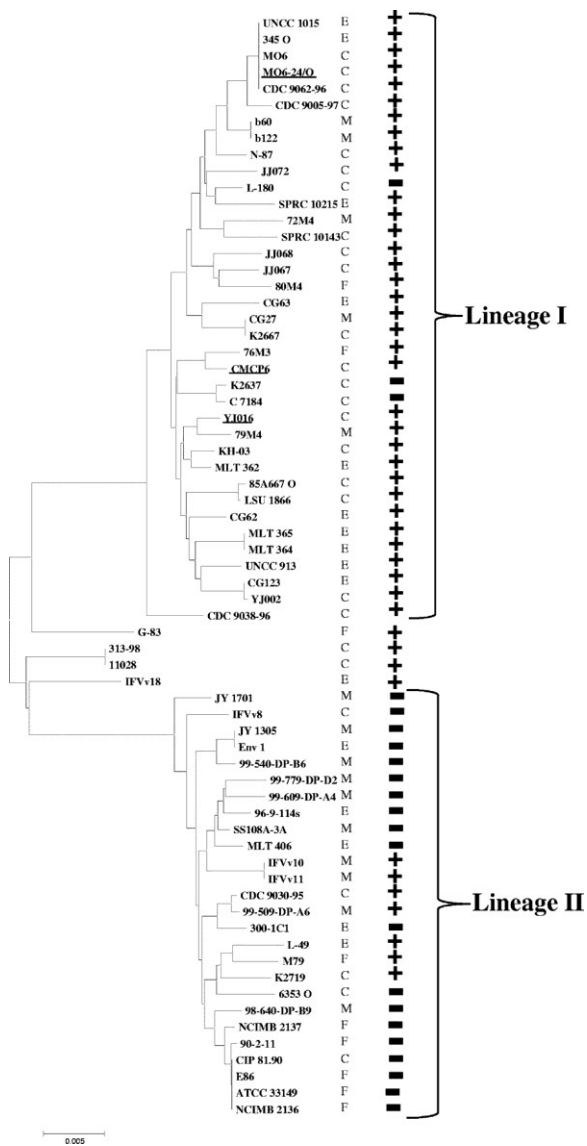


Figure 6 **Distribution of *nanA* within the *V. vulnificus* phylogeny.** The phylogenetic tree of *V. vulnificus* is based on the analysis of six housekeeping genes using the Kimura method and constructed using the neighbor-joining method as previously described (12). PCR assays were performed using *nanA*-specific primers and genomic DNA of *V. vulnificus* strains as templates. Positive and negative PCR results are indicated by “+” and “-,” respectively. The three sequenced *V. vulnificus* strains are underlined. The source of each isolate is also shown where C is for clinical, E for environmental, F for fish, and M for mollusk.

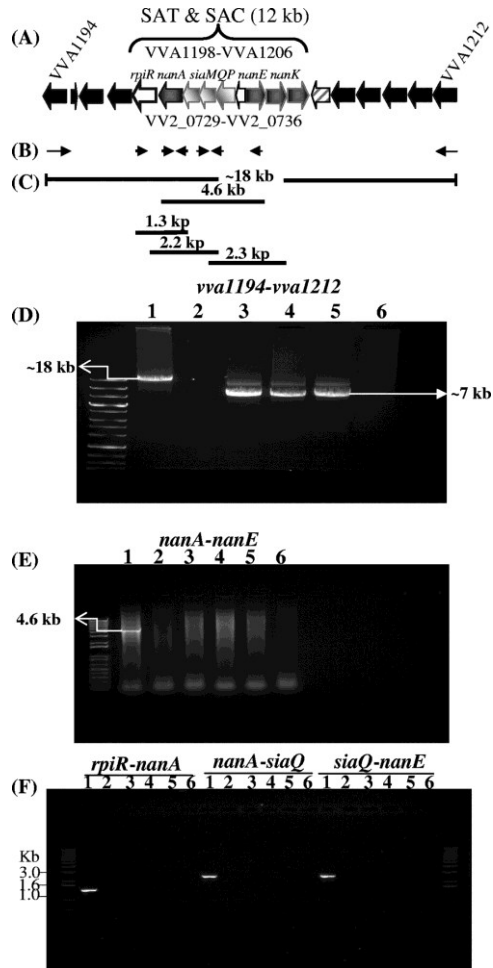


Figure 7 **PCR analysis of *V. vulnificus* *nanA*-negative strains. PCR analysis of *V. vulnificus* *nanA*-negative strains.** (A) Schematic of region examined. Solid arrows represent ORFs and black filled arrows represent ORFs outside the SAT and SAC region. Numbers above and below ORFs represent locus tags for strains YJ016 and CMCP6, respectively. (B) Line arrows indicate locations of primers used in PCR assays. (C) Black solid lines indicate regions amplified by primer pairs. (D) Long-range PCR assay. The lane to the left of lane 1 shows a 1 kb plus DNA ladder (Invitrogen). Lanes: 1, *nanA*-positive strain YJ016; 2 to 5, *nanA*-negative strains K2637, JY1701, E86, and L-180; 6, negative control, no template. A product of ~18 kb was obtained from YJ016, whereas a ~7-kb band was obtained from all other strains except K2637. (E) *nanA*-to-*nanE* PCR assay. Lanes 1 to 6 are as in panel D. A product of 4.6 kb was obtained from YJ016 only. (F) PCR assays for *rpiR*-*nanA*, *nanA*-*siaQ*, and *siaQ*-*nanE*. Lanes 1 to 6 are as in panel D. PCR products were obtained from YJ016 only.

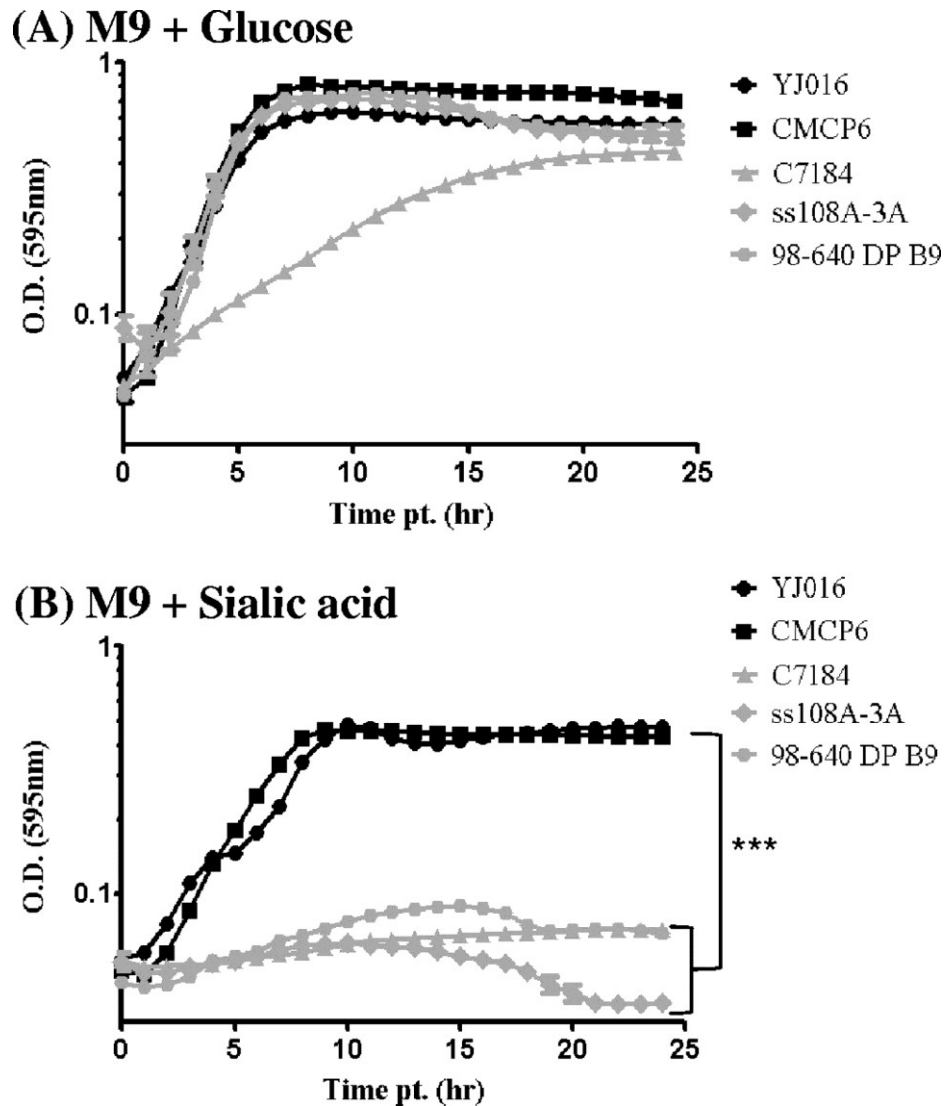


Figure 8 **Growth analysis of *V. vulnificus* in M9 minimal medium supplemented with glucose (A) or *N*-acetylneuraminic acid (sialic acid) (B) as a sole carbon source.** Two *V. vulnificus* strains that carry the sialic acid catabolism and transporter gene clusters (YJ016 and CMCP6) and three *nanA*-negative strains (C7184, ss108A-3A, and 98-640 DP B9) were examined in minimal medium supplemented with glucose (A) or sialic acid (B). All cultures were grown in triplicate, and each experiment was performed at least twice using two biological replicates. Plots are represented on a natural log scale. OD, optical density. Error bars indicate standard deviations. An unpaired Student t test was used to determine statistically significant difference between cells grown in glucose and cells grown in *N*-acetylneuraminic acid. ***, $P < 0.001$.

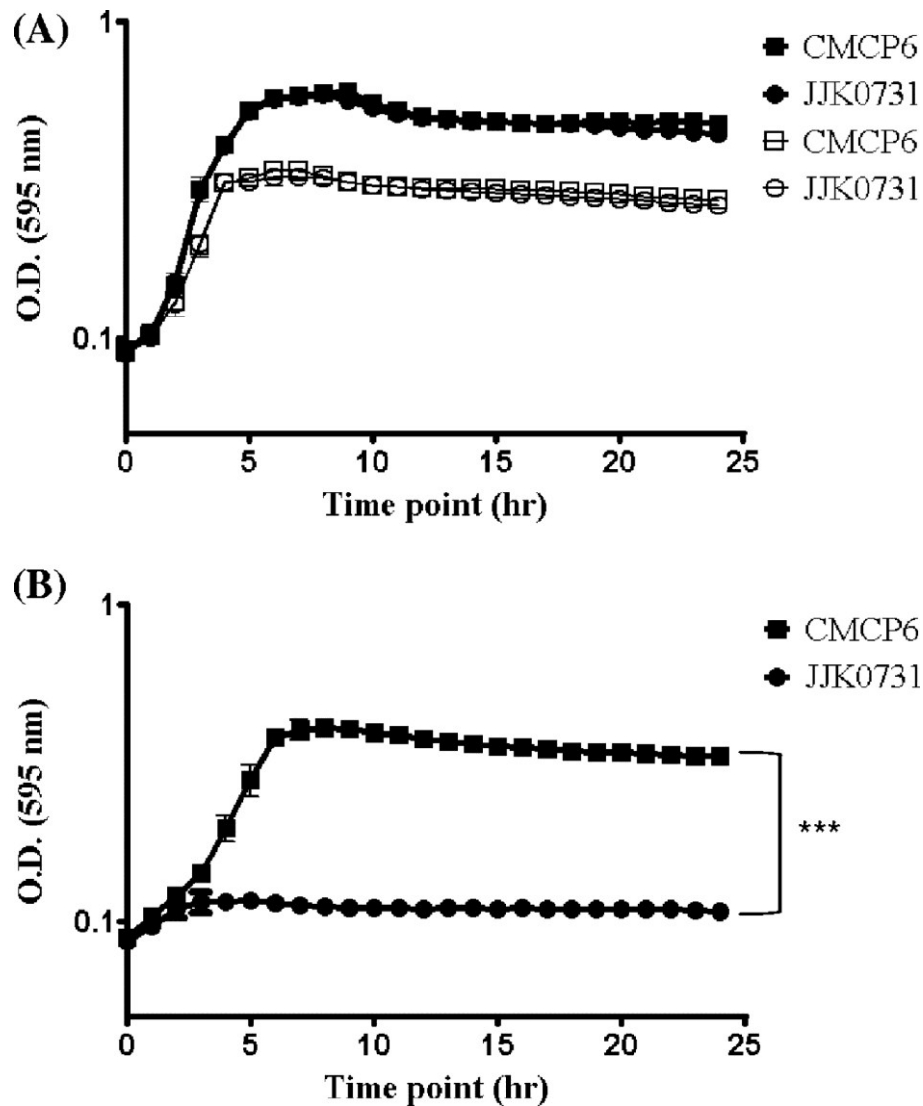


Figure 9 **Growth analysis of *V. vulnificus* wild-type strain CMCP6 and its nonpolar *siaM* deletion mutant strain JJK0731 in M9 minimal medium supplemented with glucose or *N*-acetylglucosamine (NAG) (A) or *N*-acetylneuraminic acid (sialic acid) (B).** (A) Upper two lines with symbols of solid squares and circles indicate the growth pattern in M9 plus glucose, and the lower two are of M9 plus NAG. Plots are represented on natural log scale. OD, optical density. All cultures were grown in triplicate, and each experiment was performed at least twice using two biological replicates. Error bars indicate standard deviation. An unpaired Student t test was used to determine statistical difference between mutant strain cells and wild-type strain cells grown in *N*-acetylneuraminic acid (sialic acid). ***, $P < 0.001$.

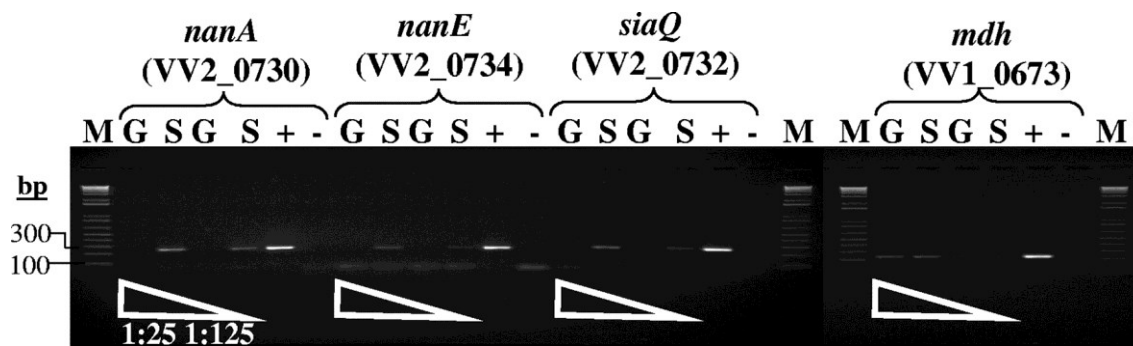


Figure 10 **Expression analysis of sialic acid catabolism (e.g., *nanA*, *nanE*) and transporter (e.g., *siaQ*) genes, and a reference (housekeeping) gene (*mdh*) in *V. vulnificus* strain CMCP6 in the presence of glucose (G) or sialic acid (S). cDNA samples were diluted 1:25 and 1:125 and used as templates for semiquantitative RT-PCRs. Genomic DNA of CMCP6 and a PCR mixture without any DNA were used as positive (+) and negative (-) controls, respectively. The values on the left are the molecular mass (bp) standard of 1 kb plus DNA ladder (Invitrogen).**

| Table 1 Bacterial strains and plasmids used in this study | | |
|---|--|------------|
| Strain or plasmid | Description ^a | Reference |
| <i>Vibrio vulnificus</i> | | |
| YJ016 | SAC ⁺ SAT ⁺ ; clinical isolate | 11 |
| CMCP6 | SAC ⁺ SAT ⁺ ; clinical isolate | This study |
| JJK0731 | CMCP6 Δ <i>siaM</i> (VV2_0731) | |
| <i>Escherichia coli</i> | | |
| DH5 α λ -pir | <i>pir80dlacZ</i> Δ M15 δ (<i>lacZYA-argF</i>)U169 <i>recA1 hsdR17 deoR thi-1 supE44 gyrA96 relA1</i> | This study |
| β 2155 DAP | Donor for bacterial conjugation; <i>thr1004 pro thi strA hsdS lacZ</i> Δ M15 (F <i>lacZ</i> Δ M15 <i>lacTRQJ36proAB</i>) <i>dapA</i> Erm ^r <i>pirRP4</i> (Km ^r from SM10) | |
| DH5 α λ -pir Δ <i>siaM</i> | DH5 α λ -pir containing pDS132 Δ <i>siaM</i> | This study |
| β 2155 DAP- Δ <i>siaM</i> | β 2155 harboring pDS132 Δ <i>siaM</i> | This study |
| Plasmids | | |
| pDS132 | Suicide plasmid, Cm ^r , SacB | 32 |
| pDS132 Δ <i>siaM</i> | pDS132 harboring truncated <i>siaM</i> | This study |

- ^a SAC, sialic acid catabolism; SAT, sialic acid transport.

Table 2 Primers used in this study

| Primer name | Sequence (5'-3') | T_m (°C) | Product size (bp) |
|-------------------|---|------------|-------------------|
| SOE PCR primers | | | |
| SOEAsiaQF | GCTCTAGAGTGTTGTCCTTGGAAGCTGCG | 57 | 527 |
| SOEBsiaMR | ATGGCCAACCATGGATTTGGCA | 57 | |
| SOECsiaMF | TGCCAAATCCATGGTTGGCCAT GCATCGGCGGTTCGGGATTGA | 59 | 573 |
| SOEDnanAR | CGAGCTCAACGATACTCAGAGCCCCCGT | 57 | |
| SOEFLsiaQF | CTCATTGGCTGTGCCATCGCT | 58 | 1,998 |
| SOEFLnanAR | CAAGGCCCGATCGCGGAAGT | 60 | 1,224 |
| RT-PCR primers | | | |
| nanA-QF | TTGGCTACTCTCAGCGCGCG | 62 | 250 |
| nanA-QR | TTGCCACTTCCGCGATCGGG | 62 | |
| nanE-QF | TCTTGCTTCGCGGATGGGCA | 62 | 236 |
| nanE-QR | CGTGTGATGGCCGAGCCCAC | 63 | |
| siaQ-QF | AGCCCGCCAAGGGGTAAACTG | 62 | 247 |
| siaQ-QR | TGTCGCTCATTGGCTGTGCCA | 62 | |
| mdh-QF | CCCGTTTCGATCAAAGGTTA | 52 | 229 |
| mdh-QR | CAATTGGCACAGTGGTGTTTC | 54 | |
| PCR assay primers | | | |
| nanAF | TCGCGCATTTTCGCCACGAC | | |
| nanER | GCGGCGAGTTGAGGCGTGTT | 65 | 4,562 |
| rpiRF | TACGCAAGCCCAGCGGCATG | | |
| nanAR | TTGCCACTTCCGCGATCGGG | 65 | 1,299 |

| Primer name | Sequence (5'-3') | T_m (°C) | Product size (bp) |
|-------------|-----------------------|------------|-------------------|
| nanAF | TTGGCTACTCTCAGCGCGCG | | |
| siaQR | TGTCGCTCATTGGCTGTGCCA | 65 | 2,233 |
| siaQF | AGCCCGCCAAGGGGTAAACTG | | |
| nanER | CGTGTGATGGCCGAGCCCAC | 65 | 2,309 |

Chapter 3

GENOMIC AND METABOLIC PROFILING OF NONULOSONIC ACIDS IN VIBRIONACEAE REVEAL BIOCHEMICAL PHENOTYPES OF ALLELIC DIVERGENCE IN *VIBRIO VULNIFICUS*

Introduction

Nonulosonic acids (NulOs) are a family of negatively charged nine-carbon backbone α -keto sugars that include the neuraminic (a.k.a. sialic), legionaminic, and pseudaminic acids (Angata and Varki, 2002b; Lewis et al., 2009). The sialic acids are the best understood among NulOs and are found in prominent outermost positions on the surfaces of all vertebrate cells (Varki, 2007). In mammals, the most common NulO is sialic acid, a molecule found at particularly high levels at mucosal surfaces of mammals. Pseudaminic and legionaminic acids are not expressed in animals. In their various locations on microbial surfaces, different NulO structures have been implicated in a variety of host-microbe interactions. NulOs of the sialic, legionaminic, and pseudaminic acid types are involved in bacterial behaviors like biofilm formation, autoagglutination and motility (Anderson et al.,; Naito et al.,; Swords et al., 2004; Guerry et al., 2006; Ewing et al., 2009) as well as direct protein-carbohydrate interactions between host and pathogen (Khatua et al.,; Jones et al., 2003; Swords et al., 2004; Carlin et al., 2007; Carlin et al., 2009). In particular, sialic acid-containing bacterial glycans participate in strategies of immune suppression and subversion, likely contributing to clinical conditions ranging from urogenital, airway and ear infections, to systemic bacteremia, meningitis, and the induction of autoimmunity

(Anderson et al.,; Houlston et al.,; Wessels et al., 1989; Vimr and Lichtensteiger, 2002; Vimr. et al., 2004b; Komagamine and Yuki, 2006; Wu and Jerse, 2006).

Sialic acids were once thought to be unique to the deuterostome lineage of 'higher' animals and absent from most protostome, fungi, plants and protists (Warren, 1963) In fact, the biosynthetic pathways for sialic acids appear to be quite ancient, likely predating the divergence of the three domains of life (Lewis et al., 2009). Recent studies show that nonulosonic acid biosynthetic (nab) gene clusters are encoded in a surprising variety of bacterial strains and species, including a large number of γ -Proteobacteria, including the family Vibrionaceae (Lewis et al., 2009). Different Proteobacteria have been shown to express NulOs as modifications of polymerized cell surface molecules such as capsular polysaccharides (Gil-Serrano et al., 1999; Le Quere et al., 2006) lipopolysaccharides (Li et al.,; Perepelov et al.,; Shashkov et al., 2007) and flagella (Logan et al., 2002; Schirm et al., 2003; McNally et al., 2006; McNally et al., 2007; Logan et al., 2009). Among the Vibrionaceae, strains of *V. parahaemolyticus*, *V. vulnificus*, *Aliivibrio salmonicida*, and *Photobacterium profundum* have also been shown to express NulOs (Edebrink et al., 1996; Bogwald and Hoffman, 2006; Lewis et al., 2009; Vinogradov et al., 2009). However, little is known about the larger distribution patterns, the natural history of NulOs in Vibrionaceae, or the biology of these molecules in aquatic or host-associated niche environments.

As a group, the Vibrionaceae engage in a full spectrum of lifestyles, from free-living states to colonization or infection of both aquatic and terrestrial hosts (Austin et al., 2009). *Vibrio vulnificus* is an excellent example of the range of environmental and host niches that can be occupied by different members of the same *Vibrio* species.

Vibrio vulnificus is an obligate halophile, found in estuarine and marine coastal environments worldwide (Tamplin et al., 1982; Kaysner et al., 1987; Kaysner et al., 1989; Oliver, 1995). It is found in association with zooplankton, crabs, and various filter feeders such as oysters and mussels (Depaola et al., 1994; Motes et al., 1998; Heidelberg et al., 2002a; b). *V. vulnificus* is also a highly invasive pathogen of both fish and humans, and in humans, infection is characterized by primary septicemia and wound infections with mortality rates greater than 50% in susceptible individuals (Linkous and Oliver, 1999; Oliver, 2005b; Jones and Oliver, 2009a). Multilocus sequence typing (MLST) analysis of six housekeeping genes and genotyping data has previously divided *V. vulnificus* isolates into at least three distinct clusters or lineages; lineage I is comprised exclusively of biotype 1 isolates recovered mainly from clinical sources, lineage II contains biotype 1 and all biotype 2 isolates recovered from environmental sources including diseased fish, and the third lineage is comprised of biotype 3 (Warner and Oliver, 1999a; Bisharat et al., 2005; Bisharat et al., 2007; Bisharat et al., 2007; Cohen et al., 2007a; Warner and Oliver, 2008). Biotype 3 isolates, which are recovered from one geographic region and associated with one fish species, were shown to be genetically identical and distinct from lineage I and II isolates (Bisharat et al., 2005; Bisharat et al., 2007).

We hypothesize that the family Vibrionaceae may be a particularly active lineage of NulO evolution. Here we combine genomic and biochemical approaches to more systematically investigate and document the distribution, phylogeny, and functional activity of homologous NulO biosynthetic pathways in members of the Vibrionaceae.

Materials and Methods

Abbreviations used.

DMB, 1,2-diamino-4,5-methylene dioxybenzene; HPLC, high performance liquid chromatography; Kdo, 3-Deoxy-D-*manno*-octulosonic acid; NAB, nonulosonic acid biosynthesis; NulO, nonulosonic acid; TBA, thiobarbituic acid.

Bacterial strains and culture conditions.

Bacterial strains used in this study are listed in Tables 3 and 4. Unless otherwise noted, all strains were grown aerobically (250 rpm) at 37°C in Luria-Bertani broth (Fisher Scientific) with a final NaCl concentration of 2% (Fisher Scientific). A total of 67 *V. vulnificus* isolates examined in this study were temporally (1980 to 2005) and geographically (Asia, Europe and North America) widespread encompassing all 3 biotype groups as previously reported (Cohen, A. L. et al., 2007a). Of the 67 isolates examined, 27 were recovered from clinical sources (wound infections and blood) and 40 from environmental sources (clam, oyster, mussel, fish, seawater and sea sediment). All *V. vulnificus* strains were grown in LB supplemented with 2% NaCl and stored at -80 °C in LB broth with 20% (v/v) glycerol.

Molecular analysis.

Chromosomal DNA was extracted from each of the *V. vulnificus* isolates using the Genome DNA isolation kit from Bio 101 as previously described (Cohen, A. L. et al.,) PCR primers to amplify the *nab1* (VV0316) and *nab1* (VV0312) genes from *V. vulnificus* YJ016, and *nab1* (VV1_0803) and *nab2* (VV1_0808) genes from *V. vulnificus* CMCP6 were designed based on the sequence of each strain and purchased from Integrated DNA Technologies (Coralville, IA) (**Table 5**). Polymerase chain

reactions were performed in a 25 µl reaction mixture using the following program: an initial denaturation step at 94°C for 1 min followed by 30 cycles of denaturation at 94°C for 30 sec, 30 sec of primer annealing at 57-61°C, and 60 sec of primer extension at 72°C. PCR products were visualized on agarose gels.

Bioinformatic and phylogenetic analysis of *nab* genes.

We performed BLAST searches (BLASTP) against the sequenced genome database using as seeds the sequences of proteins encoded by *nab1*, *nab2*, *nab3* and *nab4* from YJ016 and CMCP6. Phylogenetic analysis was performed on Nab1 and Nab2 from 21 strains encompassing 12 species. The *nab1* gene alleles from two of the 3 *nab* clusters in *A. salmonicida* are pseudogenes and were not included in the analysis of Nab1 proteins. Complete protein sequences were aligned using ClustalW 2.0 or MUSCLE V3.8, and the alignment was manually checked using GENEDOC for invariant and conserved regions (Edgar, 2004; Larkin et al., 2007). We used Neighbor Joining (NJ), as implemented in MEGA 4 (Guindon and Gascuel, 2003; Guindon et al., 2005; Tamura et al., 2007). The Bootstrap values for NJ trees were obtained after 1000 generations and MEGA 4 tree viewer was used to visualize the trees and calculate confidence values (Huson, 1998; Tamura et al., 2007).

Nucleotide sequence accession numbers.

The 16S rRNA gene sequence accession numbers used to construct *Vibrio* phylogeny were as follows: *Vibrio cholerae* CECT 514, X76337; *Vibrio furnissii* ATCC 35016, X76336; *Vibrio fluvialis* NCTC 11327, X76335; *Vibrio brasiliensis* LMG 20546, AJ316172; *Vibrio mimicus* ATCC 33653T, X74713; *Vibrio metschnikovii* CIP69.14T, X74711; *V. vulnificus* ATCC 27562, X76333; *Vibrio*

alginolyticus ATCC 17749, X56576; *Vibrio splendidus* LMG 4042, AJ515230; *Vibrio parahaemolyticus* ATCC 17802, AF388386; *Vibrio harveyi* NCIMB1280T, AY750575; *Vibrio tubiashii* ATCC 19109, X74725; *Vibrio orientalis* ATCC 33934T, X74719; *Vibrio sinaloensis* CAIM 797, DQ451211; *Vibrio rotiferatus* LMG 21460, AJ316187; *Vibrio navarrensis*, X74715; *Vibrio sp.* AND4, AF025960; *Vibrio sp.* EX25, CP001805; *Vibrio coralliilyticus* LMG 20984, AJ440005; *Vibrio shiloni* AK1, AF007115.1; *Listonella anguillarum*, AM235737; *Photobacterium damsela* ATCC 33539, AB032015; *Photobacterium angustum* ATCC 25915, D25307; *Photobacterium profundum* DSJ4, D21226; *Grimontia hollisae* LMG 17719, AJ514909; *Aliivibrio fischeri* ATCC 774T, X74702; *Aliivibrio salmonicida* NCMB 2262, X70643; *Vibrio ordalii* ATCC 33509T, X74718; *Shewanella benthica* ATCC 43992, X82131. PCR primers for *V. vulnificus* YJ016 and CMCP6 *nab1* and *nab2* were designed using accession numbers VV0316 (NP_933109.1), VV0312 (NP_933105.1), VV1_0803 (NP_759780.1), and VV1_0808 (NP_759785.1) respectively. The accession numbers for the other *Vibrio nab* genes used, including those used for BLAST analysis and tree construction, are as follows. The *nab1* accession numbers for *V. vulnificus* (2 strains), *Vibrio sp.* EX25, *V. parahaemolyticus*, *V. salmonicida*, *V. fischeri*, *Photobacterium profundum* (2 strains), *V. harveyi*, *V. splendidus*, *V. coralliilyticus*, *V. shilonii*, *V. mimicus*, and *Grimontia hollisae* are NP_759780.1, NP_933109.1, ZP_04922879.1, NP_796582.1, YP_002264336.1, YP_203530.1, YP_002154944.1, ZP_01218688.1, YP_130889.1, ZP_00989910.1, YP_001443906.1, ZP_01867489.1, ZP_06040339.1, ZP_06054134.1, and ZP_06053975.1. The *nab2* accession numbers for *V. vulnificus* (2 strains), *Vibrio sp.* EX25, *V. parahaemolyticus*, *V. salmonicida*, *V. fischeri*, *P. profundum* (2 strains), *V.*

harveyi, *V. splendidus*, *V. coralliilyticus*, *V. shilonii*, *V. mimicus*, and *G. hollisae* are NP_759785.1, NP_933105.1, ZP_04922882.1, NP_796579.1, YP_002261714.1, YP_002261791.1, YP_002264335.1, YP_203526.1, YP_002154946.1, ZP_01218684.1, YP_130887.1, YP_001443899.1, ZP_00989905.1, ZP_05888524.1, ZP_01867488.1, ZP_06040343.1, ZP_06054132.1, and ZP_06053977.1.

Release of NulOs by mild acid hydrolysis.

NulO sugars were released from extensively washed culture pellets with mild acid hydrolysis using 2N acetic acid for 3 hours at 80 °C as previously described (Lewis et al., 2004) Supernatants were filtered over 10K molecular weight cutoff centrifugal filtration cassettes (Centricon). The low molecular weight fraction was then lyophilized and stored at -20 °C for use in thiobarbitic acid (TBA), 1,2-Diamino-4,5-methylene dioxybenzene high performance liquid chromatography (DMB-HPLC), or mass spectrometric analyses as described below.

Thiobarbitic acid assays.

The thiobarbitic acid (TBA) assay is relatively simple, fast, and inexpensive, and has been used extensively for studies of nonulosonic acids such as *N*-acetylneuraminic acid. Potential NulOs released from vibrios (see above) were treated for 30 min at 37 °C with 0.1N sodium hydroxide (final concentration) followed by neutralization as previously described (Higa et al., 1989) Measurement of thiobarbitic acid reactive species (TBARs) was performed on this material as previously described (Warren, 1959) Group B and Group A Streptococci were used as positive and negative controls respectively; the former displays high levels of surface

sialic acids, while the latter does not. A standard curve for TBARs was generated in each experiment using *N*-acetylneuraminic acid (Sigma). Results were normalized to total protein content from bacterial culture pellet lysates that were set aside prior to NulO hydrolysis. Protein content was measured using the bicinchoninic assay (Pierce).

DMB derivatization and high performance liquid chromatography.

NulOs released by mild acid hydrolysis were derivatized with 1, 2-diamino-4, 5-methylene dioxybenzene (DMB). Reactions consisted of 7mM DMB, 18mM sodium hydrosulfite, 1.4M acetic acid, and 0.7M 2-mercaptoethanol and were carried out for 2 hours at 50 °C in the dark. DMB-NulO derivatives were resolved by HPLC using a reverse phase C18 column (Varian) eluted isocratically at a rate of 0.9ml/min over 50 minutes using 85% MQ-water, 7% methanol, 8% acetonitrile as previously described (Lewis et al., 2004; Lewis et al., 2009) Detection of fluorescently labeled NulO sugars was achieved at excitation and emission wavelengths of 373nm and 448nm respectively. 3-Deoxy-D-manno- octulosonic acid (Kdo) is an eight-carbon backbone α -keto acid that forms part of the conserved core portion of lipopolysaccharide in virtually all Gram negative bacteria. Kdo was released and derivatized under the same conditions as the related nonulosonic acid α -keto acids and served as an internal control in these assays to express relative levels of NulOs. The Mann Whitney nonparametric test was used for statistical evaluation of differences between NulO/Kdo ratio between strains.

Electrospray mass spectrometry.

DMB-derivatized extracts or individually isolated HPLC peaks were analyzed at the University of California San Diego Glycotechnology core resource, using a ThermoFinnigan LC-Q ion-trap mass spectrometer with tandem HPLC.

Results

Frequency of *nab* gene clusters in Vibrionaceae.

As of September 2010, there were 24 species and 66 strains of the family Vibrionaceae in the genome database (www.ncbi.nlm.nih.gov/genomes/lproks.cgi). This includes 27 strains of *V. cholerae*, four strains from the closely related species *V. mimicus*, seven *V. parahaemolyticus* genome sequences, and 21 additional species with either two or a single genome represented. Nonulosonic acid (NulO) biosynthetic (NAB) pathways are encoded by *nab* gene clusters, which share a common core portion comprised of *nab1*, a homolog of CMP-*N*-acetylneuraminic acid synthetase, *nab2*, a homolog of *N*-acetylneuraminic acid synthase, and *nab3*, a homolog of UDP-*N*-acetylglucosamine 2-epimerase. Many of these sequenced *Vibrio* species encoded a putative NAB pathway. BLAST analysis of *nab* genes identified 12 species and a total of 21 strains encoding *nab* gene clusters; *V. vulnificus* (2 strains), *V. parahaemolyticus* (6), *V. mimicus* (1), *V. harveyi* (2), *V. shilonii* (1), *V. splendidus* (1), *V. coralliilyticus* (1), *V. fischeri* (2), *V. salmonicida* (1), *Vibrio sp. EX25* (1), *Photobacterium profundum* (2), and *Grimontia hollisae* (1) (**Fig. 11**). However, about 50% (13/27) of fully sequenced Vibrionaceae species isolates did *not* encode homologous pathways for NulO biosynthesis (**Fig. 12**).

Evolution of NulO biosynthesis in Vibrionaceae.

Analysis of the distribution and arrangement of *nab* gene clusters among Vibrionaceae lineages reveals a complex evolutionary history. Within many lineages, there is a conspicuous presence or absence of homologous NAB pathways with some notable exceptions. For example, among the seven *V. parahaemolyticus* strains examined, only strain AN-5034 lacked the *nab* cluster and *nab* genes from 5/6 other strains shared 100% amino acid sequence identity. *V. parahaemolyticus* strain 16 shared only 90% amino acid identity with *nab* genes from the other strains. Among the 27 *V. cholerae* genomes, none encoded *nab* genes. Yet, within sequenced isolates of *V. mimicus*, a species closely related to *V. cholerae*, 1 of the 4 sequenced strains (MB451) contained a *nab* region with divergent gene order compared to related species (**Fig. 11**).

For other vibrios, phylogenetic analysis of Nab amino acid sequences revealed that members of the same species sometimes encode NAB pathways that are highly divergent from each other. One of the clearest examples of phylogenetic divergence involved the two sequenced strains of *V. vulnificus* (YJ016 and CMCP6), both clinical biotype 1 strains from Asia (Chen et al., 2003a). The *nab* gene cluster within *V. vulnificus* YJ016 encompasses ORFs VV0311 to VV0316 on chromosome 1. In strain CMCP6, the NAB cluster encompasses ORFs VV1_0803 to VV1_0808 and is also encoded on chromosome 1 (**Fig. 11**). Both Nab1 and Nab2 from CMCP6 and YJ016 are found on two divergent lineages (a and b in **Fig. 13A** and **13B**). Nab2 from YJ016 is closely related to Nab2 from *V. fischeri* ES114 and *P. profundum* 3TCK whereas Nab2 from CMCP6 is closely related to Nab1 from *V. splendidus* and *V. harveyi* (a and b in **Fig. 13B**).

Representative members of other species, (*A. salmonicida* and *G. hollisae*), encode multiple paralogous *nab* gene clusters within the same genome. In *A. salmonicida*, open reading frames (ORFs) VSAL_I0164 to VSAL_I0172 are duplicated at position VSAL_I0250 to VSAL_I0259 but on the negative strand and the *nab1* gene is a pseudogene. A third copy of the *nab* cluster is found in this species at ORFs VSAL_I3009 to VSAL_I3013 but the region shares low sequence similarity with the other two clusters and has a unique gene arrangement (**Fig. 11**). Flanking all three *nab* regions in *A. salmonicida* is a transposase. In the *G. hollisae* genome, two copies of the *nab* region are present but the regions share less than 65% amino acid identity, ORFs VHA_003148 to VHA_003151 and VHA_003308 to VHA_003011, however, the gene order is identical. Taken together, these observations suggest that *nab* gene clusters in Vibrionaceae are prone to duplication, divergence, and horizontal transfer.

Gene cluster organization matches phylogenetic signatures of Nab1 and Nab2 in Vibrionaceae.

Initial observations of the *nab* gene clusters in sequenced strains of Vibrionaceae and other γ - Proteobacteria suggested that there are at least three divergent *nab* gene alleles encoded within different gene cluster arrangements (**Fig. 11**). To examine this more carefully, selected *nab* gene clusters were aligned (**Fig. 13C**) and compared to phylogenetic branching patterns of Nab1 (**Fig. 13A**) and Nab2 (**Fig. 13B**) amino acid sequences. There was a strong correlation between *nab* gene cluster arrangement and phylogenetic lineage of Nab1 and Nab2 amino acid sequences (**Fig. 13 'a'&'b'**). These data also revealed examples of apparent recombination between the different *nab* alleles. For example, while most of the Vibrionaceae

encoded *nab1* and *nab2* alleles that both cluster in phylogenetic clade 'a', or both in phylogenetic clade 'b', the *Vibrio sp.* Ex25 strain encoded *nab1* and *nab2* alleles that clustered in different phylogenetic clades (b and a respectively) (**Fig. 13**).

Biochemical analyses of Vibrionaceae isolates confirm that many species express NulOs.

To determine whether NAB pathways are functional in Vibrionaceae, analytical approaches were applied to investigate the potential production of NulOs in different lineages. Initially, Vibrionaceae isolates (28 strains representing 14 species) were subjected to the classic thiobarbitic acid (TBA) assay, a method originally used to evaluate the distribution and levels of sialic acids expressed by different animal lineages (Warren, 1963) Indeed, many of the vibrios expressed thiobarbitic acid reactive species (TBARs) when grown under standard culture conditions (**Fig. 14A**). However, as suggested by genomic observations of *nab* gene clusters in sequenced vibrios, many of the Vibrionaceae isolates did not show TBARs above levels observed in negative controls. The method of thiobarbitic acid reactivity has some limitations, including the potential for interfering molecular species that may confound interpretation of the results (Warren, 1959). To further characterize potential NulO expression, selected isolates were analyzed using a method of derivatization that relies specifically on the α -keto acid shared by all types of nonulosonic acids. Briefly, mild acid hydrolysates of selected *Vibrio* isolates were subjected to derivatization (fluorescence tagging) of NulOs with DMB (1, 2- diamino-4, 5-methylene dioxybenzene). Molecular species of DMB-NulOs were then resolved by high performance liquid chromatography (HPLC). Chromatograms revealed multiple peaks of DMB-derivatized molecules in several *Vibrio* isolates (**Fig. 14B**).

Further verification that HPLC peaks of DMB-derivatized molecules correspond to masses characteristic of NulOs was achieved by mass spectrometry (**Fig. 15**). These experiments show several retention times of DMB-derivatized molecules that correspond to masses of di-*N*-acetylated nonulosonic acids (*m/z* 450-451) (Lewis et al., 2009) Due to the multiple epimers and modifications of NulOs that can occur naturally (Knirel et al., 2003) identical masses found within many of the HPLC peaks could not be assigned unambiguously to specific chemical structures. However, it is clear from these studies that a variety of di-*N*-acetylated nonulosonic acids are produced by multiple strains of *V. parahaemolyticus*, *V. fischeri*, and *V. vulnificus*. Taken together, these experiments conclusively show that many Vibrionaceae encode functional NAB pathways.

Distribution of nab alleles among diverse *V. vulnificus* isolates.

To more clearly define potential associations between the different *nab* alleles and bacterial phylogenetic lineages, a more directed approach within a single species was utilized. *Vibrio vulnificus* was chosen for these studies due to the phylogenetically divergent *nab* gene clusters encoded in the two available reference genome strains (YJ016 and CMCP6) (**Fig. 13** and **Fig. 16**). Allele typing of *nab1* and *nab2* was performed on a collection of 67 *V. vulnificus* strains whose phylogenetic relationships are known, using a set of primer pairs for *nab1* and *nab2* alleles designed using genomic sequences from reference strains YJ016 and CMCP6 (alleles hereafter referred to as YJ-like and CM-like, **Table 4**). Four PCR assays were performed (**Table 5**) using genomic DNA isolated from the 67 *V. vulnificus* strains (**Table 4**), 40 of which were from environmental sources and 27 from clinical sources. We then

mapped the presence of YJ-like or CM-like *nab1* and/or *nab2* alleles onto the *V. vulnificus* phylogenetic tree (Cohen et al., 2007a) (**Fig. 16**).

PCR assays were negative for thirteen of the 67 isolates examined, including biotype 3 isolates, suggesting these strains may either lack the genes or contain unique untypeable *nab* genes (**Fig. 16**). YJ-like alleles of *nab1* and *nab2* were identified in 26 strains, while 16 strains encoded CM- like alleles of both genes. Among the lineage I isolates, which are mostly from clinical sources, both YJ-like and CM-like alleles of *nab1* and *nab2* were present. However, among the lineage II isolates, which are predominantly environmental and fish isolates, the YJ-like allele was by far the most common (**Fig. 16**). Interestingly, two *V. vulnificus* isolates encoded a CM-like *nab1* allele with a YJ- like *nab2* allele (**Fig. 16**). Taken together with data presented in **Fig. 13**, these observations further support the conclusion that members of the Vibrionaceae sometimes engage in horizontal exchange and recombination of different *nab* gene cluster alleles.

NulOs are expressed at higher levels in lineage I clinical isolates with CMCP6-like alleles.

We hypothesized that allelic differences in *nab* genes may predict functional differences in the level of NulO production by isolates of *V. vulnificus*. To test this hypothesis, we subjected isolates of *V. vulnificus*, representing all three lineages, and two *nab* allele types to DMB-HPLC analysis. The structurally related 8-carbon α -keto acid known as Kdo served as a convenient internal standard for normalization of NulO expression, since it is present as part of the conserved core structure of lipopolysaccharide in Gram negative bacteria and also reacts with DMB. Relative NulO production was determined for the different isolates, by comparing HPLC peak

areas at characteristic retention times of NulO and Kdo in *V. vulnificus* as described in the materials and methods (**Fig. 17A**). Relative NulO levels were compared among lineage I and lineage II isolates (**Fig. 17B**) and among isolates having YJ-like and CM-like *nab1* and *nab2* alleles (**Fig. 17C**). These data show that NulO expression levels are much higher in isolates that encode CM-like *nab* alleles (**Fig. 17C**), and that these strains tend to belong to *V. vulnificus* phylogenetic lineage I (mostly clinical isolates) (**Fig. 17B**). Alternatively, isolates that encoded YJ-like *nab* alleles expressed much lower levels of NulOs. Nearly all of the lineage II (mostly environmental) isolates encoded YJ-like *nab* alleles and had low levels of NulOs (**Fig. 17C**). Interestingly, the data also show that most of the isolates that were "untypeable" by these methods did in fact express NulOs at levels that were significantly higher than strains with YJ-like *nab* genes, but significantly lower than strains with CM-like *nab* genes. Taken together, these data strongly suggest that there are at least 3 alleles of *nab* genes that correspond to low (YJ-like), intermediate (untypeable), or high (CM-like) levels of NulO expression.

Discussion

These studies illustrate processes of evolution within the family Vibrionaceae by analysis of genetic and phenotypic patterns related to the nine carbon backbone α -keto acid sugars (NulOs). We show that biosynthetic pathways for NulOs are widespread in Vibrionaceae, but by no means universal (Figs. 7 & 8). The distribution and phylogeny of *nab* pathways in *Vibrio* suggests that some lineages or strains have lost, while others have apparently duplicated these gene clusters (Figs. 7 & 8 and text). Multiple biochemical approaches confirm that NAB pathways are indeed active in a variety of *Vibrio* isolates (Figs. 10 & 11) and can participate in the biosynthesis of

multiple structural variations of NulOs within a given strain (**Fig. 15A**). Genomic comparisons revealed multiple allele types of NAB pathways reflected by similar patterns of gene arrangement and phylogeny (**Fig. 13**), and which correspond to functional differences in NulO expression levels (**Fig. 17**). In particular, clinical isolates of the CMCP6-like allele expressed on average, nearly 100-fold higher levels of NulOs compared to environmental isolates with the YJ016 allele. Moreover, the data show several examples of apparent recombination between *nab* gene cluster alleles (**Fig. 13** and **Fig. 16**). Taken together, these studies indicate a relatively plastic state of NAB pathway evolution in Vibrionaceae. These observations highlight the family Vibrionaceae and the species *Vibrio vulnificus* as interesting models for investigations of the biological functions of NulOs.

During the completion of this study, the genome sequence of a third *V. vulnificus* strain MO6- 24/O, a clinical isolate from the USA, became available. We found that strain MO6-24/O contains a NAB cluster identical to CMCP6 and produces high levels of NulOs confirming our genomic predictions (Figs. 12 & 13). Lastly, our data also strongly suggest the presence of a third (and possibly more) NAB cluster type that is present among *V. vulnificus* natural isolates. We identified a total of 13 strains that were untypeable by our PCR method, however our analysis on NulO levels demonstrates that these strains produce intermediate levels of NulO indicating the presence of *nab* genes unrelated to YJ016 or CMCP6. Given the limited number of *V. vulnificus* isolates that we examined it is tempting to speculate that there may be even more heterogeneity in *nab* gene content within this species and the challenge going forward will be to determine the functional role of this diversity in survival and fitness. Nonulosonic acids

(NulOs) are generally expressed on the surfaces of cells - in both 'higher' animals and on bacteria. Vibrionaceae species likely express NulOs as part of one or more surface structures such as capsular polysaccharides, lipopolysaccharides, or flagella (Li et al.,; Perepelov et al.,; Gil-Serrano et al., 1999; Logan et al., 2002; Schirm et al., 2003; Le Quere et al., 2006; McNally et al., 2006; McNally et al., 2007; Shashkov et al., 2007; Logan et al., 2009). For example, strains of *Campylobacter jejuni* can simultaneously express pseudaminic and legionaminic acids as flagellar modifications and sialic acids as lipopolysaccharide modifications (Linton et al., 2000; Logan et al., 2009). It is possible that different NAB alleles in Vibrionaceae encode slightly different NulO structures, and/or that NulO sugars may be intended for different surface molecules (i.e. capsule, LPS, flagella). Alternatively, the different NAB alleles in *V. vulnificus* could be responsible for NulO modifications at different densities on the same molecule. *Vibrio* NulOs may be involved in motility, biofilm formation, relative phage susceptibility, or other phenotypes relevant to the marine ecosystem niche. In addition, *Vibrio* NulOs may have functional implications during opportunistic pathogenesis of aquatic or terrestrial animals.

In summary, the further study of NulO biology in Vibrionaceae will require careful analysis of the genetics and biochemistry of cell surface NulO modifications. Taken together with the many known roles of NulOs in host-microbe interactions, these studies provide a basis for further investigations of NulOs in bacterial behaviors and host-pathogen interactions involving the Vibrionaceae.

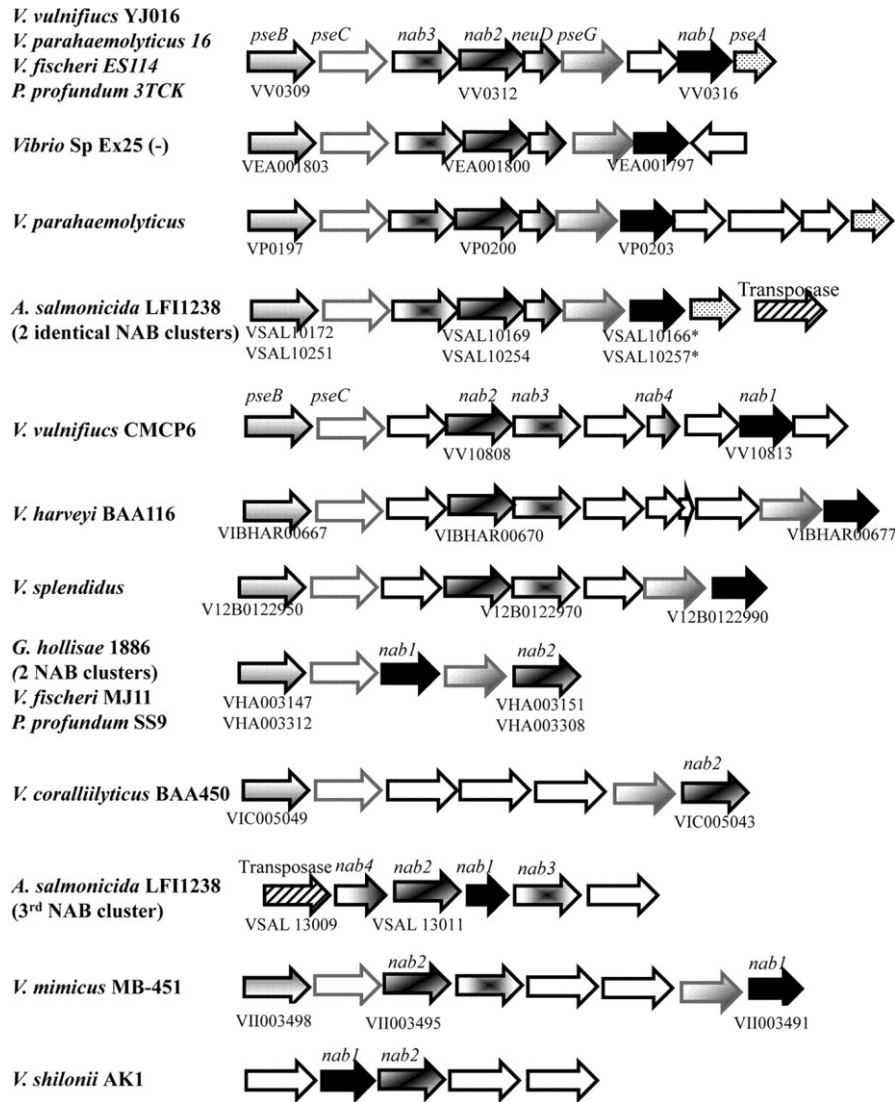


Figure 11 **Genetic structure of the nab gene cluster among sequenced Vibrionaceae species.** Shown is a schematic representation of the gene arrangement of NAB clusters among sequenced isolates of members of the family Vibrionaceae. The annotated homologs of the ORFs are *nab1* (CMP-NeuAc synthase homolog), *nab2* (*N*-acetylneuraminic acid synthase homolog), *nab3* (UDP-*N*-acetylglucosamine 2 epimerase homolog), *neuD* (acetyltransferase homolog), *pseA* (flagellin modification protein homolog), *pseB* (polysaccharide biosynthesis homolog), *pseC* (DegT aminotransferase homolog), and *pseG* (nucleotidyl/sugar P transferase homolog). Strains with identical gene orders are shown only once with isolate names listed on the left. Accession numbers for *nab* genes are shown below schematic ORFs.

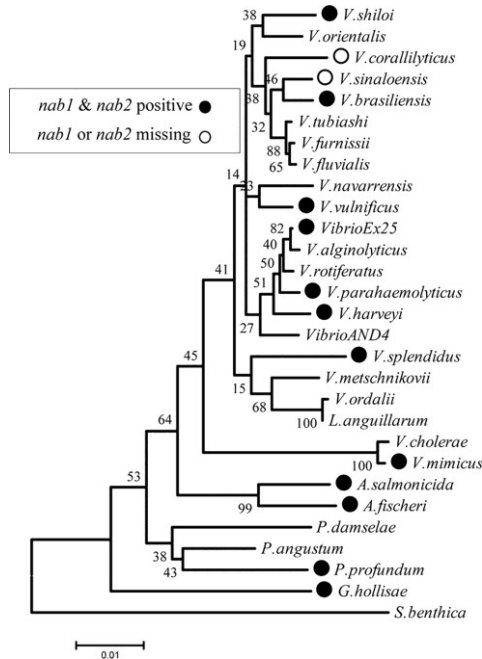


Figure 12 **Distribution of nab genes among sequenced members of the family Vibrionaceae.** A phylogenetic tree of completely sequenced members of the family Vibrionaceae based on 16S rRNA sequences was constructed. Evolutionary history was inferred by the NJ method. The bootstrap consensus tree inferred from 500 replicates. Branches corresponding to partitions reproduced in less than 50% bootstrap replicates are collapsed. The evolutionary distances were computed using the Kimura 2-parameter method and are expressed as the number of base substitutions per site. All positions containing gaps and missing data were eliminated from the data set (complete deletion option). There were a total of 1,191 positions in the final data set. *Shewanella benthica* 16S rRNA served as the outgroup. Strains that contain *nab* genes are indicated by circles on the right.

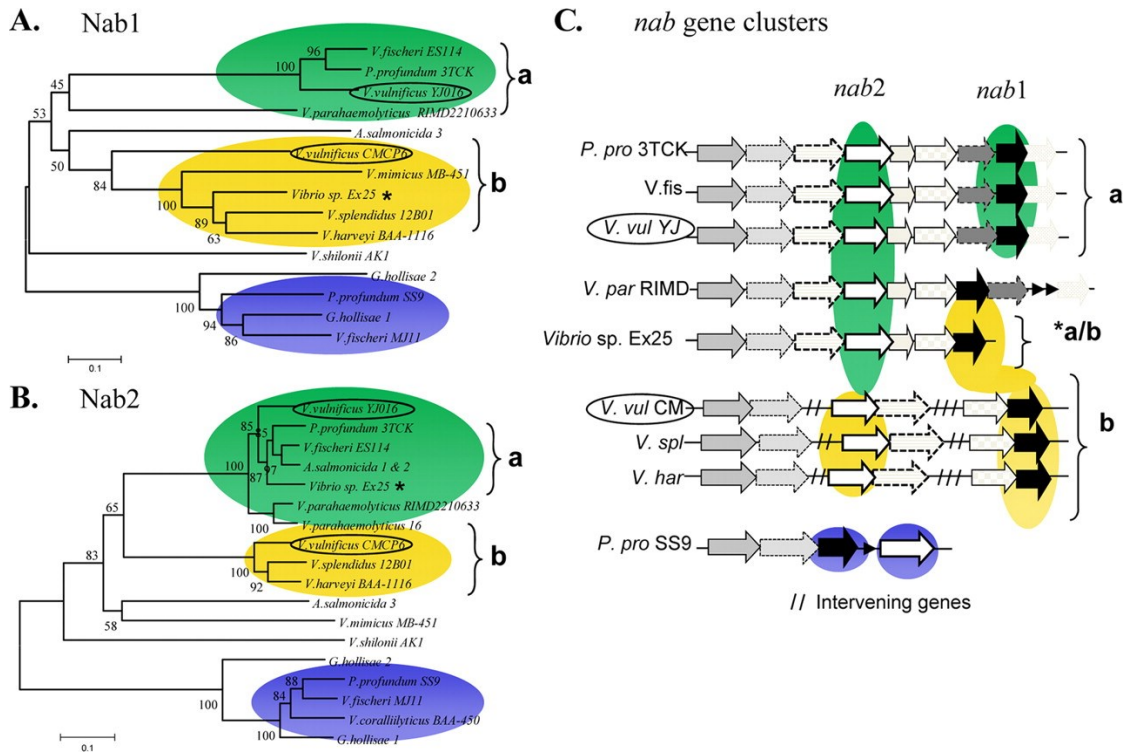


Figure 13 **Correlation of phylogenetic branching patterns and analysis of Nab1 and Nab2 among Vibrionaceae species.** Evolutionary relationships of Nab1 (A) and Nab2 (B) amino acid sequences from 12 species of the family Vibrionaceae was inferred by the NJ method. The bootstrap consensus tree inferred from 500 replicates. Evolutionary distances were computed using the Poisson correction method and are expressed as the number of amino acid substitutions per site. All positions containing alignment gaps and missing data were eliminated only in pairwise sequence comparisons (pairwise deletion option). There were a total of 432 positions in the final data set. The lowercase letters a and b refer to similar phylogenetic clades and gene cluster arrangements shown in green and yellow, respectively. Asterisks highlight *Vibrio sp. EX25*, which exhibits evidence of recombination between the a and b gene cluster alleles. See Fig. 1 for a complete description of gene identifiers and accession numbers.

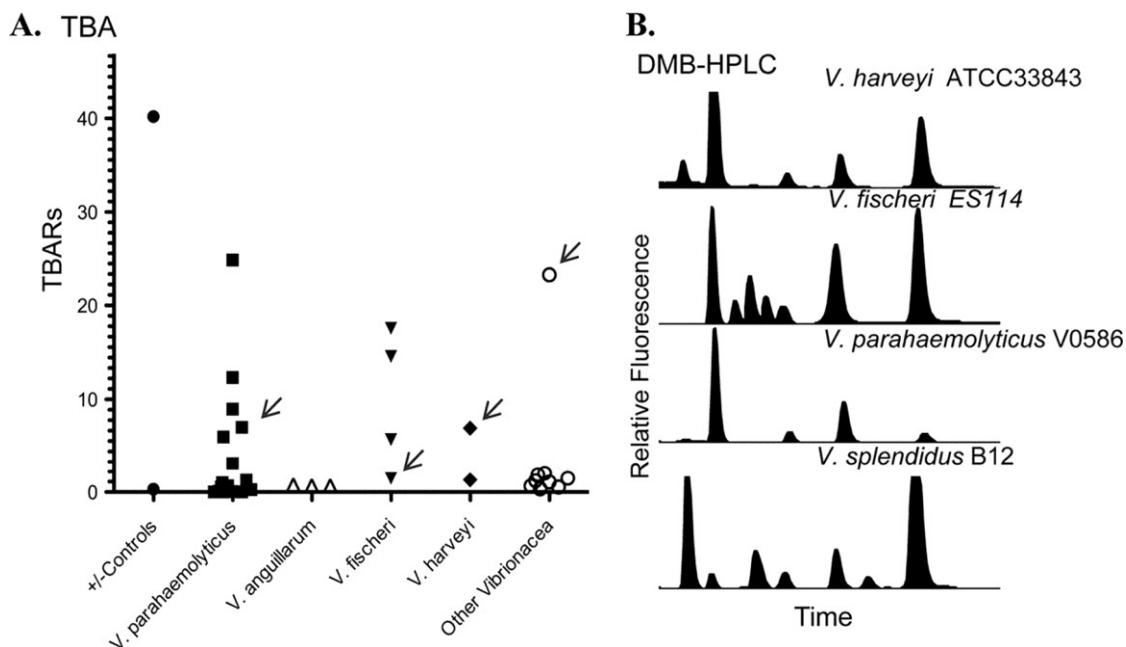


Figure 14 **Analysis of putative NulOs in Vibrionaceae.** (A) A TBA assay of *Vibrio* strains listed in Table 1 was carried out as described in Materials and Methods. Results were normalized to total protein content and expressed as TBARS. Controls gave the expected results and included *Streptococcus agalactiae* (group B), which is known to express sialic acids, and *Streptococcus pyogenes* (group A), which does not express sialic acids (+ and –, respectively). (B) Putative NulOs released from selected strains (indicated by arrows in panel A) were fluorescently derivatized with DMB as described in Materials and Methods. DMB-derivatized α -keto acids were then resolved by HPLC with reverse-phase separation.

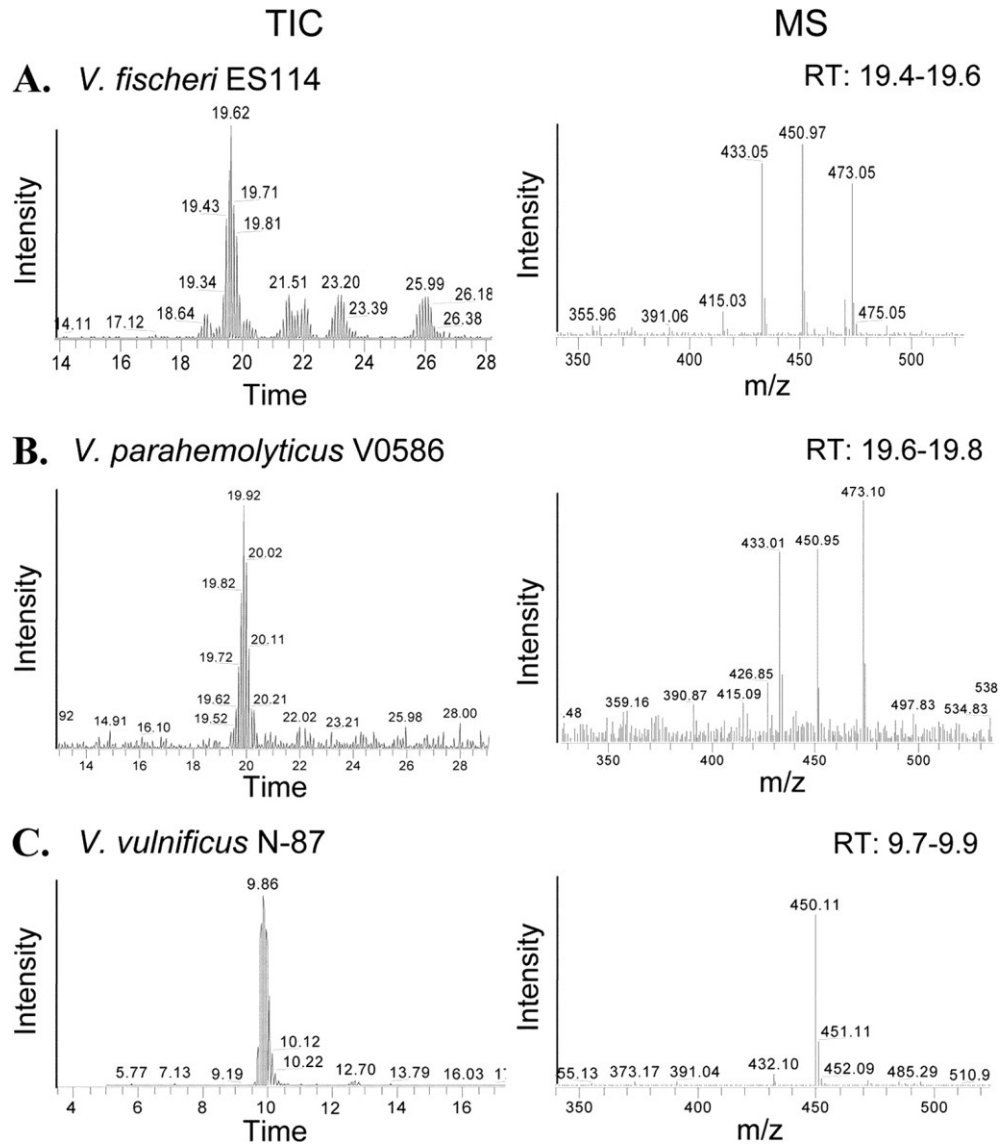


Figure 15 **Mass spectrometry reveals masses of DMB-derivatized di-N-acetylated NulOs in Vibrionaceae.** *V. fischeri* (ES114*) (A), *V. parahaemolyticus* (518-01 and V0586*) (B), and *V. vulnificus* (CDC903896, N-87*, MLT362, MO6-24/O, and SS108A3A) (C) were subjected to electrospray ionization mass spectrometry performed in tandem with HPLC separation of DMB-NulOs. Asterisks indicate data representative of the strains tested. The total ion currents (TIC) of selected m/z 450 to 451 during HPLC elution are shown on the left, while mass spectra are shown on the right along with the retention times (RT).

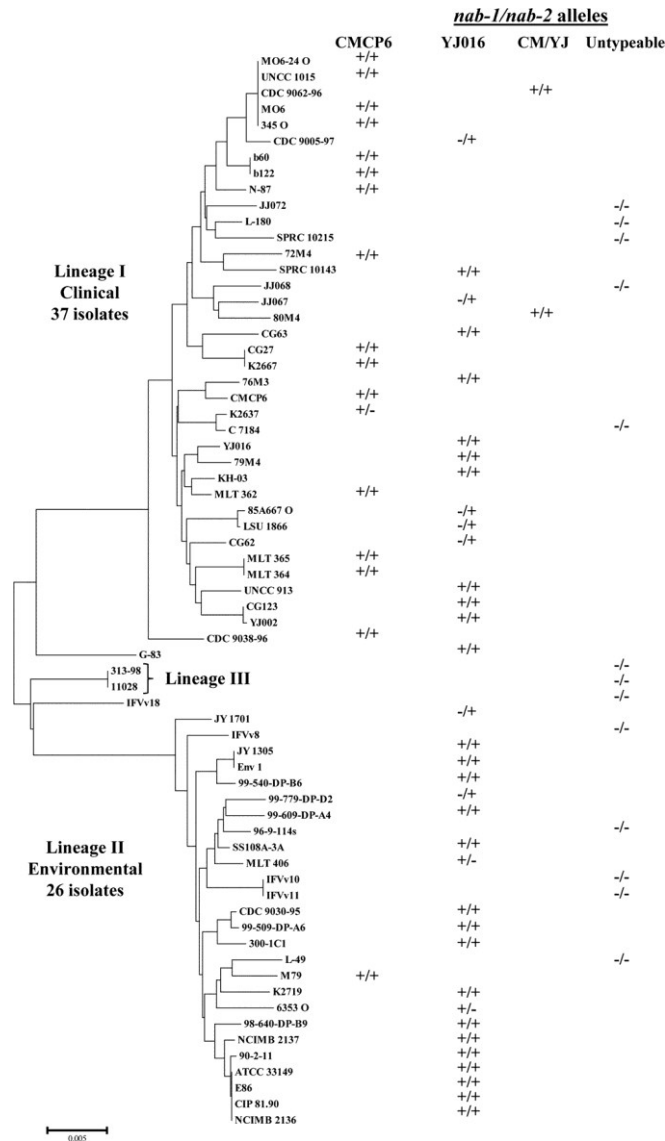


Figure 16 **Distribution of *nab1* and *nab2* allele types among *V. vulnificus*.** PCR diagnosis of *nab* alleles was carried out using genomic DNA template from 67 strains of *V. vulnificus* and primers specific to the *nab1* and *nab2* alleles from reference strains YJ016 and CMCP6. If only one gene allele was positive, a minus sign was used to indicate a negative PCR result for the other allele. Strains that were negative in all PCR assays are indicated as “untypeable” here (-/-), since biochemical investigations revealed that they do, in fact, express NulOs (see Fig. 11). The phylogenetic tree of *V. vulnificus* is based on a phylogenetic analysis of six housekeeping genes as previously described.

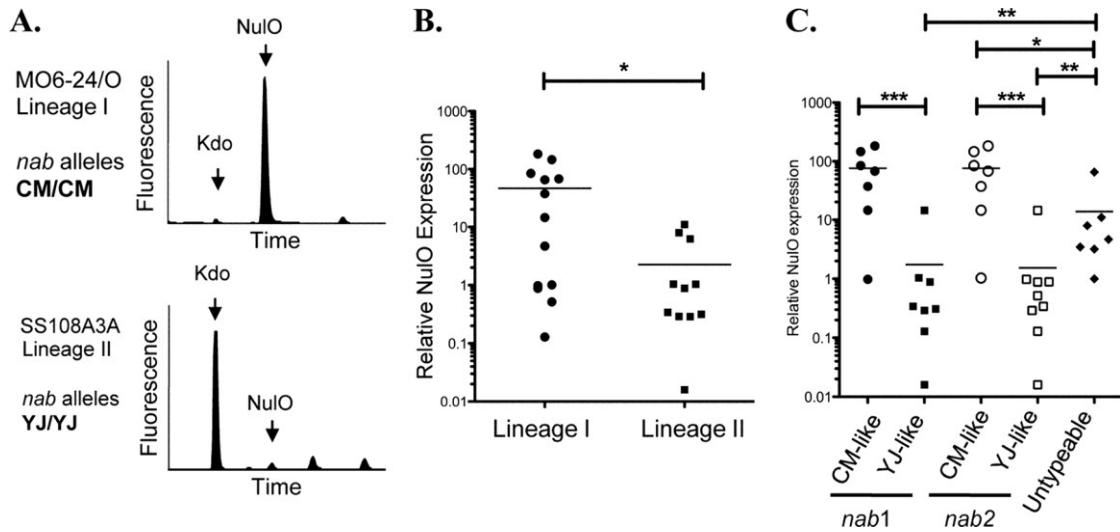


Figure 17 **CMCP6-like *nab* alleles are associated with high levels of NulO expression in mostly clinical strains.** DMB HPLC analysis of diverse *V. vulnificus* isolates was carried out, and NulO expression levels were normalized to an internal control monosaccharide (Kdo) that is a part of the conserved core portion of LPS. (A) Raw HPLC data from strains representing the major *V. vulnificus* lineages (I and II) and common *nab* allele types (CMCP6 and YJ016). (B) Relative NulO expression levels in lineage I and II strains. (C) *V. vulnificus* isolates with CM-like alleles of *nab* genes have significantly higher levels of NulOs than isolates with YJ-like alleles. Most of the “untypeable” isolates do, in fact, express detectable NulOs but at levels that are intermediate compared to those of isolates with YJ-like or CM-like alleles. (B and C) The Mann-Whitney test was used for statistical evaluation (*, $P < 0.05$; **, $P < 0.01$; ***, $P < 0.0001$). Note the log scales.

Table 3 Species and strains examined in this study

| Species | Isolate name |
|--------------------------------|--------------|
| <i>Listonella anguillarum</i> | B559 |
| <i>Listonella anguillarum</i> | B561 |
| <i>Listonella anguillarum</i> | B563 |
| <i>Vibrio angustum</i> | B70 |
| <i>Vibrio fischeri</i> | ATCC 33983 |
| <i>Vibrio fischeri</i> | 394 |
| <i>Vibrio fischeri</i> | 63 |
| <i>Vibrio fischeri</i> | ES114 |
| <i>Vibrio harveyi</i> | ATCC 33843 |
| <i>Vibrio harveyi</i> | L222 |
| <i>Vibrio logei</i> | B583 |
| <i>Vibrio ordalii</i> | B572 |
| <i>Vibrio orientalis</i> | B717 |
| <i>Vibrio pelagius</i> | B98 |
| <i>Vibrio splendidus</i> | B12 |
| <i>Vibrio parahaemolyticus</i> | 428/01 |
| <i>Vibrio parahaemolyticus</i> | 30824 |
| <i>Vibrio parahaemolyticus</i> | 9808/1 |
| <i>Vibrio parahaemolyticus</i> | UCMA178 |
| <i>Vibrio parahaemolyticus</i> | 090-96 |
| <i>Vibrio parahaemolyticus</i> | 906-97 |
| <i>Vibrio parahaemolyticus</i> | 190-2004 |
| <i>Vibrio parahaemolyticus</i> | 155-05 |
| <i>Vibrio parahaemolyticus</i> | 357-99 |
| <i>Vibrio parahaemolyticus</i> | 518-01 |
| <i>Vibrio parahaemolyticus</i> | VP81 |
| <i>Vibrio parahaemolyticus</i> | Vphy191 |
| <i>Vibrio parahaemolyticus</i> | V0441 |
| <i>Vibrio parahaemolyticus</i> | V0586 |

Table 4 *V. vulnificus* strains used in this study and their *nab* alleles

| Strain name | <i>nab1</i> allele | <i>nab2</i> allele | Place of isolation | Source | Yr of isolation |
|--------------|--------------------|--------------------|--------------------|----------|-----------------|
| YJ002 | YJ016-like | YJ016-like | Taiwan | Clinical | 1993 |
| JJ068 | | | Taiwan | Clinical | 1993 |
| JJ072 | | | Taiwan | Clinical | 1993 |
| JJ067 | | YJ016-like | Taiwan | Clinical | 1993 |
| YJ016 | YJ016-like | YJ016-like | Taiwan | Clinical | 1993 |
| L-180 | | | Japan | Clinical | 1980 |
| N-87 | CMCP6-like | CMCP6-like | Japan | Clinical | 1987 |
| KH-03 | YJ016-like | YJ016-like | Japan | Clinical | 2003 |
| SPRC 10143 | YJ016-like | YJ016-like | NK ^a | Clinical | NK |
| CMCP6 | CMCP6-like | CMCP6-like | Korea | Clinical | NK |
| CDC 9038-96 | CMCP6-like | CMCP6-like | Texas | Clinical | 1996 |
| CDC 9062-96 | CMCP6-like | YJ016-like | Louisiana | Clinical | 1996 |
| CDC 9005-97 | | YJ016-like | Louisiana | Clinical | 1997 |
| CDC 9030-95 | YJ016-like | YJ016-like | Florida | Clinical | 1995 |
| 313-98 | | | Israel | Clinical | 1998 |
| 11028 | | | Israel | Clinical | NK |
| CIP 81.90 | YJ016-like | YJ016-like | France | Clinical | 1980 |
| LSU 1866 | | YJ016-like | NK | Clinical | NK |
| M06 | CMCP6-like | CMCP6-like | United States | Clinical | NK |
| M06-24/O | CMCP6-like | CMCP6-like | California | Clinical | NK |
| 6353/O | YJ016-like | | Maryland | Clinical | NK |
| 85A667/O | | YJ016-like | California | Clinical | NK |
| K2637 | CMCP6-like | | Louisiana | Clinical | 2005 |
| K2667 | CMCP6-like | CMCP6-like | Louisiana | Clinical | 2005 |
| K2719 | YJ016-like | YJ016-like | Louisiana | Clinical | 2005 |
| C-7184 | | | United States | Clinical | NK |
| IFVv8 | | | Florida | Clinical | NK |
| CG27 | CMCP6-like | CMCP6-like | Taiwan | Oyster | 1993 |
| 98-640 DP-B9 | YJ016-like | YJ016-like | Louisiana | Oyster | 1998 |
| 99-609 DP-A4 | YJ016-like | YJ016-like | Oregon | Oyster | 1999 |

Table 4 continued

| Strain name | <i>nab1</i> allele | <i>nab2</i> allele | Place of isolation | Source | Yr of isolation |
|--------------|--------------------|--------------------|--------------------|--------|-----------------|
| 99-779 DP-D2 | | YJ016-like | Louisiana | Oyster | 1999 |
| 99-509 DP-A6 | YJ016-like | YJ016-like | Texas | Oyster | 1999 |
| 99-540 DP-B6 | YJ016-like | YJ016-like | Texas | Oyster | 1998 |
| 300-1C1 | YJ016-like | YJ016-like | NK | Oyster | NK |
| JY1701 | | YJ016-like | Louisiana | Oyster | NK |
| Env1 | YJ016-like | YJ016-like | Louisiana | Oyster | NK |
| SS108A-3A | YJ016-like | YJ016-like | NK | Oyster | NK |
| b60 | CMCP6-like | CMCP6-like | India | Oyster | NK |
| b122 | CMCP6-like | CMCP6-like | India | Oyster | NK |
| IFVv10 | | | France | Mussel | NK |
| IFVv11 | | | France | Mussel | NK |
| 72M4 | CMCP6-like | CMCP6-like | India | Clam | NK |
| 79M4 | YJ016-like | YJ016-like | India | Clam | NK |
| 76M3 | YJ016-like | YJ016-like | India | Fish | NK |
| 80M4 | CMCP6-like | YJ016-like | India | Fish | NK |
| G-83 | YJ016-like | YJ016-like | Korea | Fish | NK |
| NCIMB 2136 | YJ016-like | YJ016-like | Japan | Eel | NK |
| 90-2-11 | YJ016-like | YJ016-like | Norway | Eel | NK |
| ATCC 33149 | YJ016-like | YJ016-like | Japan | Eel | NK |
| NCIMB 2137 | YJ016-like | YJ016-like | Japan | Eel | NK |
| E86 | YJ016-like | YJ016-like | Spain | Eel | 1990 |
| M79 | CMCP6-like | CMCP6-like | Spain | Eel | NK |

Table 4 continued

| Strain name | <i>nab1</i> allele | <i>nab2</i> allele | Place of isolation | Source | Yr of isolation |
|-------------|--------------------|--------------------|--------------------|---------------|-----------------|
| IFVv18 | | | France | Seawater | NK |
| MLT362 | CMCP6-like | CMCP6-like | Hawaii | Seawater | 1991 |
| MLT364 | CMCP6-like | CMCP6-like | Hawaii | Seawater | 1991 |
| MLT406 | YJ016-like | | Florida | Seawater | 1991 |
| SPRC 10215 | | | NK | Seawater | NK |
| CG62 | | YJ016-like | Taiwan | Seawater | 1993 |
| CG63 | YJ016-like | YJ016-like | Taiwan | Seawater | 1993 |
| CG123 | YJ016-like | YJ016-like | Taiwan | Seawater | 1993 |
| 96-9-114s | | | Denmark | Sediment | NK |
| L-49 | | | Japan | Environmental | 1988 |
| JY1305 | YJ016-like | YJ016-like | Louisiana | Environmental | NK |
| UNCC 1015 | CMCP6-like | CMCP6-like | North Carolina | Environmental | NK |
| MLT 365 | CMCP6-like | CMCP6-like | Florida | Environmental | NK |
| UNCC 913 | YJ016-like | YJ016-like | North Carolina | Environmental | NK |
| 345/O | CMCP6-like | CMCP6-like | Louisiana | Environmental | NK |

- [↪](#) NK, not known.

Table 5 Primers used for PCR assays in this study

| Oligonucleotide name | Sequence (5'-3') | Product size (bp) | T _m (°C) |
|----------------------|-----------------------------------|-------------------|---------------------|
| VV0312F | CGA AGC ACT GGC GTT TAA A | | |
| VV0312R | GCT CGA GCA TCT CCC AAT ACT | 986 | 61 |
| VV0316F | GGC CAC CCC TTC AAT TGA G | | |
| VV0316R | GTC GCA TAC ACA ACC GTG G | 435 | 60 |
| VV10808F | TAT TCG TTT AGC CAA ACA GTT GA | | |
| VV10808R | CCA CTT CAT CCC AAC GCG TT | 902 | 57 |
| VV10803F | TTA TCG GCG ACA AGG TGA | | |
| VV10803R | ATC CAT TAC ATA GGC AAA TAT G | 346 | 60 |

Chapter 4

SIALIC ACID-LIKE MOLECULES EXPRESSED ON *VIBRIO VULNIFICUS* LIPOPOLYSACCHARIDE ARE ESSENTIAL FOR BLOODSTREAM SURVIVAL IN A MURINE MODEL OF SEPTICEMIA

Introduction

Sialic acids are found on all vertebrate cells, positioned at the terminal end of glycan chains that modify proteins and lipids. In mammals, sialic acids perform a wide range of functions such as cell-cell interactions, and immune modulation (Varki and Schauer, 2009). Sialic acids also appear to form part of the basis for what has been called “self-associated molecular patterns” in mammals (Lewis et al., 2009). In fact, many bacterial pathogens synthesize or acquire sialic acids and incorporate these molecules into surface structures such as flagella, capsular polysaccharides and lipopolysaccharides (Logan et al., 2002; Le Quéré et al., 2006; Li et al., 2010). At high levels, bacterial sialic acids have been shown to dampen host complement activity and neutrophil responses (Parsons et al., 1988; Carlin et al., 2007) and to promote bacterial survival in the bloodstream and dissemination to other tissues (Zelmer et al., 2008). Many other bacteria synthesize “sialic acid-like” amino sugars, but whether these related structures impact systemic virulence in mammalian hosts is unknown.

Sialic acids are part of a larger family of nine-carbon backbone α -keto sugars called nonulosonic acids (NulOs) (Angata and Varki, 2002). *N*-acetylneuraminic acid (Neu5Ac) is the most common sialic acid in humans and the most widely studied of

the NulOs. Legionaminic and pseudaminic acids [derivatives of 5,7-diacetamido-3,5,7,9-tetra-deoxy-D-glycero-D-galacto-nonulosonic acid (Leg5,7Ac₂) and 5,7-diacetamido-3,5,7,9-tetra-deoxy-L-glycero-L-manno-nonulosonic acid (Pse5,7Ac₂)] were first characterized in lipopolysaccharides of *Legionella pneumophila* (Knirel et al., 1997) and *Pseudomonas aeruginosa* (Knirel et al., 1984) respectively.

The importance of sialic acid modified bacterial surface structures has been determined in several organisms. The removal of sialic acid from the K1 capsule of *E. coli* LP1674 increased complement mediated killing and lead to attenuation in bacteremia in 3 day old rats (Mushtaq et al., 2004). Capsular polysaccharide sialylation of *Streptococcus agalactiae* allows interaction with sialic acid binding Ig-like lectins (Siglecs), expressed on the surface of neutrophils and monocytes, which can dampen immune responses (Carlin et al., 2007). The O-antigen of lipopolysaccharide (LPS) is sialylated in *Neisseria meningitidis* B1940 and was found to inhibit IgM binding and complement deposition leading to resistance to serum mediated killing (Vogel et al., 1997). Sialylation of LPS in *Haemophilus influenzae* strains 375 and 477 has also been shown to confer resistance to human serum and promote virulence in the chinchilla ear model (Hood et al., 1999; Bouchet et al., 2003). The protective effect of sialylated LPS is further confirmed in *Campylobacter jejuni* MSC57360, as sialic acid synthesis mutants exhibited decreased serum resistance (Guerry et al., 2000). By far, the effects of NulO modification on survival in host systems has been shown in bacteria that utilize the canonical *N*-acetylneuraminic acid and not its molecular mimics, legionaminic and pseudaminic acid. The impact of these sialic acid-like molecules on virulence have been extensively studied in *Campylobacter*. *Campylobacter jejuni* is an interesting case as it utilizes *N*-

acetylneuraminic acid, legionaminic acid, and pseudaminic acid in parallel (Michael et al., 2002; Guerry et al., 2006; Schoenhofen et al., 2009). In *C. jejuni* the LPS is sialylated with *N*-acetylneuraminic acid and its unsheathed flagellum is heavily modified with either legionaminic or pseudaminic acid residues (Thibault et al., 2001; Logan et al., 2002). Mutations in key genes in the pseudaminic acid biosynthetic pathway of *C. jejuni* NCTC 11168 resulted in non-motile phenotypes, defects in autoagglutination, and adherence to epithelial cells, as well as defects in the ability to cause diarrhea in ferrets (Guerry et al., 2006). However, mutations in the legionaminic acid biosynthetic gene cluster in *C. jejuni* NCTC 11168 H (hyper-motile variant) did not impact motility, but did lead to decreased hydrophobicity, reduced biofilm formation and were also required for optimal intestinal colonization in the chicken model (Howard et al., 2009). Taken together, these studies show that NulO residues can have important roles in the persistence of pathogens *in vivo*.

Vibrio vulnificus is a Gram-negative rod shaped halophile found in estuarine and coastal environments (Blackwell and Oliver, 2008). It is a disease causing agent in humans, causing gastroenteritis, wound infections and rapid onset septicemia (Jones and Oliver, 2009). *Vibrio vulnificus* commonly comes in to contact with humans due to the consumption of raw or undercooked shellfish and is the leading cause of seafood related death in the United States with an alarming 50% case fatality rate in susceptible individuals (Bross et al., 2007). Indeed, *V. vulnificus* mortality appears to result from rapid progression of a localized infection (wound or gut) to a systemic infection of the blood. However, little is known at the molecular level about virulence factors that allow *V. vulnificus* to evade killing in the bloodstream to cause rapid onset septicemia.

It was previously predicted through bioinformatic analysis that *V. vulnificus* encodes homologs of NulO biosynthesis (Lewis et al., 2009), and further, that clinical isolates CMCP6 and YJ016 have divergent alleles of putative NulO biosynthetic enzymes (Lewis et al., 2011). Biochemical analysis further revealed that *V. vulnificus* produce di-*N* acetylated NulOs and strains encoding CMCP6-like alleles produced on average 100-fold higher levels of NulO than their YJ016-like counterparts. Finally, strains that encoded CMCP6-like alleles were also much more likely to be clinical isolates, suggesting that NulO molecules may have a role in virulence (Lewis et al., 2011).

Here we sought to formally characterize the genetic basis for NulO biosynthesis in *V. vulnificus* and to investigate the potential biological and clinical significance of NulO production in the strain CMCP6 and YJ016. Taken together, our results demonstrate that NulO residues modify lipopolysaccharides in *V. vulnificus* and that production of these molecules is important for biological functions in the aquatic environment, such as motility and biofilm formation, and for systemic virulence in the mammalian host. The data provides the first demonstration of sialic acid-like molecules as important for survival of a pathogen in the bloodstream.

Materials and Methods

Strains and culture conditions

This study utilized the *V. vulnificus* clinical isolates CMCP6 and YJ016. Strains and plasmids used are listed in **Table 6**. All strains were grown aerobically at 30°C in Luria-Bertani broth (LB) (Fisher Scientific, Fair Lawn, NJ) containing 2%

NaCl or Marine Broth 2216 (MB) as noted (BD, Franklin Lakes, NJ). Stationary growth cultures were prepared with a single colony and allowed to grow for 16 hours. Logarithmic phase cultures were produced from a 2% inoculum of stationary phase culture, which was grown for 4 hrs in fresh medium.. Growth analysis of strains was performed by measuring optical density (O.D.) at 595 nm every hour for 24 h using a Genios microplate reader and Magellan plate reader software (Tecan US, Durham, NC).

Allelic exchange mutagenesis in *V. vulnificus*

The *V. vulnificus* CMCP6 and YJ016 genome sequences were used for primer design and oligonucleotides were purchased from Integrated DNA Technologies (Coralville, IA) (**Table 7**). An in-frame deletion mutant of *V. vulnificus* CMCP6 *nab2* (VV1_0808) gene was constructed using splicing by overlap extension (SOE) PCR and allelic exchange (Horton et al., 1989). A 411-bp deletion was constructed in the CMCP6 *nab2* gene as follows. Primers were designed to PCR amplify two gene fragments that flank the targeted 411 bp deletion region within *nab2*. The fragments were annealed, ligated, and amplified to construct a truncated *nab2* gene fragment. The truncated gene was inserted into the high copy cloning vector pJET 1.2 Amp^r (Thermo Fisher Scientific, Waltham, MA) and transformed into *Escherichia coli* cloning strain DH5 α λ -pir. The cloned fragment was then subcloned into suicide vector pDS132 Cm^r (Philippe et al., 2004) and transformed into the diaminopimelic acid (DAP) auxotroph *E. coli* β 2155 donor strain for conjugation to *V. vulnificus* by cross-streaking on to LB containing 0.3mM DAP (Sigma-Aldrich, St. Louis, MO). Subsequent growth was plated on LB 2% NaCl containing 25 μ g/ml chloramphenicol to isolate recombinants of *V. vulnificus* containing pDS132. *V. vulnificus* conjugants

were cultured overnight without antibiotics to allow a second round of homologous recombination to occur, eliminating pDS132 and producing an in-frame deletion mutant of *nab2*. The resulting overnight culture was plated onto LB 2% NaCl supplemented with 10% sucrose, which is lethal to strains harboring pDS132, to recover colonies that contain a double crossover. A 396 bp deletion in the YJ016 *nab2* (VV0312) allele and an 837 bp deletion in the CMCP6 *flhF* (VV1_1950) gene, were constructed as described above. Deletion mutants were confirmed by PCR using SOE flanking primers and by sequencing. CMCP6 $\Delta nab2$ was complemented by amplifying gene VV1_0808 using the primers listed in **Table 7**. The gene was cloned into pBBR1MCS Cm^r, and selection for the complemented strain was achieved by plating on LB 2% NaCl containing 25 μ g/ml chloramphenicol.

HPLC analysis

Bacterial cultures grown under various conditions were subjected to mild acid hydrolysis in 2N acetic acid at 80°C for 3 hours, as previously described (Lewis et al., 2004). After mild acid treatment to release NulO residues, cellular debris were removed by centrifugation, and the low molecular weight fraction was isolated using 10 kD molecular weight cutoff centrifugal filtration. The filtrate was derivatized with 1,2-diamino-4,5-methylene dioxybenzene (DMB), which is specific to the keto acid portion of NulO residues. Reactions consisted of: 7mM DMB, 18 mM sodium hydrosulfite, 1.4 M acetic acid and 0.7 M 2-mercaptoethanol (Sigma-Aldrich) and were carried out in the dark at 50°C for 2 hours. Derivatized NulO residues were resolved by HPLC using a C18 column (Tosoh Bioscience, King of Prussia, PA)

eluted isocratically using 85% Milli-Q ultrapure water, 8% acetonitrile, and 7% methanol at a rate of 0.9 ml/min for a period of 50 min as previously described (Lewis et al., 2004). Detection of fluorescent NulO derivatives was achieved using an excitation wavelength of 373 nm and emission wavelength of 448 nm. 2-keto-3-deoxy-D-manooctulosonic acid (Kdo) is an 8-carbon backbone monosaccharide related to the nonulosonic acids that is a conserved component of the lipopolysaccharide core. Kdo is also released by mild acid hydrolysis and derivatized by DMB and thus serves as a convenient internal positive control in the analyses and can also be used to calculate relative levels of NulO production.

Lipopolysaccharide analysis

Lipopolysaccharide was isolated by the method detailed in Amaro et al., with minor modifications (1992). Briefly, 1.5 ml of logarithmic cultures in sterile marine broth were adjusted to O.D. 0.8 at 600 nm, centrifuged at 400 x g for 5 min, and resuspended in 50 µl of Laemmli buffer. Samples were boiled for 10 min and 25 µg of proteinase K in 10 µl of Laemmli buffer was added and incubated at 60°C for 1 h. The extracted LPS was separated by SDS-PAGE using a 4-15% acrylamide gradient gel (Bio-Rad) and visualized by 1 %periodic acid oxidation incubation for 2 h at room temperature and fluorescent labeling with Pro-Q® Emerald 300 stain (Molecular Probes/Invitrogen, Carlsbad, CA, USA).

Antibiotic sensitivity

Sensitivity to polymyxin-B was assessed by zone of clearance formed from 100 µg polymyxin-B discs (Sigma). The following antibiotic discs (BD) were used to

determine general sensitivity of the strains: tetracycline 30 µg, ciprofloxacin 5 µg, nalidixic acid 30 µg, erythromycin 15 µg gentamicin 10 µg. Logarithmic cultures were plated onto LB 2% NaCl and allowed to dry for 10 min. Assay was performed in duplicate or triplicate (polymyxin-B) on each strain and incubated at 30°C overnight.

Preparation of flagellin monomers for NulO analysis

Flagellin monomers were isolated from *V. vulnificus* by the method detailed in McCarter et al. (1988). Briefly, 10 ml logarithmic cultures of *V. vulnificus* were vigorously vortexed for 2 min, centrifuged at 6000 x g and 4°C for 10 min, and the subsequent pellet is resuspended and the process repeated to separate free flagella from the cells. The flagella were pelleted by centrifugation at 38,700 x g and 4°C for 40 min. Pelleted flagella were resuspended in 40 µl of Laemmli buffer and separated by SDS-PAGE by a 7.5% acrylamide gel (Bio-Rad Hercules, CA, USA). Proteins were visualized by Bio-safe coomassie stain (Bio-Rad). Isolated flagella from *Campylobacter coli* was used as a positive control for NulO modification and *Listeria monocytogenes* used as a negative control of NulO modification was kindly provided to us by Susan Logan, (Institute for Biological Sciences, National Research Council, Ottawa, ON, Canada). Flagellin monomers were excised from the gel, ground by micropipette tip in 100 µl of 4N acetic acid, and NulO was released by mild acid hydrolysis at 80°C for 3 h. Acrylamide gel fragments were removed by 10 kD molecular weight cutoff centrifugal filtration and DMB-derivitization and HPLC analysis was performed on the filtrate as previously described (Lewis et al., 2004).

V. vulnificus motility

Motility was assessed by inoculating 1 μ l of logarithmic cultures in the center of a Marine Broth (MB) soft agar plate (0.3% agar). Motility was measured as diameter of bacterial growth in mm after incubation for 16 hours at room temperature. The average diameter of distance swam was then recorded. Measurements were performed in triplicate with at least two biological replicates.

Electron microscopy of *V. vulnificus* flagellation

Electron microscopy was used visualize defects in flagellation and quantify the percentage of the population that contained defects. 100 bacteria were counted for each strain and performed in duplicate. Samples were allowed to absorb onto formvar/carbon-coated copper grids (Ted Pella Inc., Redding CA) for 10 min. Grids were washed in dH₂O and stained with 1% aqueous uranyl acetate (Ted Pella Inc.) for 1 min. Excess liquid was gently wicked off and grids were allowed to air dry. Samples were viewed on a JEOL 1200EX transmission electron microscope (JEOL USA, Peabody, MA) at an accelerating voltage of 80kV.

Biofilm assay

The ability to form biofilms was assessed by inoculating 96 well plates with 1:100 dilutions of stationary cultures in marine broth (MB). 1, 4, 6 and 24 h incubation periods, non agitated, at room temperature, were assessed for biofilm formation. The culture media was removed and the wells were washed three times with sterile PBS. 100 μ l of 0.1% crystal violet was added to each well and incubated for 30 min at room temperature. The crystal violet was then removed and, wells were washed three times with 100 μ l of sterile PBS. Crystal violet was extracted using 100 μ l of DMSO, and

average O.D. at 595 nm was recorded. Biofilm assays were performed in triplicate on at least two biological replicates.

Mouse infection model

Animal infection studies were performed in accordance with approved protocols from the Washington University Division of Comparative Research. Bacterial strains were grown overnight aerobically at 30°C in LB 2%. A 2% inoculum of overnight cultures was used to grow samples to log phase and *V. vulnificus* wild type (WT) and streptomycin resistant (Sm^r) mutant were mixed 1:1 by O.D. measurement. 1×10^7 CFU in 100 μ l of sterile PBS was used to infect male 8-10 week old CD1 mice (Charles River, Wilmington, MA) by tail vein injection. Cheek bleeds were performed at 30 min post infection and 90 min post infection. The animals were sacrificed 90 min post infection and the liver was harvested and homogenized in sterile PBS. The collected samples were serially diluted and plated on to LB plates, with and without streptomycin to distinguish WT from mutant colonies. Half life ($T_{1/2}$) is defined as the time in minutes required for clearance of 50% of bacterial titers in the bloodstream between 30 and 90 min. $T_{1/2}$ is calculated as follows: $t_{1/2} = \text{time (60min)} \times \log_2 / \log(\text{CFU/ml 30 min} / \text{CFU/ml 90 min})$. The competitive index (CI) was determined as follows: $CI = \text{ratio out}_{(WT/mutant)} / \text{ratio in}_{(WT/mutant)}$. A $CI > 1$ indicates that the WT has the ability to out-compete the mutant while conversely a $CI < 1$ indicates that the WT is less fit compared with the mutant. A 1:10 dilution of 1:1 WT and mutant strains were made in 1 ml of LB 2% and utilized for *in vitro* competition assays. Samples were incubated at 30°C for 30 and 90 min, and analyzed for CI index as described above.

Results

HPLC analysis establishes the genetic basis of nonulosonic acid biosynthesis in *V. vulnificus*

As was shown in our previously in chapter 3, *V. vulnificus* CMCP6 and YJ016 contain distinct clusters attributed to the production of NulO and HPLC analysis revealed that CMCP6 produced much larger amounts of NulO compared to YJ016. To definitively determine the genetic basis for NulO production in *V. vulnificus*, we performed in-frame deletion of the gene encoding the homolog of *N*-acetylneuraminic acid synthase VV1_0808 (*nab2*) in CMCP6 (gene cluster shown in **Fig. 18A**). The mutant strain did not exhibit substantial defects in growth in either LB (**Fig. 18B**) or MB (**Fig. 18C**). To examine NulO production by the WT strain and determine the effect of deletion of *nab2* in the putative NulO biosynthesis pathway, NulO residues were released by mild acid hydrolysis, and derivatized with the fluorescent molecule 1,2-diamino-4,5-methylene dioxybenzene (DMB), which reacts with the alpha-keto acid of NulOs. HPLC was then used to separate and quantify NulOs. DMB-HPLC analysis of total cellular-associated NulOs revealed a complete absence of NulO expression in the $\Delta nab2$ strain (**Fig. 18D**). Relative NulO production in the WT strain was shown to be similar in logarithmic and stationary growth as well as in LB and MB. We note that while NulO synthesis was only restored in the complemented strain, NulO levels were not significantly lower ($p > 0.05$) in the complemented strain compared to WT. Deletion of the putative *nab2* in YJ016 also lead to loss of NulO expression (data not shown). This analysis formally demonstrates the genetic basis for NulO synthesis in *V. vulnificus*, showing that the *N*-acetylneuraminic acid synthase homolog encoded by *nab2* is required for NulO biosynthesis.

V. vulnificus LPS is modified with NulO residues, which contribute to the natural resistance of *V. vulnificus* to the LPS-binding antibiotic polymyxin-B

The LPS O-antigen is a frequent site of NulO modification in Gram-negative organisms (Knirel et al., 1984; Knirel et al., 1997; Li et al., 2010; Post et al., 2012). To investigate whether *V. vulnificus* LPS contains NulO residues, LPS was isolated from WT CMCP6 and CMCP6 $\Delta nab2$. Polyacrylamide gel electrophoresis followed by glycan staining using the ProQ Emerald stain (Molecular Probes/Invitrogen) found CMCP6 $\Delta nab2$ to contain a lower molecular weight band than is present in WT CMCP6 (**Fig. 19A**). Complementation of CMCP6 $\Delta nab2$ led to a partial restoration of the high molecular weight band observed in the WT CMCP6. Investigation into the LPS of YJ016 WT and YJ016 $\Delta nab2$ yielded the same shift in the molecular weight of the mutant band (**Fig. 20B**). *V. vulnificus* has a natural resistance to the cationic LPS-binding antibiotic polymyxin-B (Oliver et al., 1992). To investigate whether NulO residues on *V. vulnificus* LPS influence sensitivity to polymyxin-B, an antibiotic sensitivity assay was conducted. Plates swabbed with late logarithmic cultures of all strains were incubated overnight in the presence of filter paper discs containing 100 μg discs of polymyxin-B and incubated overnight at 30°C. This experiment revealed that disruption of NulO biosynthesis does in fact significantly increase sensitivity to polymyxin-B (**Fig. 19B**). The zone of clearance for WT CMCP6 was negligible, consistent with the reported natural resistance of *V. vulnificus* to this antibiotic. In contrast, CMCP6 $\Delta nab2$ yielded a significant ($p < .001$) zone of clearance, suggesting that the NulO modification of LPS may be shielding *V. vulnificus* LPS from interaction with polymyxin-B. Complementation of the mutant restored the WT phenotype of polymyxin-B resistance. To examine whether the increased sensitivity of the $\Delta nab2$ strain to polymyxin-B was specific, or whether the mutation may have

weakened the bacterial surface architecture, generally increasing antibiotic sensitivity, we examined bacterial sensitivity to a broader range of antibiotics (**Fig. 19C**). These experiments demonstrated no significant differences between CMCP6 WT and CMCP6 $\Delta nab2$ in their susceptibility to tetracycline, ciprofloxacin, nalidixic acid, erythromycin, or gentamicin. The complemented strain exhibited a significant increase in susceptibility to tetracycline, erythromycin, and gentamicin, most likely due to the growth defect in this strain. Together, these results strongly suggest that NulO modifications of LPS are responsible for the natural resistance of *V. vulnificus* to polymyxin-B.

To determine whether in *V. vulnificus* CMCP6 the flagellum is also modified with NulO, flagella of CMCP6 WT and CMCP6 $\Delta nab2$ were isolated and flagellin monomers were resolved by SDS-PAGE. Positive and negative controls of NulO modification included flagellar preparations from *Campylobacter* and *Listeria* respectively. Mild acid hydrolysis and DMB-HPLC analysis was performed on the isolated protein bands as previously described (Lewis et al., 2004). Using this method, the positive and negative control bands from *Campylobacter* and *Listeria* respectively, gave the expected results; however, we were unable to detect the presence of NulO on the *V. vulnificus* flagellin monomers by this method, strongly suggesting that the *V. vulnificus* flagella is not modified by NulO (**Fig. 21**).

To further establish that flagellum is not the primary target for sialic acid-like modification, a flagellum mutant was constructed and examined by DMB-HPLC analysis, as previously described. We constructed a deletion in the *flhF* gene of CMCP6 (VV1_1950), which has been shown in *V. vulnificus* and *V. cholerae* to encode a regulator of flagella synthesis, producing an aflagellar, non-motile strain

(Correa et al., 2005; Kim et al., 2012). No motility was detected for CMCP6 $\Delta flhF$ on MB soft agar plates (0.3% agar) after 16 h, confirming the aflagellar phenotype (data not shown). DMB- HPLC analysis of CMCP6 $\Delta flhF$ and the WT demonstrated the presence of WT levels of NulO production in the mutant (**Fig. 22**). As we did not see a decrease in NulO production between the WT strain and the aflagellar mutant, we can potentially conclude that there is no loss of total NulO due to the absence of the flagella, yielding further evidence that the flagellin monomers of *V. vulnificus* are not modified by NulO.

NulO synthesis is essential for full motility in *V. vulnificus*

We next examined whether NulO residues are required for motility in *V. vulnificus*. Swimming motility was assessed by spotting CMCP6 WT and CMCP6 $\Delta nab2$ strains onto marine agar plates (0.3%) and measuring zones of motility following 16 hours of growth at room temperature. These experiments demonstrated that disruption of NulO synthesis in *V. vulnificus* resulted in a significant ($p < 0.001$) decrease in the ability of bacteria to engage in swimming motility on soft agar plates (**Fig. 23A-B**). Visualization of flagella filaments using transmission electron microscopy determined that the deletion of *nab2* in CMCP6 resulted in a missing or shortened flagella (**Fig. 23C**). While the vast majority (~80%) of individual bacteria in the WT population produced a single long polar flagellum characteristic of this organism (**Fig. 23D**), the CMCP6 $\Delta nab2$ population contained a much higher proportion of individual bacteria with a shortened or missing flagellum, with only ~23% of the population exhibiting a long polar flagellum ($p < 0.01$) (**Fig. 23D**). Independent deletion of *nab2* in the YJ016 strain background had exactly the same effect on flagella morphology and motility (**Fig. 20**), a finding that strongly argues

against the possibility that mutation of *nab2* had a polar effect that impacted motility. The complemented CMCP6 *nab2* mutant exhibited an increase in the percentage of bacteria with WT flagellum morphology (**Fig. 23D**); however, the mutant did not regain WT levels of motility on soft agar plates (**Fig. 23A, 23D**).

A likely possibility for the motility phenotype in the complemented strain relates to the fact that complementation did not fully restore NulO biosynthesis to the WT level (**Fig. 18D**). This is also consistent with the results of the LPS analysis, where the complemented strain expressed both the higher and lower molecular weight bands characteristic of the WT and $\Delta nab2$ strains respectively (**Fig. 19A**).

V. vulnificus NulO residues play a role in biofilm formation

Next, we evaluated the potential role of *V. vulnificus* NulO modifications on biofilm generation on abiotic surfaces. A biofilm assay was conducted with 1:100 diluted WT CMCP6 and CMCP6 $\Delta nab2$ strains on 96-well polystyrene plates at 1-, 4-, 6- and 24-hour time points- (6 hour time point shown in **Fig. 23E**). The results indicate that impairment of NulO synthesis in *V. vulnificus* significantly ($p < .001$) reduces its ability to form biofilms. Data collected at the other time points (not shown) were similar to observations shown in **Fig. 23E**. Similarly, in YJ016 $\Delta nab2$ reduced biofilm formation was also observed (**Fig. 20**). Complementation of CMCP6 $\Delta nab2$ restored its ability to form biofilms to WT levels. This would indicate that NulO present on surface components facilitates biofilm formation in this organism.

NulO confers a competitive advantage in systemic infection of the mouse

To determine whether NulO plays a role in *V. vulnificus* virulence, a tail-vein injection mouse model was developed to mimic the septicemia typical of the organism when infecting susceptible human hosts. WT CMCP6 and CMCP6 $\Delta nab2$ were

competed in mouse bloodstream to investigate if NulO conferred an advantage in survival or proliferation. A 1:1 mixed culture of CMCP6 WT and CMCP6 $\Delta nab2$ strains was used to infect mice by tail vein injection. Blood was taken at 30 and 90 min time points and the liver was harvested at 90 min to determine systemic infection. CFU outputs of WT and $\Delta nab2$ at 30 and 90 min were used to determine the half-life (T1/2) of each strain, which indicates the time in minutes required to clear 50% of the strain present in the bloodstream between 30 and 90 min. The results show that CMCP6 $\Delta nab2$ has a significantly shorter ($p < 0.03$) T1/2 of 10.62 min compared to 43.03 min in WT strain (**Fig. 24A**). This indicates that CMCP6 $\Delta nab2$ has a decreased ability to survive in the host bloodstream. YJ016 $\Delta nab2$ was found to also have a shorter T1/2 of 19.76 min compared to 45.70 min in WT strain (data not shown). The competitive index (CI) of WT CMCP6 versus CMCP6 $\Delta nab2$ at 30 min was 16.2 and at 90 min was 234.9. These data demonstrate the ability of the WT strain to outcompete the mutant *in vivo*. In addition, it was found that the WT significantly outcompeted ($p < 0.03$) the *nab2* CMCP6 mutant in dissemination to the liver with a CI of 64.3 (**Fig. 24B**). As we have previously shown, *V. vulnificus* CMCP6 produces significantly more NulOs than YJ016, therefore we were interested to see if this would play a role in the competitive indices of their respective $\Delta nab2$ strains (Lewis et al., 2011). We observed that similar to CMCP6, YJ016 also has a competitive advantage over YJ016 $\Delta nab2$ in the mouse bloodstream (30 min CI = 1.9, 90 min CI = 14.2) as well as in dissemination to the liver (CI = 5.2) (**Fig. 24B**). However, the effect of the loss of NulO production is much less pronounced in YJ016 compared to CMCP6, with significantly ($p < 0.03$) greater competitive indices seen for CMCP6 in the blood and liver (**Fig. 24B**). This result demonstrates that NulO modification of *V. vulnificus*

surface structures confers a competitive advantage *in vivo*. The much lower competitive indices in YJ016 relative to CMCP6 may indicate that the greater amount of NulO in CMCP6 provides more protection from the host immune system.

In order to demonstrate that the attenuation of the *nab2* mutant *in vivo* was the result of the NulO defect and not due to its impaired motility and biofilm formation we examined the aflagellar non-motile CMCP6 $\Delta flhF$ strain *in vivo*. As described previously, a 1:1 mixed culture of CMCP6 WT and CMCP6 $\Delta flhF$ strains was used to infect mice by tail vein injection and blood samples 30 and 90 min post-infection were examined. The CI WT CMCP6 versus CMCP6 $\Delta flhF$ at 30 min was 1.11 and at 90 min was 14.7, with WT also outcompeting $\Delta flhF$ in dissemination in to the liver with a CI of 4.3 (**Fig. 21b**). In *in vitro* competition assays, we found no difference in the CI of CMCP6 WT and $\Delta flhF$ mutant strains at 30 min and 90 min (data not shown). Our results show that while CMCP6 WT has a competitive advantage over CMCP6 $\Delta flhF$ in the mouse bloodstream, it is much less pronounced than what was seen in CMCP6 $\Delta nab2$ (**Fig. 24B**). Overall the data demonstrate that the defect in the *nab2* mutant is due predominately to NulO production and not defects in motility or biofilm formation.

Discussion

This study sought to determine the role that sialic acid-like modifications played in *V. vulnificus* fitness and survival. Our previous study showed that *V. vulnificus* contained at least two divergent gene clusters responsible for NulO production and that this genetic difference correlated with relative amounts of NulO produced by a given strain (Lewis et al., 2011). The NulO produced by *V. vulnificus* was defined as not being the more commonly studied *N*-acetylneuraminic acid, but an

acetaminidino modified version of either pseudaminic acid or legionaminic acid (Lewis et al., 2011). In this study, the construction of CMCP6 $\Delta nab2$ confirmed the gene as the sole NulO synthase in the organism, and that elimination of NulO production does not significantly alter growth in this organism (**Fig. 18**). Analysis of *V. vulnificus* LPS revealed that the structure is modified with NulO and that absence of NulO leads to an increase in sensitivity to polymyxin-B (**Fig. 19**). This result is in agreement with analysis of *V. vulnificus* ATCC strain 27562, where Vinogradov and colleagues demonstrated the presence of pseudaminic acid residues at the terminal end of the LPS (Vinogradov et al., 2009). However, a report examining the presence of NulO on *V. vulnificus* YJ016 LPS, by Senchenkova and co-workers detected no NulO on its LPS (Senchenkova et al., 2009). It is possible that during LPS purification in this study that the NulO residue was lost prior to analysis, since our previous studies (Lewis et al., 2011), and our present results demonstrate that YJ016 does utilize NulO and it is LPS associated (**Fig. 21**). Analysis of flagellin from *V. vulnificus* CMCP6 strongly suggests that that the flagellum is not directly modified by NulOs. Investigation into the effects of NulO modification on *V. vulnificus* demonstrated a defect in motility (**Fig. 23**) but not a completely non-motile phenotype as seen in *Campylobacter* spp. NulO mutants (Goon et al., 2003). The partial motility phenotype of the *nab2* mutant may be due to alteration in the composition of the flagellum sheath, which has been shown in *V. cholerae* to contain LPS residues (Fuerst and Perry, 1988). HPLC analysis of our non-motile CMCP6 $\Delta flhF$ strain which is flagellin negative, demonstrated that it contains the same level of NulO as the parent strain (**Fig. 22**). This data further strengthen the case that *V. vulnificus* flagellum is not modified with NulO. Consistent with studies investigating NulO production, biofilm formation in CMCP6 $\Delta nab2$ was significantly

reduced compared to the parent strain (**Fig. 23**), though it is unclear how much of this reduction is directly due to the loss of NulO. Flagella defects are known to cause decreases in biofilm formation in *Vibrio* (Yildiz and Visick, 2009) and the non-motile CMCP6 $\Delta flhF$, exhibited similar levels of biofilm accumulation to CMCP6 $\Delta nab2$ (**Fig. 25A**). *In vivo* competition experiments of WT CMCP6 versus CMCP6 $\Delta nab2$ revealed that NulO modification confers a pronounced competitive advantage in the mouse blood stream (**Fig. 24**). This may be attributed to decreased survivability of CMCP6 $\Delta nab2$ relative to WT CMCP6. The ability of WT CMCP6 to survive longer in the bloodstream may be due to the protective effects that NulO modification confers to complement mediated killing, as was observed in sialic acid modification of the LOS and CPS of *C. jejuni* and *S. agalactiae*, respectively (Edwards et al., 1982; Guerry et al., 2000). Interestingly, WT YJ016 was found to have a smaller competitive advantage against YJ016 $\Delta nab2$ (**Fig. 24**). We surmise that this is due to lower overall levels of NulO present on the surface of YJ016, which would lead to a smaller effect on survivability on the organism in the absence of NulO. As motility is a well-studied virulence factor, we investigated the impact motility plays in our bloodstream model by competing WT CMCP6 with CMCP6 $\Delta flhF$. Our results show that while WT CMCP6 is able to out-compete the non-motile strain in our model, it is at a much lower level than what is seen in CMCP6 $\Delta nab2$ (**Fig. 25**). We can then conclude that the increased survival of the WT strain *in vivo* is primarily due to the presence of NulO modification.

Mass spectral analysis concludes that *V. vulnificus* is producing a di-*N* acetylated pseudaminic or legionaminic acid, and not the canonical *N*-acetylneuraminic acid. This is consistent with the phylogenetic analysis of *nab* genes

in this organism (Lewis et al., 2009), which were found to be legionaminic acid producing homologs, and a recent study which discovered that the closely related species, *V. fischeri*, contained legionaminic acid modified LPS (Post et al., 2012). We have shown in this study that the sialic acid-like molecules serve as a mimic to *N*-acetylneuraminic acid despite having stereochemical differences in their structures. The phenotypes present in *V. vulnificus* NulO mutants provides further evidence of the ability of pseudaminic or legionaminic acids to perform the same roles as *N*-acetylneuraminic acid, in regards to structural integrity of the organism and host-pathogen interactions. As of the completion of this study we do not have evidence on which sialic acid-like molecule is being produced by *V. vulnificus*, and whether the genetic differences present in CMCP6 and YJ016 correlates to different moieties. Further studies will be done to investigate any potential structural differences in the NulO yielded from the CMCP6 and YJ016 alleles. The ability of *V. vulnificus* to form capsules is a known virulence factor in this organism (Simpson et al., 1987; Wright et al., 1990). As of now, we have not investigated whether the capsule in *V. vulnificus* is modified by NulO, as has been shown in other pathogenic species (Severi et al., 2007). There is precedence for the potential of more than one structure to be modified (Kahler et al., 1998; Schoenhofen et al., 2009), and it could potentially explain the differences seen in level of NulO production in CMCP6 and YJ016.

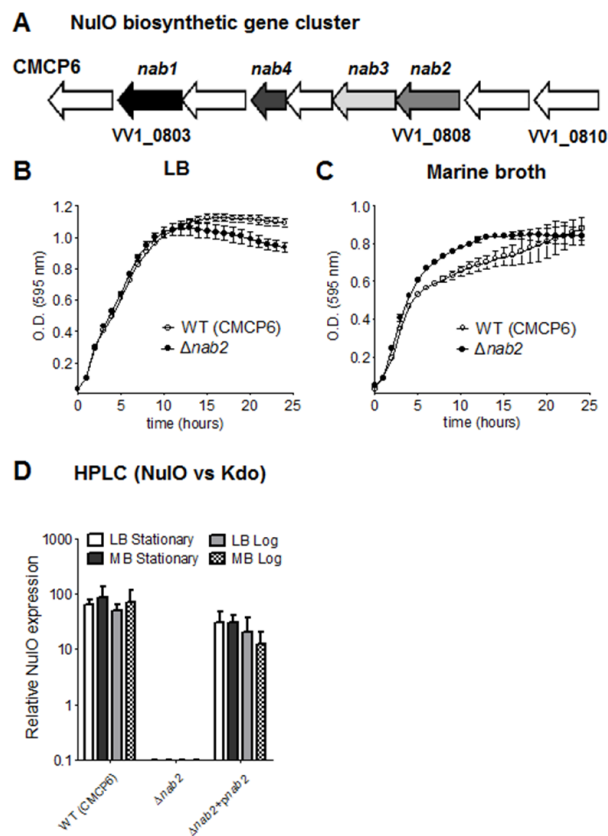


Figure 18 ***V. vulnificus nab2* is essential for NulO expression.** (A) Schematic of the *V. vulnificus* sialic acid-like biosynthetic cluster. Open reading frames and direction of transcription are designated by arrows. *nab1* (CMP-neuraminic acid synthase homolog), *nab2* (*N*-acetylneuraminic acid synthase homolog), *nab3* (UDP-*N* acetylglucosamine 2 epimerase homolog), *nab4* (acetyltransferase homolog) are highlighted. WT CMCP6 and CMCP6 $\Delta nab2$ have comparable growth in LB (B) or MB (C) media. (D) DMB-HPLC analysis of CMCP6 WT and CMCP6 $\Delta nab2$. HPLC analysis confirms that *nab2* encodes the *V. vulnificus* NulO synthase. Nonulosonic acids are synthesized at similar levels in all tested growth phases and media conditions. NulO expression is normalized to 3-D3-Deoxy-D-manno-oct-2-ulosonic acideoxy-D-manno-oct-2-ulosonic acid (KDO) for each strain and condition. Error bars represent standard deviation of three experiments. . An unpaired Student's *t*-test in GraphPad Prism 5.0 was used to determine statistically significant differences in NulO production.

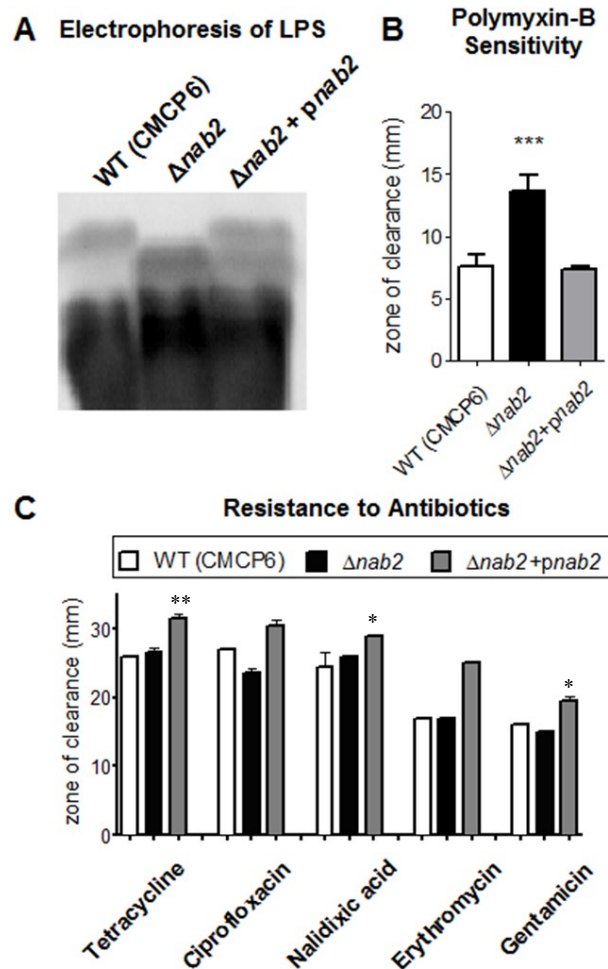


Figure 19 *V. vulnificus* LPS is modified with NuLO. (A) *V. vulnificus* CMCP6 LPS analyzed by SDS-PAGE and fluorescent glycan staining, demonstrates a small LPS or lipooligosaccharide. CMCP6 $\Delta nab2$ LPS exhibits a molecular weight shift that is restored upon complementation of WT *nab2* gene. (B) CMCP6 $\Delta nab2$ is significantly more sensitive to the LPS-binding antibiotic polymyxin B (100 μ g) than WT and complemented strains. (C) Antibiotic sensitivity is specific to polymyxin-B. Other antibiotics tested gave comparable zones of clearance in WT and NuLO mutant. Error bars represent standard deviation of at least two experiments. An unpaired Student's *t*-test in GraphPad Prism 5.0 was used to determine statistically significant differences in antibiotic zone of clearance. ***, $p < 0.001$, **, $p < 0.01$, *, $p < 0.05$

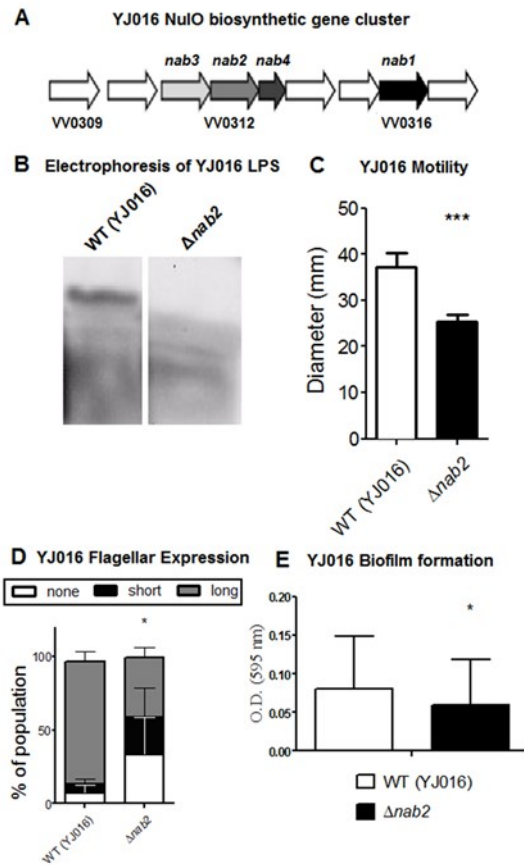


Figure 20 **Functional analysis of *V. vulnificus* YJ016 *nab2*.** (A) Schematic of the *V. vulnificus* YJ016 sialic acid-like biosynthetic cluster. Open reading frames and direction of transcription are designated by arrows. *nab1* (CMP-neuraminic acid synthase homolog), *nab2* (*N*-acetylneuraminic acid synthase homolog), *nab3* (UDP-N acetylglucosamine 2 epimerase homolog), *nab4* (acetyltransferase homolog) are highlighted. (B) *V. vulnificus* YJ016 LPS analyzed by SDS-PAGE and fluorescent glycan staining, demonstrates molecular weight shift in YJ016 $\Delta nab2$. (C) Motility in YJ016 $\Delta nab2$ significantly decreased and (D) transmission electron microscopy revealed defects in the flagella morphology of YJ016 $\Delta nab2$ with an increased population exhibiting shortened or missing flagella. (E) Biofilm assay in polystyrene 96 well plates confirms decreased biofilm formation in YJ016 $\Delta nab2$. Error bars represent standard deviation of at least two experiments. A paired Student's t-test in GraphPad Prism 5.0 was used to compare biofilm accumulation between strains. *, p < .03

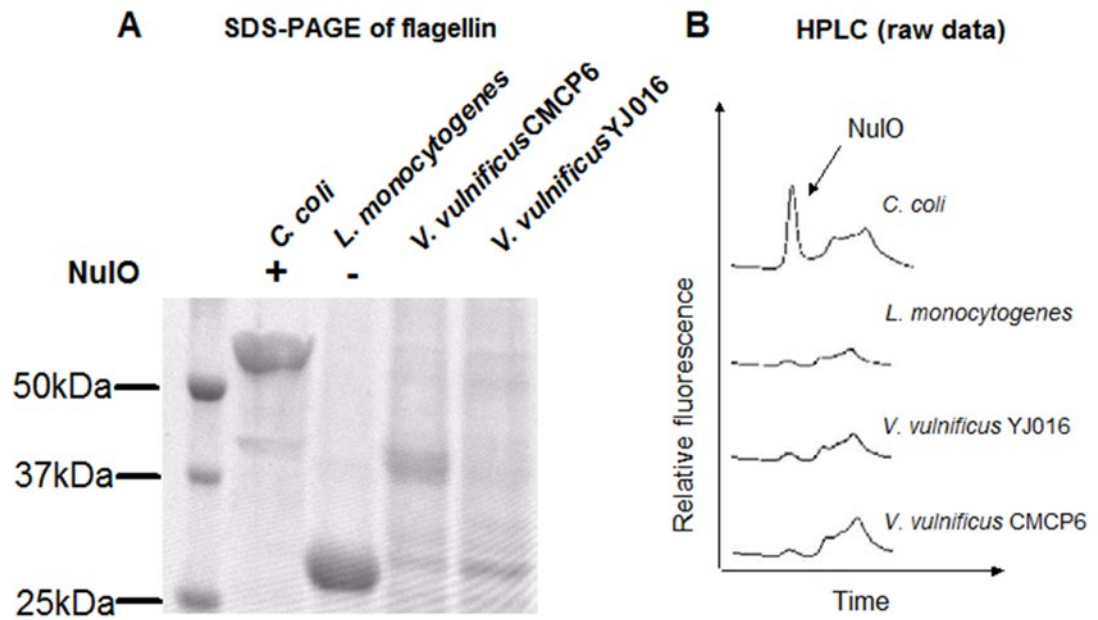


Figure 21 **SDS-PAGE of *V. vulnificus* flagellin.** (A) Purified flagellin from *Campylobacter coli* (MW 59 kDa), and *Listeria monocytogenes* (MW 30kDa) was used as a positive and negative control respectively for NulO modification of flagellin monomers. (B) *V. vulnificus* CMCP6 and YJ016 flagellin (39-41 kDa) (A), was determined to contain no NulO by HPLC analysis of purified flagellin bands.

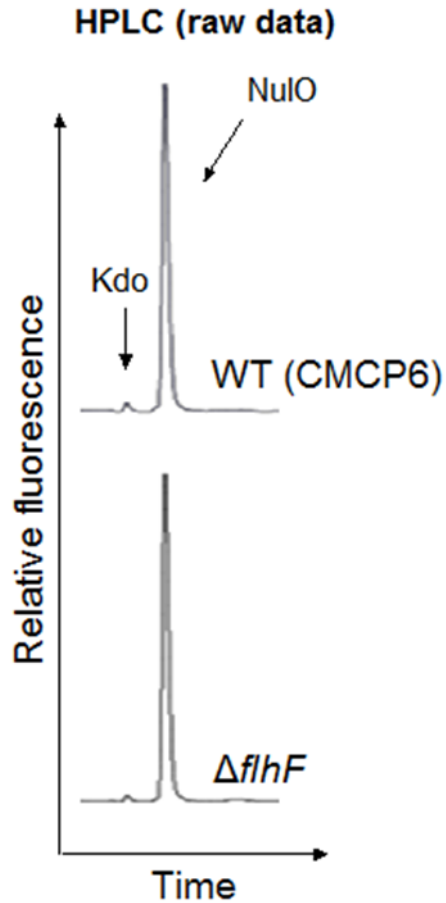


Figure 22 **HPLC analysis of aflagellar, non-motile $\Delta flhF$ shows no decrease in NuO levels.** DMB-HPLC analysis of CMCP6 WT and CMCP6 $\Delta flhF$ confirms that in the absence of flagella synthesis NuO production from whole cell lysates remains unchanged. This would indicate that the flagella of *V. vulnificus* CMCP6 does not undergo NuO glycosylation.

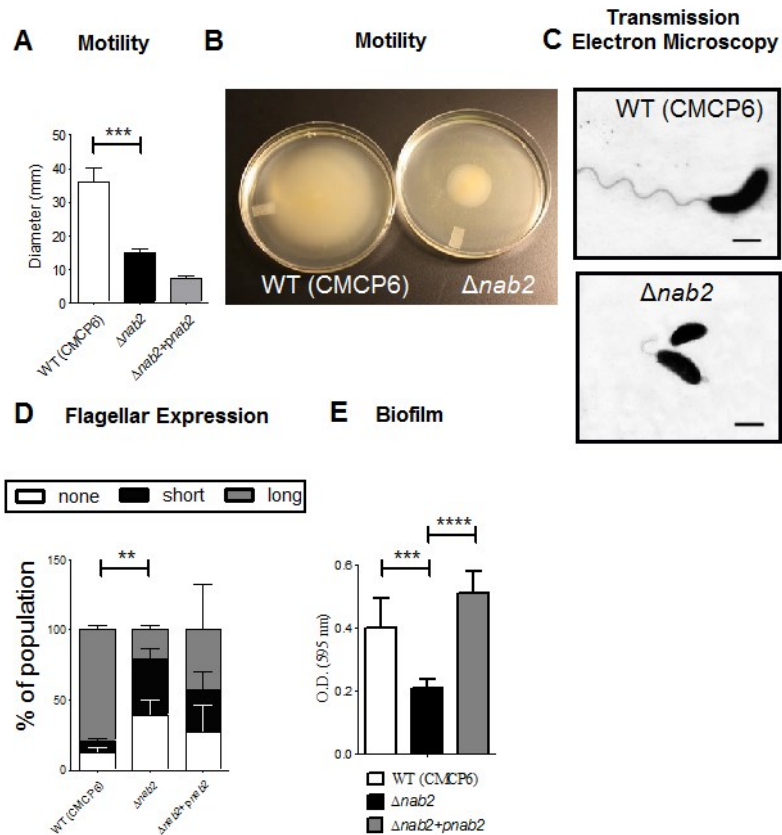


Figure 23 **Impairment of NulO Biosynthesis leads to a defect in Motility.** (A, B) A 16 h swim assay on MB 0.3% agarose to determine motility in *V. vulnificus*. Motility in CMCP6 $\Delta nab2$ significantly decreased. (C) Transmission electron microscopy revealed defects in the flagella morphology of *V. vulnificus nab2* mutant (D) with increased proportions of the population exhibiting shortened or missing flagella in CMCP6 $\Delta nab2$. (E) Biofilm assay conducted on polystyrene 96 well plates. Biofilm accumulation at 6 h is significantly greater in WT CMCP6 relative to CMCP6 $\Delta nab2$. Complementation of CMCP6 $\Delta nab2$ restores biofilm accumulation to WT levels. Optical density of 0.1% crystal violet stained biofilm measured at 595 nm. Error bars represent standard deviation of at least two experiments. An unpaired Student's *t*-test in GraphPad Prism 5.0 was used to determine statistically significant differences between the strains. **, $p < 0.01$ ***, $p < 0.001$, **** $p < 0.0001$

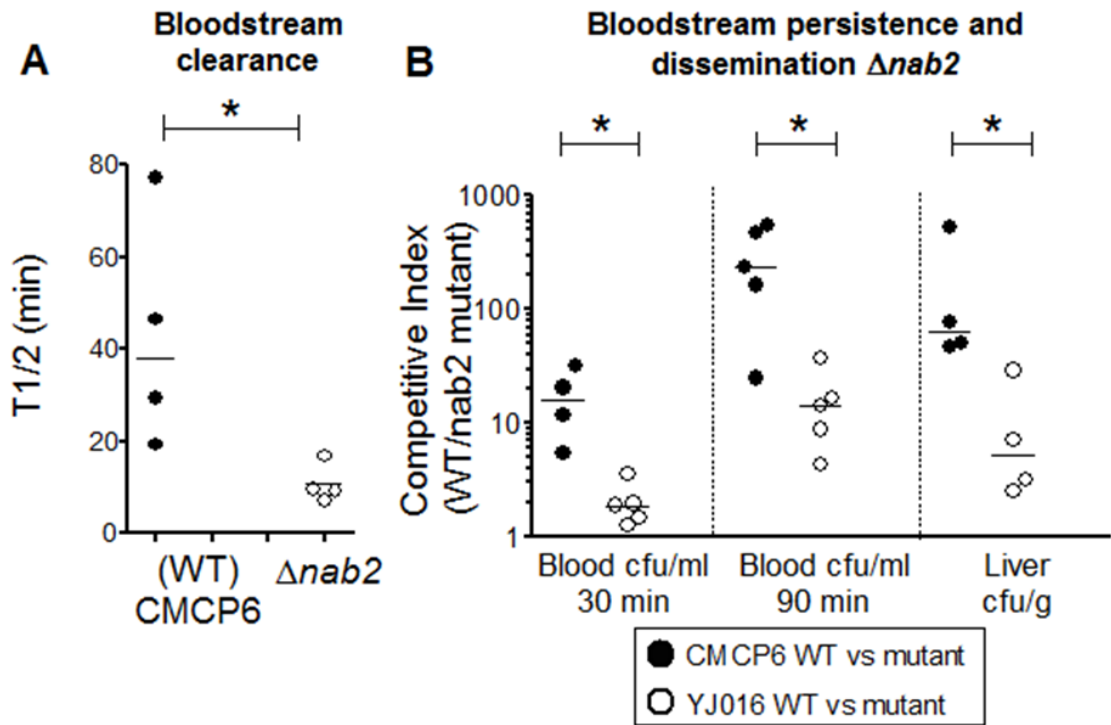


Figure 24

Elaboration of NulO is required for *V. vulnificus* bacteremia.

Bloodstream survival of *V. vulnificus* WT and mutant strains. The T1/2 represents half-life of the bacterial strains in the mouse bloodstream, the time required for clearance of 50% *V. vulnificus* titers from the host system. (A) WT CMCP6 has a significantly greater T1/2 relative to CMCP6 $\Delta nab2$ in the mouse bloodstream, indicating decreased survivability of mutant strain. (B) Competitive index of WT CMCP6 and CMCP6 $\Delta nab2$ increases from a period 30 to 90 min in the mouse blood stream. A comparable competitive index was found in the liver after 90 min. As previously shown, (26) NulO production in WT CMCP6 is much greater than in WT YJ016 and subsequently the competitive indices of WT CMCP6 and CMCP6 $\Delta nab2$ (closed circles) are significantly larger than in WT YJ016 and YJ016 $\Delta nab2$ (open circles) (B). Competition experiments were conducted at least twice. A Mann-Whitney *U*-test in GraphPad Prism 5.0 was used to determine statistical significance, * in all cases $p < 0.03$

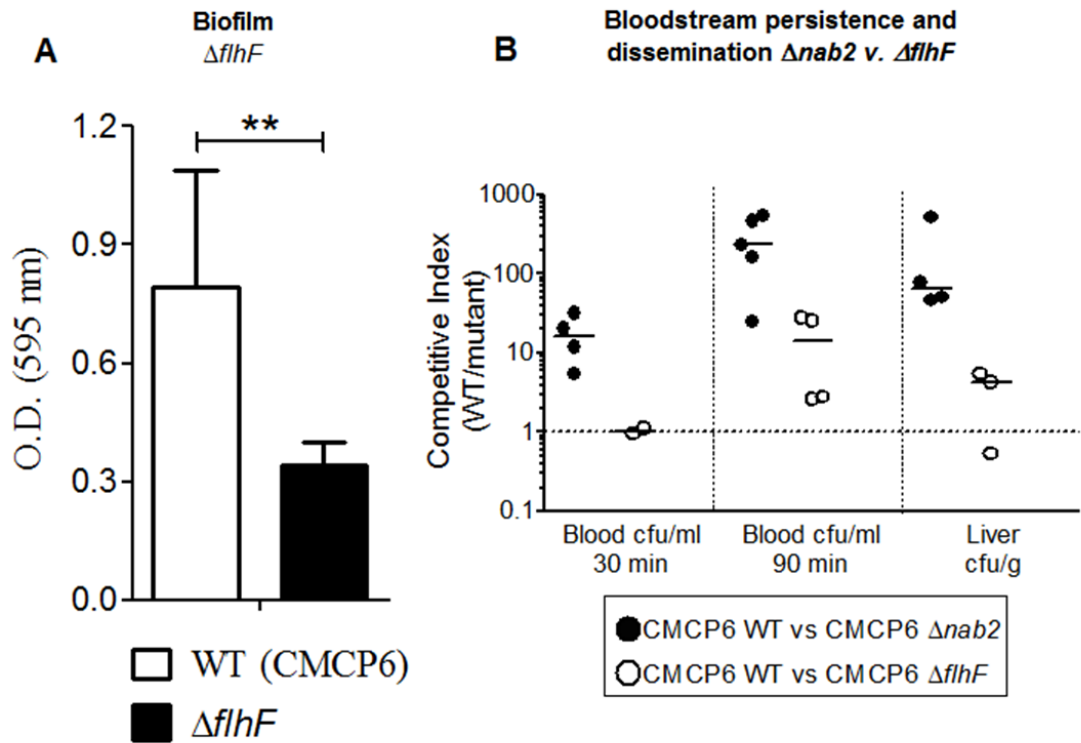


Figure 25 **Biofilm assay and in vivo competition assays of WT CMCP6 versus the $\Delta flhF$ flagellum mutant.** (A) Biofilm assay conducted on polystyrene 96 well plates reveals that motility mutant CMCP6 $\Delta flhF$ exhibits biofilm defect at 6 hours. Optical density of 0.1% crystal violet stained biofilm measured at 595 nm. (B) Competitive indices of WT CMCP6 and CMCP6 $\Delta nab2$ (closed circles) are greater than what is seen in WT CMCP6 and CMCP6 $\Delta flhF$ (open circles) as the infection persists from 30 to 90 min, as well as in dissemination into the liver. Error bars represent standard deviation. An unpaired Student's *t*-test in GraphPad Prism 5.0 was used to determine statistically significant differences in biofilm accumulation between the strains. **, $p < 0.01$

Table 6 Bacterial strains and plasmids used in this study

| Strain or plasmid | Genotype or description | Reference or source |
|---|--|---------------------|
| <i>Vibrio vulnificus</i> strains | | |
| CMCP6 | clinical isolate | |
| YJ016 | clinical isolate | (45) |
| CMCP6 $\Delta nab2$ | CMCP6 $\Delta nab2$ (VV1_0808) | This study |
| CMCP6 $\Delta nab2$ + <i>p_{nab2}</i> | CMCP6 $\Delta nab2$ + <i>pBBR1MCS_{nab2}</i> | This study |
| YJ016 $\Delta nab2$ | YJ016 $\Delta nab2$ (VV0312) | This study |
| CMCP6 $\Delta flhF$ | CMCP6 $\Delta flhF$ (VV1_1950) | This study |
| <i>Escherichia coli</i> | | |
| DH5 α λ -pir | <i>pir80dlacZ</i> Δ M15 δ (<i>lacZYA-argF</i>) <i>U169 recA1 hsdR17 deoR thi-1 supE44 gyrA96 relA1</i> | |
| β 2155 DAP | Donor for bacterial conjugation; <i>thr1004 pro thi strA hsdS lacZ</i> Δ M15 (F <i>lacZ</i> Δ M15 <i>lacTRQJ36proAB</i>) <i>dapA</i> <i>Erm^rpirRP4</i> (Km ^r from SM10) | |
| Plasmids | | |
| pJet1.2/blunt | High copy cloning vector | |
| pJet1.2-0808SOE | <i>V. vulnificus</i> VV1_0808 SOE product | This study |
| pJet1.2-0312SOE | <i>V. vulnificus</i> VV0312 SOE product | This study |
| pJet1.2-1950SOE | <i>V. vulnificus</i> VV1_1950 SOE product | This study |
| pDS132 | Suicide plasmid; Cm ^r ; SacB | (42) |
| pDS0808 | <i>V. vulnificus</i> VV1_0808 SOE product | This study |
| pDS0312 | <i>V. vulnificus</i> VV0312 SOE product | This study |
| pDS1950 | <i>V. vulnificus</i> VV1_1950 SOE product | This study |
| pBBR1MCS | Expression plasmid; Cm ^r | (46) |
| pBBR1MCS0808c | Expression plasmid (VV1_0808) | This study |

Table 7 Primers used in this study

| Primer name | Sequence (5'–3') | T_m (°C) | Product size (bp) |
|--------------------|---|---------------|----------------------|
| SOEVV1_0808 A | TCTAGACGCCAAGCACCAAAGTTATT | 60 | |
| SOEVV1_0808B | CTCTTCGTCTGGCGTTGACA | 60 | 354 |
| SOEVV1_080C | TGTC AACGCCAGACGAAGAGGCTAGCCTCGAGCCACA AGA | 60 | |
| SOEVV1_080D | GCATGCTCAAGTTGCGGATCATTTTG | 60 | 372 |
| SOEVV1_0808F LF | CCAGAGAAGAGGCACCAGTT | | |
| SOEVV1_0808F LR | CCAGAGAAGAGGCACCAGTT | 60 | 1,237 |
| VV1_0808Fc | AAGCTTCGCCAAGCACCAAAGTTATT | | |
| SOEVV0312A | CTTATGGGCCAAGGTGATAGCAG | 61 | |
| SOEVV0312B | GGTCGAAAGGAACTCAATACCC | 61 | 401 |
| SOEVV0312C | GGGTATTGAGTTCCTTTTCGACCGATTTACCTGCGGGTT ACTCTG | 60 | |
| SOEVV0312D | CTCGAGCATCTCCCAATACTG | 60 | 369 |
| SOEVV0312FL F | GTTACCTTGGGTGAAGAAGCAC | 60 | |
| SOEVV0312LR | CACTTCAGCAAAGGAAGAGACC | 60 | 1,936 |
| SOEVV1_195A | TCTAGATCGAATTGTACAGGCTGTGG | 60 | |
| SOEVV1_195B | CAAAGCGTTTGGTCATGGAT | 61 | 399 |
| SOEVV1_195C | ATCCATGACCAAACGCTTTGTCATGCAAGAGAGTGG GGAA | 61 | |
| SOEVV1_195D | GAGCTCGCTTGATCGTGTATCATATTCTCA | 59 | 377 |
| SOEVV1_1950F LF | AGGCGAACCAGCAGTCTTAC | 59 | |
| SOEVV1_1950F LR | GCCAAACCTAGGGTCACATT | 59 | 1,838 |
| VV1_0808Fc | AAGCTTCGCCAAGCACCAAAGTTATT | 60 | |
| VV1_0808Rc | TCTAGAGTGGCGGTGACTACACAGATT | 60 | 1,079 |

Chapter 5

PERSPECTIVES AND FUTURE DIRECTIONS

In this dissertation we have produced evidence to propose that sialic acid catabolism in *V. vulnificus* is likely to play a role in the acquisition of scarce nutrients in the intestinal tract upon infection and biosynthesis serves a structural role that confers an advantage in survival and fitness. *Vibrio vulnificus* has the full complement of genes necessary to catabolize and biosynthesize sialic acids and the highly divergent nab cluster of CMCP6 and YJ016 makes *V. vulnificus* an attractive model for studying the implications of biosynthetic genetic diversity. Overall, our study demonstrated that the ability to catabolize and transport sialic acid is heavily correlated with clinical isolates of *V. vulnificus*, indicating a role in the pathogenesis of this organism. Coupled with evidence of a decreased ability of catabolism deficient strains to colonize the mouse intestinal tract, it can be asserted that sialic acid catabolism is a virulence factor in this organism. This dissertation also revealed that Vibrionaceae is a “hot spot” of sialic acid evolution, producing either the bacterial specific legionaminic or pseudaminic acids, and suggests that surface sialylation plays a role in environmental fitness. We also presented compelling evidence that bacterial specific sialic acids protect *V. vulnificus* from immune responses in a host bloodstream. To our knowledge, this is first time a Neu5Ac mimic has been shown to have this ability. Also this is the first example of a *V. vulnificus* virulence factor found to be required for survival in the bloodstream, and could serve a key role in its ability to cause rapid septicemia and mortality.

Origins of sialic acid catabolism and transport diversity

In Chapter 2 we found that among the three sequenced *V. vulnificus* clinical strains, the sialic acid catabolism genes were present on chromosome II and unlike *V. cholerae*, are not associated with a pathogenicity island. Upon examination of 67 natural isolates, which phylogenetically clustered as either Lineage I clinical isolates or Lineage II environmental isolates, we found that the catabolism region was present predominantly in lineage I of *V. vulnificus*. Isolates that contain this region can utilize sialic acid as a sole carbon source and the tripartite ATP-independent periplasmic (TRAP) transporter SiaPQM is the sole transporter responsible for the uptake of sialic acid. We also concluded that environmental sialic acid had a pronounced effect on the up-regulation catabolic and transport genes in this organism. The ability of sialic acid to induce the genes responsible for its utilization would indicate a tightly regulated cluster. Strains that screened negative for *V. vulnificus nanA* could not grow solely on minimal media supplemented with sialic acid. This confirms that the negative PCR results are not due to polymorphic differences of the enzyme between strains, as was seen when studying the biosynthetic pathway. Interestingly, the inability to catabolize sialic acid was the result of the absence of the entire 12 kb region encoding the catabolism and transport genes, and not due to point mutations rendering *nanA* nonfunctional. This raises the question of how certain strains of *V. vulnificus* have come to lose or gain this ability. Unlike *V. cholerae*, the catabolism cluster is not found on a pathogenicity island, however the similarity of gene order and amino acid composition among catabolism positive *Vibrio* would suggest that this capability was lost in catabolism negative strains rather than gained. Further work needs to be done to construct the evolutionary history of the catabolic cluster in general; γ -Proteobacteria diverge widely in NanA phylogeny and nearly all enteric species contain a NanT

homolog instead of a TRAP or SSS system found in the Vibrionaceae. The consequence of what transporter is utilized in sialic acid catabolism is also worthwhile of further investigation. As previously mentioned, uptake of sialic acid requires one of four specialized transport systems: a major facilitator superfamily (MFS) permease NanT, TRAP transporter SiaPQM, a sodium solute symporter (SSS) SiaT, and an ATP-binding cassette (ABC) transport system SatABCD. It is unknown if usage of a particular transport system is correlated with prevalence of certain sialic acid derivatives in that organisms niche. The latter proposition is made somewhat less plausible with the evidence of bacterial species who coincide in the same environmental niche (i.e. human large intestine) utilizing different transport systems. However, a large scale comparison of the transport systems used in a niche by niche basis may reveal a bias towards one system. The NanT of *E. coli* BW25113, TRAP of *H. influenzae* Rd KW20 and the SSS transporter from *S. enterica* sp. typhimurium LT2, were found to uptake Neu5Ac, Neu5Gc, and KDN, albeit with a considerably lower affinity for KDN (Hopkins et al., 2013). Whether there are differences in affinity to Neu5Ac and efficacy of uptake between these four systems remains to be determined. Despite this evidence, preliminary inquiries into the specificity of *Vibrio* TRAP transporters has shown that *V. vulnificus* and *V. cholerae* are unable to uptake KDN. Furthermore, our bioinformatics studies would suggest that the human pathogen *G. vaginalis* putatively contains an ABC type transporter. This transporter has been shown by the Lewis group to be inhibited by the presence of Neu5Gc (Lewis et al., 2013). This presents the possibility of determining what the basis for sialic acid transporter promiscuity is and how the transport system can differ in their ability to uptake similarly structured compounds.

Structural diversity and environmental role of sialic acid biosynthesis

In Chapter 3, we examined the phylogenetic relationships, distribution, and function of the diverse sialic acid biosynthesis pathways of the family Vibrionaceae and *V. vulnificus* isolates. We found that roughly half the sequenced species of Vibrionaceae contained putative synthesis genes. We confirmed earlier through phylogenetic analysis that *Vibrio* spp. produce bacterial specific sialic acids, legionaminic or pseudaminic acids, and not Neu5Ac. Duplication, divergence, horizontal transfer and recombination of *nab* gene clusters was prevalent amongst Vibrionaceae, with three major clades formed. We used our collection of 67 different isolates of *V. vulnificus* to assess the distribution of CMCP6 and YJ016 alleles, which were found on highly divergent clades in analysis of the Vibrionaceae family. Our analysis showed that the CMCP6-like alleles were predominately found in the clinical lineage I isolates and that this genotype produced upwards of 40-fold higher levels of sialic acids than isolates containing YJ016-like alleles. Biochemical analysis discovered a potential third cluster in *V. vulnificus*, producing sialic acids at a level intermediate to CMCP6 and YJ016. This is consistent with the presence of three major synthesis clades at the family level. In our aim to establish a functional significance of sialic acid biosynthesis in *V. vulnificus*, the genetic basis of sialic acid biosynthesis in *V. vulnificus* was confirmed by deletion of the putative *nab2* synthase gene in the CMCP6 and YJ016 background. Chapter 4 details how loss of sialic acid synthesis led to a shift in the molecular weight of *V. vulnificus* LOS fragments indicating that the LPS modification in this organism. The removal of sialic acid from *V. vulnificus* LPS caused a significant increase in sensitivity to the LPS-associated polymyxin-B antibiotic, and this phenotype was shown to be LPS specific. In addition, we identified the role of sialic acid modification in optimal biofilm formation, motility

and flagellar construction and function. Competition experiments in a mouse model of septicemia revealed a survival advantage of the wild type CMCP6 strain versus the $\Delta nab2$ strain which was much less pronounced in the YJ016 background. This was the first phenotypic difference that could be attributed to greater amounts of sialic acid production in CMCP6. Previously, in vitro assays of $\Delta nab2$ CMCP6 and YJ016 revealed no significant differences in the resulting phenotype.

We are still uncertain why CMCP6 produces more sialic acid than YJ016. Our studies in LPS and flagellin did not provide a basis for the disparity. It is possible that the LPS of CMCP6 contains multiple sialic acid residues, and that can be determined by tandem electrospray ionization mass spectrometry (ESI-MS/MS), which would enable us to reveal any heterogeneity in the strains LOS structure. It is also possible that the capsule of CMCP6 is sialylated and this feature is either absent or less pronounced in YJ016. Pillin has been shown to undergo sialylation as well, yielding another potential target to explore (Castric et al., 2001). Investigations in to the regulation and expression of the sialic acid biosynthesis cluster would give us an indication of how CMCP6 produces more sialic acid than YJ016. Very little research has been done in this, due to the genes themselves being constitutively expressed and the propensity for research to focus on one or two strains of a species.

Whether these divergent allelic clusters produce discrete derivatives of pseudaminic acid or legionaminic acid remains to be seen. We have produced HPLC evidence to suggest that the clusters do produce different sugars and YJ016 potentially produces two varieties, however whether these were legionaminic or pseudaminic acid residues was inconclusive. 2D Nuclear Magnetic Resonance (NMR) would straightforwardly determine the structure of products of this cluster. However, a more

interesting question is whether it is possible to genetically determine, by identification of the catalytic residues, what derivatives of pseudaminic or legionaminic acid are produced. It may be possible to identify what residues are responsible for the stereoisomeric differences seen between these two structures. By the use of protein modeling and ligand binding models we could potentially be able to elucidate these residues, determine what sialic acid is being produced by amino acid composition alone, and use 2D-NMR for confirmation of our findings. Also we are exploring the use of circular dichroism as a rapid method of detecting what sialic acid derivatives are present on the surface components of *Vibrio* spp.

The specific mechanism by which sialic acid protects *V. vulnificus* in the blood stream is currently unknown. The rapid loss of $\Delta nab2$ titers seen in our mouse septicemia model would suggest the clearing of the mutant strains is complement mediated. A fluorescently labeled complement deposition assay would tell us if sialic acid residues on the surface of *V. vulnificus* inhibits this immune response to a degree not seen in the mutant strains.

Lastly it would be of interest to further examine the environmental implications of sialic acid biosynthesis, as this area is greatly understudied considering the disparate lifestyles of organisms found to contain *nab* genes. Sialylation of external components could play a role in oyster colonization. It has been reported in the literature that *V. vulnificus* strains with the environmental E phenotype dominate over clinical C types in oysters despite relatively equal distribution of their populations in the surrounding seawater (Warner and Oliver, 2008). As we see varying levels of sialylation present in environmental and clinical clades, sialic acid production could potentially play a role in oyster colonization. Biofilm formation on biotic

surfaces such as shells of crustaceans and mollusks could also be explored. Increased ability to form biofilm on chitin surfaces found in the marine environment would, not only provide a rich source of nutrition for the organism but would also promote genetic exchange, as chitin has been shown to make *Vibrio* spp. naturally competent (Gulig et al., 2009). In addition to the promotion of biofilm formation, marine organisms are known to contain lectins which can interact and bind to sialic acid molecules (Mandal, 1990). These organism specific binding proteins could play a role preferentially screening the organisms that colonize its system.

REFERENCES

- Allen, S., Zaleski, A., Johnston, J.W., Gibson, B.W., and Apicella, M.A. (2005). Novel sialic acid transporter of *Haemophilus influenzae*. *Infect Immun* 73, 5291–5300.
- Almagro-Moreno, S., and Boyd, E.F. (2009a). Insights into the evolution of sialic acid catabolism among bacteria. *BMC Evolutionary Biology* 9, 118.
- Almagro-Moreno, S., and Boyd, E.F. (2009b). Sialic Acid Catabolism Confers a Competitive Advantage to Pathogenic *Vibrio cholerae* in the Mouse Intestine. *Infect. Immun.* 77, 3807–3816.
- Almagro-Moreno, S., and Boyd, E.F. (2010). Bacterial catabolism of nonulosonic (sialic) acid and fitness in the gut. *Gut Microbes*, 1:1-6. *Gut Microbes* 1, 1–6.
- Altschul, S.F., Madden, T.L., Schaffer, A.A., Zhang, J., Zhang, Z., Miller, W., and Lipman, D.J. (1997). Gapped BLAST and PSI-BLAST: a new generation of protein database search programs. *Nucleic Acids Res* 25, 3389–3402.
- Amaro, C., and Biosca, E.G. (1996). *Vibrio vulnificus* biotype 2, pathogenic for eels, is also an opportunistic pathogen for humans. *Appl Environ Microbiol* 62, 1454–1457.
- Amaro, C., Biosca, E., Fouz, B., and Garay, E. (1992). Electrophoretic analysis of heterogeneous lipopolysaccharides from various strains of *Vibrio vulnificus* biotypes 1 and 2 by silver staining and immunoblotting. *Current Microbiology* 25, 99–104.
- Anderson, G.G., Goller, C.C., Justice, S., Hultgren, S.J., and Seed, P.C. Polysaccharide capsule and sialic acid-mediated regulation promote biofilm-like intracellular bacterial communities during cystitis. *Infect Immun* 78, 963–975.
- Angata, T., and Varki, A. (2002). Chemical diversity in the sialic acids and related alpha-keto acids: an evolutionary perspective. *Chem Rev* 102, 439–469.
- Annunziato, P., Wright, L., Vann, W., and Silver, R. (1995). Nucleotide sequence and genetic analysis of the neuD and neuB genes in region 2 of the polysialic acid gene cluster of *Escherichia coli* K1. *J. Bacteriol.* 177, 312–319.

- Austin, B. Vibrios as causal agents of zoonoses. *Vet Microbiol* *140*, 310–317.
- Barry, G.T. (1958). Colominic acid, a polymer of *N*-acetylneuraminic acid. *The Journal of Experimental Medicine* *107*, 507–521.
- Bennett, M., and Schmid, K. (1980). Immunosuppression by human plasma alpha 1-acid glycoprotein: importance of the carbohydrate moiety. *Proceedings of the National Academy of Sciences of the United States of America* *77*, 6109–6113.
- Bertin, Y., Chaucheyras-Durand, F., Robbe-Masselot, C., Durand, A., de la Foye, A., Harel, J., Cohen, P.S., Conway, T., Forano, E., and Martin, C. (2013). Carbohydrate utilization by enterohaemorrhagic *Escherichia coli* O157:H7 in bovine intestinal content. *Environ Microbiol* *15*, 610–622.
- Biosca, E.G., Amaro, C., Larsen, J.L., and Pedersen, K. (1997). Phenotypic and genotypic characterization of *Vibrio vulnificus*: proposal for the substitution of the subspecific taxon biotype for serovar. *Appl Environ Microbiol* *63*, 1460–1466.
- Bisharat, N., Cohen, D., Harding, R., Falush, D., Crook D., Peto, T., and Maiden, M.C. (2005). Hybrid *Vibrio vulnificus*. *Emerg Infect Dis.* *11*, 30–5.
- Bisharat, N., Amaro, C., Fouz, B., Llorens, A., and Cohen, D.I. (2007a). Serological and molecular characteristics of *Vibrio vulnificus* biotype 3: evidence for high clonality. *Microbiology* *153*, 847–856.
- Bisharat, N., Cohen, D.I., Maiden, M.C., Crook, D.W., Peto, T., and Harding, R.M. (2007b). The evolution of genetic structure in the marine pathogen, *Vibrio vulnificus*. *Infect Genet Evol* *7*, 685–693.
- Blackwell, K.D., and Oliver, J.D. (2008). The ecology of *Vibrio vulnificus*, *Vibrio cholerae*, and *Vibrio parahaemolyticus* in North Carolina estuaries. *J Microbiol* *46*, 146–153.
- Blix, G. (1936). Concerning the carbohydrate groups of submaxillary mucin. *H-S Z Physiol Chem* *240*, 43–54.
- Bogwald, J., and Hoffman, J. (2006). Structural studies of the O-antigenic oligosaccharide from *Vibrio salmonicida* strain C2 isolated from Atlantic cod, *Gadus morhua* L. *Carb Res* *341*, 1965–1968.

- Bouchet, V., Hood, D.W., Li, J., Brisson, J.-R., Randle, G.A., Martin, A., Li, Z., Goldstein, R., Schweda, E.K.H., Pelton, S.I., et al., (2003). Host-derived sialic acid is incorporated into *Haemophilus influenzae* lipopolysaccharide and is a major virulence factor in experimental otitis media. *Proceedings of the National Academy of Sciences* *100*, 8898–8903.
- Brigham, C., Caughlan, R., Gallegos, R., Dallas, M.B., Godoy, V.G., and Malamy, M.H. (2009). Sialic Acid (*N*-acetyl Neuraminic Acid or NANA) Utilization by *Bacteroides fragilis* Requires A Novel *N*-acetyl Mannosamine (manNAc) Epimerase. *J Bacteriol.*
- Bross, M.H., Soch, K., Morales, R., and Mitchell, R.B. (2007). *Vibrio vulnificus* infection: Diagnosis and treatment. *American Family Physician* *76*, 539–544.
- Butor, C., Diaz, S., and Varki, A. (1993). High level O-acetylation of sialic acids on *N*-linked oligosaccharides of rat liver membranes. Differential subcellular distribution of 7- and 9-O-acetyl groups and of enzymes involved in their regulation. *The J Biol Chem* *268*, 10197–10206.
- Cameron, D.J., and Churchill, W.H. (1982). Specificity of macrophage mediated cytotoxicity: role of target cell sialic acid. *The Japanese Journal of Experimental Medicine* *52*, 9–16.
- Carlin, A.F., Lewis, A.L., Varki, A., and Nizet, V. (2007). Group B Streptococcal Capsular Sialic Acids Interact with Siglecs (Immunoglobulin-Like Lectins) on Human Leukocytes. *J Bacteriol* *189*, 1231–1237.
- Carlin, A.F., Uchiyama, S., Chang, Y.C., Lewis, A.L., Nizet, V., and Varki, A. (2009). Molecular mimicry of host sialylated glycans allows a bacterial pathogen to engage neutrophil Siglec-9 and dampen the innate immune response. *Blood* *113*, 3333–3336.
- Castric, P., Cassels, F.J., and Carlson, R.W. (2001). Structural Characterization of the *Pseudomonas aeruginosa* 1244 Pilin Glycan. *J Biol Chem* *276*, 26479–26485.
- Chatzidaki-Livanis, M., Jones, M.K., and Wright, A.C. (2006). Genetic variation in the *Vibrio vulnificus* group 1 capsular polysaccharide operon. *J Bacteriol* *188*, 1987–1998.
- Chen, C.Y., Wu, K.M., Chang, Y.C., Chang, C.H., Tsai, H.C., Liao, T.L., Liu, Y.M., Chen, H.J., Shen, A.B., Li, J.C., et al., (2003). Comparative genome analysis of *Vibrio vulnificus*, a marine pathogen. *Genome Res* *13*, 2577–2587.

- Cohen, A.L., Oliver, J.D., DePaola, A., Feil, E.J., and Boyd, E.F. (2007a). Emergence of a virulent clade of *Vibrio vulnificus* and correlation with the presence of a 33-kilobase genomic island. *Appl Environ Microbiol* 73, 5553–5565.
- Cohen, A.L., J.D. Oliver, A. DePaola, E. Feil, and Boyd., E.F. (2007b). Molecular phylogeny of *Vibrio vulnificus* based on multilocus sequence analysis and a 33 kb genomic island correlates with pathogenic potential. *Appl Environ Microbiol* 73, 5553–5565.
- Condemine, G., Berrier, C., Plumbridge, J., and Ghazi, A. (2005). Function and expression of an *N*-acetylneuraminic acid-inducible outer membrane channel in *Escherichia coli*. *J Bacteriol* 187, 1959–1965.
- Correa, N.E., Peng, F., and Klose, K.E. (2005). Roles of the regulatory proteins FlhF and FlhG in the *Vibrio cholerae* flagellar transcription hierarchy. *J Bacteriol* 187, 6324–6332.
- Culling, C.F.A., Reid, P.E., Clay, M.G., and Dunn, W.L. (1974). The histochemical demonstration of O-acylated sialic acid in gastrointestinal mucins. Their association with the potassium hydroxide-periodic acid-schiff effect. *J Histochem Cytochem* 22, 826–831.
- DePaola, A., Capers, G.M., and Alexander, D. (1994). Densities of *Vibrio vulnificus* in the intestines of fish from the U.S. Gulf Coast. *Appl Environ Microbiol* 60, 984–988.
- DePaola, A., Nordstrom, J.L., Dalsgaard, A., Forslund, A., Oliver, J., Bates, T., Bourdage, K.L., and Gulig, P.A. (2003). Analysis of *Vibrio vulnificus* from market oysters and septicemia cases for virulence markers. *Appl Environ Microbiol* 69, 4006–4011.
- Edebrink, P., Jansson, P.-E., Bøgwald, J., and Hoffman, J. (1996). Structural studies of the *Vibrio salmonicida* lipopolysaccharide. *Carb Res* 287, 225–245.
- Edgar, R.C. (2004). MUSCLE: multiple sequence alignment with high accuracy and high throughput. *Nucleic Acids Res* 32, 1792–1797.
- Edwards, M.S., Kasper, D.L., Jennings, H.J., Baker, C.J., and Nicholson-Weller, A. (1982). Capsular sialic acid prevents activation of the alternative complement pathway by type III, group B streptococci. *The Journal of Immunology* 128, 1278–1283.

- Ewing, C.P., Andreishcheva, E., and Guerry, P. (2009). Functional characterization of flagellin glycosylation in *Campylobacter jejuni* 81-176. *J Bacteriol* *191*, 7086–7093.
- Finne, J., Leinonen, M., and Mäkelä, P.H. (1983). Antigenic similarities between brain components and bacteria causing meningitis. *The Lancet* *322*, 355–357.
- Fischer, M., Zhang, Q., Hubbard, R., and Thomas, G. (2010). Caught in a TRAP: substrate-binding proteins in secondary transport. *Trends Microbiol.* *18*, 471–478.
- Frerk, F. (2000). The role of seafood in bacterial foodborne diseases. *Microbes and Infection* *2*, 1651–1660.
- Fuerst, J.A., and Perry, J.W. (1988). Demonstration of lipopolysaccharide on sheathed flagella of *Vibrio cholerae* O:1 by protein A-gold immunoelectron microscopy. *J Bacteriol* *170*, 1488–1494.
- Gil-Serrano, A.M., Rodriguez-Carvajal, M.A., Tejero-Mateo, P., Espartero, J.L., Menendez, M., Corzo, J., Ruiz-Sainz, J.E., and Buendi, A.C.A.M. (1999). Structural determination of a 5-acetamido-3,5,7, 9-tetra-deoxy-7-(3-hydroxybutyramido)-L-glycero-L-manno-nonulosonic acid-containing homopolysaccharide isolated from *Sinorhizobium fredii* HH103. *Biochem J* *342 Pt 3*, 527–535.
- Glaze, P.A., Watson, D.C., Young, N.M., and Tanner, M.E. (2008). Biosynthesis of CMP-N,N'-Diacetyllegionaminic Acid from UDP-N,N'-Diacetylbaucillosamine in *Legionella pneumophila*†. *Biochemistry* *47*, 3272–3282.
- Goon, S., Kelly, J.F., Logan, S.M., Ewing, C.P., and Guerry, P. (2003). Pseudaminic acid, the major modification on *Campylobacter* flagellin, is synthesized via the Cj1293 gene. *Molecular Microbiology* *50*, 659–671.
- Grimes, D.J., Johnson, C.N., Dillon, K.S., Flowers, A.R., Noriega, N.F., 3rd, and Berutti, T. (2009). What genomic sequence information has revealed about *Vibrio* ecology in the ocean--a review. *Microb Ecol* *58*, 447–460.
- Guerry, P., Ewing, C.P., Hickey, T.E., Prendergast, M.M., and Moran, A.P. (2000). Sialylation of lipooligosaccharide cores affects immunogenicity and serum resistance of *Campylobacter jejuni*. *Infect Immun* *68*, 6656–6662.

- Guerry, P., Ewing, C.P., Schirm, M., Lorenzo, M., Kelly, J., Pattarini, D., Majam, G., Thibault, P., and Logan, S. (2006). Changes in flagellin glycosylation affect *Campylobacter* autoagglutination and virulence. *Molecular Microbiology* 60, 299–311.
- Guindon, S., and Gascuel, O. (2003). A simple, fast, and accurate algorithm to estimate large phylogenies by maximum likelihood. *Syst Biol* 52, 696–704.
- Guindon, S., Lethiec, F., Duroux, P., and Gascuel, O. (2005). PHYML Online--a web server for fast maximum likelihood-based phylogenetic inference. *Nucleic Acids Res* 33, W557–9.
- Gulig, P.A., Bourdage, K.L., and Starks, A.M. (2005). Molecular pathogenesis of *Vibrio vulnificus*. *J Microbiol* 43 Spec No, 118–131.
- Gulig, P.A., Tucker, M.S., Thiaville, P.C., Joseph, J.L., and Brown, R.N. (2009). USER friendly cloning coupled with chitin-based natural transformation enables rapid mutagenesis of *Vibrio vulnificus*. *Appl Environ Microbiol* 75, 4936–4949.
- Gulig, P.A., de Crecy-Lagard, V., Wright, A.C., Walts, B., Telonis-Scott, M., and McIntyre, L.M. (2010). SOLiD sequencing of four *Vibrio vulnificus* genomes enables comparative genomic analysis and identification of candidate clade-specific virulence genes. *BMC Genomics* 11, 512.
- Harwood, V.J., Gandhi, J.P., and Wright, A.C. (2004). Methods for isolation and confirmation of *Vibrio vulnificus* from oysters and environmental sources: a review. *J Microbiol Methods* 59, 301–316.
- Hashii, N., Isshiki, Y., Iguchi, T., Hisatsune, K., and Kondo, S. (2003). Structure and serological characterization of 5,7-diamino-3,5,7,9-tetra-deoxy-non-2-ulosonic acid isolated from lipopolysaccharides of *Vibrio parahaemolyticus* O2 and O-untypable strain KX-V212. *Carb Res* 338, 1055–1062.
- Hayat, U., Reddy, G.P., Bush, C.A., Johnson, J.A., Wright, A.C., and Morris, J.G., Jr. (1993). Capsular types of *Vibrio vulnificus*: an analysis of strains from clinical and environmental sources. *J Infect Dis* 168, 758–762.
- Heidelberg, J.F., Heidelberg, K.B., and Colwell, R.R. (2002a). Bacteria of the gamma-subclass Proteobacteria associated with zooplankton in Chesapeake Bay. *Appl Environ Microbiol* 68, 5498–5507.

- Heidelberg, J.F., Heidelberg, K.B., and Colwell, R.R. (2002b). Seasonality of Chesapeake Bay bacterioplankton species. *Appl Environ Microbiol* 68, 5488–5497.
- Higa, H.H., Butor, C., Diaz, S., and Varki, A. (1989). O-acetylation and de-O-acetylation of sialic acids. O-acetylation of sialic acids in the rat liver Golgi apparatus involves an acetyl intermediate and essential histidine and lysine residues--a transmembrane reaction? *J Biol Chem* 264, 19427–19434.
- Ho, J.J., Cheng, S., and Kim, Y.S. (1995). Access to peptide regions of a surface mucin (MUC1) is reduced by sialic acids. *Biochemical and Biophysical Research Communications* 210, 866–873.
- Hood, D.W., Makepeace, K., Deadman, M.E., Rest, R.F., Thibault, P., Martin, A., Richards, J.C., and Moxon, E.R. (1999). Sialic acid in the lipopolysaccharide of *Haemophilus influenzae*: strain distribution, influence on serum resistance and structural characterization. *Molecular Microbiology* 33, 679–692.
- Hopkins, A.P., Hawkhead, J.A., and Thomas, G.H. (2013). Transport and catabolism of the sialic acids *N*-glycolylneuraminic acid and 3-keto-3-deoxy-D-glycero-D-galactonononic acid by *Escherichia coli* K-12. *FEMS Microbiol Lett* 347, 14–22.
- Horton, R.M., Hunt, H.D., Ho, S.N., Pullen, J.K., and Pease, L.R. (1989). Engineering hybrid genes without the use of restriction enzymes: gene splicing by overlap extension. *Gene* 77, 61–68.
- Houliston, R.S., Vinogradov, E., Dzieciatkowska, M., Li, J., St Michael, F., Karwaski, M.F., Brochu, D., Jarrell, H.C., Parker, C.T., Yuki, N., et al., The lipooligosaccharide of *Campylobacter jejuni*: Similarity with multiple types of mammalian glycans beyond gangliosides. *J Biol Chem*.
- Howard, S.L., Jagannathan, A., Soo, E.C., Hui, J.P.M., Aubry, A.J., Ahmed, I., Karlyshev, A., Kelly, J.F., Jones, M.A., Stevens, M.P., et al., (2009). *Campylobacter jejuni* glycosylation island important in cell charge, legionaminic acid biosynthesis, and colonization of chickens. *Infect Immun* 77, 2544–2556.
- Hunt, D.E., Gevers, D., Vahora, N.M., and Polz, M.F. (2008). Conservation of the chitin utilization pathway in the Vibrionaceae. *Appl. Environ. Microbiol.* 74, 44–51.
- Huson, D.H. (1998). SplitsTree: analyzing and visualizing evolutionary data. *Bioinformatics* 14, 68–73.

- Inoue, S., and Kitajima, K. (2006). KDN (deaminated neuraminic acid): dreamful past and exciting future of the newest member of the sialic acid family. *Glycoconjugate Journal* 23, 277–290.
- Jeong, H.G., Oh, M.H., Kim, B.S., Lee, M.Y., Han, H.J., and Choi, S.H. (2009). The capability of catabolic utilization of *N*-Acetylneuraminic Acid, a sialic acid, is essential for *Vibrio vulnificus* pathogenesis. *Infect. Immun.* 77, 3209–3217.
- Jermyn, W.S., and Boyd, E.F. (2002). Characterization of a novel *Vibrio* pathogenicity island (VPI-2) encoding neuraminidase (nanH) among toxigenic *Vibrio cholerae* isolates. *Microbiology* 148, 3681–3693.
- Jermyn, W.S., and Boyd, E.F. (2005). Molecular evolution of *Vibrio* pathogenicity island-2 (VPI-2): mosaic structure among *Vibrio cholerae* and *Vibrio mimicus* natural isolates. *Microbiology* 151, 311–322.
- Jones, M.K., and Oliver, J.D. (2009). *Vibrio vulnificus*: disease and pathogenesis. *Infect Immun* 77, 1723–1733.
- Jones, C., Virji, M., and Crocker, P.R. (2003). Recognition of sialylated meningococcal lipopolysaccharide by siglecs expressed on myeloid cells leads to enhanced bacterial uptake. *Mol Microbiol* 49, 1213–1225.
- Kahler, C.M., Martin, L.E., Shih, G.C., Rahman, M.M., Carlson, R.W., and Stephens, D.S. (1998). The (α 2→8)-Linked Polysialic Acid Capsule and Lipooligosaccharide Structure Both Contribute to the Ability of Serogroup B *Neisseria meningitidis* To Resist the Bactericidal Activity of Normal Human Serum. *Infect Immun* 66, 5939–5947.
- Kasper, D.L., Winkelhake, J.L., Zollinger, W.D., Brandt, B.L., and Artenstein, M.S. (1973). Immunochemical similarity between polysaccharide antigens of *Escherichia Coli* 07:K1(L):NM and Group B *Neisseria Meningitidis*. *The Journal of Immunology* 110, 262–268.
- Kaysner, C.A., Abeyta, C., Jr., Wekell, M.M., DePaola, A., Jr., Stott, R.F., and Leitch, J.M. (1987). Virulent strains of *Vibrio vulnificus* isolated from estuaries of the United States West Coast. *Appl Environ Microbiol* 53, 1349–1351.
- Kaysner, C.A., Tamplin, M.L., Wekell, M.M., Stott, R.F., and Colburn, K.G. (1989). Survival of *Vibrio vulnificus* in shellstock and shucked oysters (*Crassostrea gigas* and *Crassostrea virginica*) and effects of isolation medium on recovery. *Appl Environ Microbiol* 55, 3072–3079.

- Kazatchkine, M.D., Fearon, D.T., and Austen, K.F. (1979). Human alternative complement pathway: membrane-associated sialic acid regulates the competition between B and beta1 H for cell-bound C3b. *Journal of Immunology (Baltimore, Md. : 1950)* *122*, 75–81.
- Khatua, B., Ghoshal, A., Bhattacharya, K., Mandal, C., Saha, B., and Crocker, P.R. Sialic acids acquired by *Pseudomonas aeruginosa* are involved in reduced complement deposition and siglec mediated host-cell recognition. *FEBS Lett* *584*, 555–561.
- Kim, B.S., Hwang, J., Kim, M.H., and Choi, S.H. (2011). Cooperative regulation of the *Vibrio vulnificus* nan gene cluster by NanR protein, cAMP receptor protein, and *N*-acetylmannosamine 6-phosphate. *J Biol Chem* *286*, 40889–40899.
- Kim, I.H., Wen, Y., Son, J.-S., Lee, K.-H., and Kim, K.-S. (2013). The Fur-Iron Complex Modulates Expression of the Quorum-Sensing Master Regulator, SmcR, To Control Expression of Virulence Factors in *Vibrio vulnificus*. *Infect Immun* *81*, 2888–2898.
- Kim, M.Y., Park, R.Y., Choi, M.H., Sun, H.Y., Kim, C.M., Kim, S.Y., Rhee, J.H., and Shin, S.H. (2006). Swarming differentiation of *Vibrio vulnificus* downregulates the expression of the vvhBA hemolysin gene via the LuxS quorum-sensing system. *J Microbiol* *44*, 226–232.
- Kim, S.M., Lee, D.H., and Choi, S.H. (2012). Evidence that the *Vibrio vulnificus* flagellar regulator FlhF is regulated by a quorum sensing master regulator SmcR. *Microbiology* *158*, 2017–2025.
- Knirel, Y.A., Vinogradov, E.V., L'Vov V, L., Kocharova, N.A., Shashkov, A.S., Dmitriev, B.A., and Kochetkov, N.K. (1984). Sialic acids of a new type from the lipopolysaccharides of *Pseudomonas aeruginosa* and *Shigella boydii*. *Carb Res* *133*, C5–8.
- Knirel, Y.A., Rietschel, E.T., Marre, R., and ZÄHringer, U. (1994). The structure of the O-specific chain of *Legionella pneumophila* serogroup 1 lipopolysaccharide. *European Journal of Biochemistry* *221*, 239–245.
- Knirel, Y.A., Moll, H., Helbig, J.H., and Zahringer, U. (1997). Chemical characterization of a new 5,7-diamino-3,5,7,9-tetradexynonulosonic acid released by mild acid hydrolysis of the *Legionella pneumophila* serogroup 1 lipopolysaccharide. *Carb Res* *304*, 77–79.

- Knirel, Y.A., Shashkov, A.S., Tsvetkov, Y.E., Jansson, P.E., and Zahringer, U. (2003). 5,7-Diamino-3,5,7,9-tetraoxynon-2-ulosonic acids in bacterial glycopolymers: chemistry and biochemistry. *Advances in Carbohydrate Chemistry and Biochemistry* 58, 371–417.
- Komagamine, T., and Yuki, N. (2006). Ganglioside mimicry as a cause of Guillain-Barre syndrome. *CNS Neurol Disord Drug Targets* 5, 391–400.
- Kovach, M.E., Phillips, R.W., Elzer, P.H., Roop, R.M., 2nd, and Peterson, K.M. (1994). pBBR1MCS: a broad-host-range cloning vector. *BioTechniques* 16, 800–802.
- Kundig, F.D., Aminoff, D., and Roseman, S. (1971). The Sialic Acids. *J Biol Chem* 246, 2543–2550.
- Kurniyati, K., Zhang, W., Zhang, K., and Li, C. (2013). A surface-exposed neuraminidase affects complement resistance and virulence of the oral spirochaete *Treponema denticola*. *Mol Microbiol* 89, 842–856.
- Kwak, J.S., Jeong, H.G., and Satchell, K.J. (2011). *Vibrio vulnificus* rtxA1 gene recombination generates toxin variants with altered potency during intestinal infection. *Proc Natl Acad Sci U S A* 108, 1645–1650.
- Lanoue, A., Batista, F.D., Stewart, M., and Neuberger, M.S. (2002). Interaction of CD22 with alpha2,6-linked sialoglycoconjugates: innate recognition of self to dampen B cell autoreactivity? *European Journal of Immunology* 32, 348–355.
- Larkin, M.A., Blackshields, G., Brown, N.P., Chenna, R., McGettigan, P.A., McWilliam, H., Valentin, F., Wallace, I.M., Wilm, A., Lopez, R., et al., (2007). Clustal W and Clustal X version 2.0. *Bioinformatics* 23, 2947–2948.
- Lee, J.H., Kim, M.W., Kim, B.S., Kim, S.M., Lee, B.C., Kim, T.S., and Choi, S.H. (2007). Identification and characterization of the *Vibrio vulnificus* rtxA essential for cytotoxicity in vitro and virulence in mice. *J Microbiol* 45, 146–152.
- Lewis, A.L., Nizet, V., and Varki, A. (2004). Discovery and characterization of sialic acid O-acetylation in group B *Streptococcus*. *Proceedings of the National Academy of Sciences of the United States of America* 101, 11123–11128.
- Lewis, A.L., Hensler, M.E., Varki, A., and Nizet, V. (2006). The Group B *Streptococcal* Sialic Acid O-Acetyltransferase Is Encoded by neuD, a Conserved Component of Bacterial Sialic Acid Biosynthetic Gene Clusters. *J Biol Chem* 281, 11186–11192.

- Lewis, A.L., Desa, N., Hansen, E.E., Knirel, Y.A., Gordon, J.I., Gagneux, P., Nizet, V., and Varki, A. (2009). Innovations in host and microbial sialic acid biosynthesis revealed by phylogenomic prediction of nonulosonic acid structure. *Proceedings of the National Academy of Sciences* *106*, 13552–13557.
- Lewis, A.L., Lubin, J.B., Argade, S., Naidu, N., Choudhury, B., and Boyd, E.F. (2011). Genomic and metabolic profiling of nonulosonic acids in *Vibrionaceae* reveal biochemical phenotypes of allelic divergence in *Vibrio vulnificus*. *Appl Environ Microbiol* *77*, 5782–5793.
- Lewis, W.G., Robinson, L.S., Gilbert, N.M., Perry, J.C., and Lewis, A.L. (2013). Degradation, Foraging, and Depletion of Mucus Sialoglycans by the Vagina-adapted Actinobacterium *Gardnerella vaginalis*. *J Biol Chem* *288*, 12067–12079.
- Li, X., and Roseman, S. (2004). The chitinolytic cascade in *Vibrios* is regulated by chitin oligosaccharides and a two-component chitin catabolic sensor/kinase. *Proceedings of the National Academy of Sciences of the United States of America* *101*, 627–631.
- Li, X., Perepelov, A.V., Wang, Q., Senchenkova, S.N., Liu, B., Shevelev, S.D., Guo, X., Shashkov, A.S., Chen, W., Wang, L., et al., (7). Structural and genetic characterization of the O-antigen of *Escherichia coli* O161 containing a derivative of a higher acidic diamino sugar, legionaminic acid. *Carb Res* *345*, 1581–1587.
- Linkous, D.A., and Oliver, J.D. (1999). Pathogenesis of *Vibrio vulnificus*. *FEMS Microbiol Lett* *174*, 207–214.
- Linton, D., Karlyshev, A.V., Hitchen, P.G., Morris, H.R., Dell, A., Gregson, N.A., and Wren, B.W. (2000). Multiple *N*-acetyl neuraminic acid synthetase (neuB) genes in *Campylobacter jejuni*: identification and characterization of the gene involved in sialylation of lipo-oligosaccharide. *Mol Microbiol* *35*, 1120–1134.
- Litwin, C.M., Rayback, T.W., and Skinner, J. (1996). Role of catechol siderophore synthesis in *Vibrio vulnificus* virulence. *Infect Immun* *64*, 2834–2838.
- Logan, S.M., Kelly, J.F., Thibault, P., Ewing, C.P., and Guerry, P. (2002). Structural heterogeneity of carbohydrate modifications affects serospecificity of *Campylobacter* flagellins. *Molecular Microbiology* *46*, 587–597.

- Logan, S.M., Hui, J.P., Vinogradov, E., Aubry, A.J., Melanson, J.E., Kelly, J.F., Nothhaft, H., and Soo, E.C. (2009). Identification of novel carbohydrate modifications on *Campylobacter jejuni* 11168 flagellin using metabolomics-based approaches. *The FEBS Journal*.
- Mandal, C. (1990). Sialic acid binding lectins. *Experientia* 46, 433–441.
- Marion, C., Aten, A.E., Woodiga, S.A., and King, S.J. (2011). Identification of an ATPase, MsmK, which energizes multiple carbohydrate ABC transporters in *Streptococcus pneumoniae*. *Infect Immun* 79, 4193–4200.
- Martinez, J., Steenbergen, S., and Vimr, E. (1995). Derived structure of the putative sialic acid transporter from *Escherichia coli* predicts a novel sugar permease domain. *J Bacteriol* 177, 6005–6010.
- Mazumder, K., Choudhury, B., Nair, G.B., and Sen, A. (2008). Identification of a novel sugar 5,7-diacetamido-8-amino-3,5,7,8,9-pentadeoxy-d-glycero-d-galacto-non-2-ulosonic acid present in the lipooligosaccharide of *Vibrio parahaemolyticus* O3:K6. *Glycoconj J* 25, 345–354.
- McCarter, L., Hilmen, M., and Silverman, M. (1988). Flagellar dynamometer controls swarmer cell differentiation of *V. parahaemolyticus*. *Cell* 54, 345–351.
- McNally, D.J., Hui, J.P., Aubry, A.J., Mui, K.K., Guerry, P., Brisson, J.R., Logan, S.M., and Soo, E.C. (2006). Functional characterization of the flagellar glycosylation locus in *Campylobacter jejuni* 81-176 using a focused metabolomics approach. *The J Biol Chem* 281, 18489–18498.
- McNally, D.J., Aubry, A.J., Hui, J.P., Khieu, N.H., Whitfield, D., Ewing, C.P., Guerry, P., Brisson, J.R., Logan, S.M., and Soo, E.C. (2007). Targeted metabolomics analysis of *Campylobacter coli* VC167 reveals legionaminic acid derivatives as novel flagellar glycans. *The J Biol Chem* 282, 14463–14475.
- Michael, F.S., Szymanski, C.M., Li, J., Chan, K.H., Khieu, N.H., Larocque, S., Wakarchuk, W.W., Brisson, J.-R., and Monteiro, M.A. (2002). The structures of the lipooligosaccharide and capsule polysaccharide of *Campylobacter jejuni* genome sequenced strain NCTC 11168. *European Journal of Biochemistry* 269, 5119–5136.
- Morris, J.G., Jr., Wright, A.C., Roberts, D.M., Wood, P.K., Simpson, L.M., and Oliver, J.D. (1987). Identification of environmental *Vibrio vulnificus* isolates with a DNA probe for the cytotoxin-hemolysin gene. *Appl Environ Microbiol* 53, 193–195.

- Motes, M.L., DePaola, A., Cook, D.W., Veazey, J.E., Hunsucker, J.C., Garthright, W.E., Blodgett, R.J., and Chirtel, S.J. (1998a). Influence of water temperature and salinity on *Vibrio vulnificus* in Northern Gulf and Atlantic Coast oysters (*Crassostrea virginica*). *Appl Environ Microbiol* *64*, 1459–1465.
- Motes, M.L., DePaola, A., Cook, D.W., Veazey, J.E., Hunsucker, J.C., Garthright, W.E., Blodgett, R.J., and Chirtel, S.J. (1998b). Influence of Water Temperature and Salinity on *Vibrio vulnificus* in Northern Gulf and Atlantic Coast Oysters (*Crassostrea virginica*). *Appl Environ Microbiol* *64*, 1459–1465.
- Mulligan, C., Geertsma, E.R., Severi, E., Kelly, D.J., Poolman, B., and Thomas, G.H. (2009). The substrate-binding protein imposes directionality on an electrochemical sodium gradient-driven TRAP transporter. *Proc Natl Acad Sci U S A* *106*, 1778–1783.
- Mulligan, C., Fischer, M., and Thomas, G.H. (2011a). Tripartite ATP-independent periplasmic (TRAP) transporters in bacteria and archaea. *FEMS Microbiol Rev.* *35*, 68–86.
- Mulligan, C., Leech, A.P., Kelly, D.J., and Thomas, G.H. (2011b). The membrane proteins, SiaQ and SiaM, form an essential stoichiometric complex in the sialic acid TRAP transporter SiaPQM (VC1777-1779) from *Vibrio cholerae*. *J Biol Chem*.
- Mushtaq, N., Redpath, M.B., Luzio, J.P., and Taylor, P.W. (2004). Prevention and Cure of Systemic *Escherichia coli* K1 Infection by Modification of the Bacterial Phenotype. *Antimicrobial Agents and Chemotherapy* *48*, 1503–1508.
- Naito, M., Fridrich, E., Fields, J.A., Pryjma, M., Li, J., Cameron, A., Gilbert, M., Thompson, S.A., and Gaynor, E.C. Effects of sequential *Campylobacter jejuni* 81-176 lipooligosaccharide core truncations on biofilm formation, stress survival, and pathogenesis. *J Bacteriol* *192*, 2182–2192.
- Nees, S., Schauer, R., and Mayer, F. (1976). Purification and characterization of *N*-acetylneuraminidase from *Clostridium perfringens*. *Hoppe Seylers Z Physiol Chem* *357*, 839–853.
- Nilsson, W.B., Paranjypte, R.N., DePaola, A., and Strom, M.S. (2003). Sequence polymorphism of the 16S rRNA gene of *Vibrio vulnificus* is a possible indicator of strain virulence. *J Clin Microbiol* *41*, 442–446.

- Nyholm, S.V., Stabb, E.V., Ruby, E.G., and McFall-Ngai, M.J. (2000). Establishment of an animal–bacterial association: Recruiting symbiotic vibrios from the environment. *Proceedings of the National Academy of Sciences* 97, 10231–10235.
- Ogasawara, Y., Namai, T., Yoshino, F., Lee, M.C., and Ishii, K. (5). Sialic acid is an essential moiety of mucin as a hydroxyl radical scavenger. *FEBS Letters* 581, 2473–2477.
- Oliver, J.D. (1995). The viable but non-culturable state in the human pathogen *Vibrio vulnificus*. *FEMS Microbiol Lett* 133, 203–208.
- Oliver, J.D. (2005). Wound infections caused by *Vibrio vulnificus* and other marine bacteria. *Epidemiol Infect* 133, 383–391.
- Oliver, J.D., Warner, R.A., and Cleland, D.R. (1982). Distribution and ecology of *Vibrio vulnificus* and other lactose-fermenting marine vibrios in coastal waters of the southeastern United States. *Appl Environ Microbiol* 44, 1404–1414.
- Oliver, J.D., Warner, R.A., and Cleland, D.R. (1983). Distribution of *Vibrio vulnificus* and other lactose-fermenting vibrios in the marine environment. *Appl Environ Microbiol* 45, 985–998.
- Oliver, J.D., Guthrie, K., Preyer, J., Wright, A., Simpson, L.M., Siebeling, R., and Morris, J.G., Jr. (1992). Use of colistin-polymyxin B-cellobiose agar for isolation of *Vibrio vulnificus* from the environment. *Appl Environ Microbiol* 58, 737–739.
- Ozkan, A.N., and Ninnemann, J.L. (1985). Suppression of in vitro lymphocyte and neutrophil responses by a low molecular weight suppressor active peptide from burn-patient sera. *Journal of Clinical Immunology* 5, 172–179.
- Paranjpye, R.N., and Strom, M.S. (2005). A *Vibrio vulnificus* Type IV Pilin Contributes to Biofilm Formation, Adherence to Epithelial Cells, and Virulence. *Infect Immun* 73, 1411–1422.
- Parsons, N.J., Patel, P.V., Tan, E.L., Andrade, J.R., Nairn, C.A., Goldner, M., Cole, J.A., and Smith, H. (1988). Cytidine 5'-monophospho-*N*-acetyl neuraminic acid and a low molecular weight factor from human blood cells induce lipopolysaccharide alteration in gonococci when conferring resistance to killing by human serum. *Microbial Pathogenesis* 5, 303–309.

- Perepelov, A.V., Liu, B., Senchenkova, S.N., Shashkov, A.S., Shevelev, S.D., Feng, L., Wang, L., and Knirel, Y.A. Structure of the O-antigen and characterization of the O-antigen gene cluster of *Escherichia coli* O108 containing 5,7-diacetamido-3,5,7,9-tetra-deoxy-L-glycero-D-galacto-non-2-ulose (8-epilegionaminic) acid. *Biochemistry (Mosc)* 75, 19–24.
- Petersen, M., Fessner, W.-D., Frosch, M., and Lüneberg, E. (2000). The *siaA* gene involved in capsule polysaccharide biosynthesis of *Neisseria meningitidis* B codes for *N*-acylglucosamine-6-phosphate 2-epimerase activity. *FEMS Microbiology Letters* 184, 161–164.
- Philippe, N., Alcaraz, J.P., Coursange, E., Geiselmann, J., and Schneider, D. (2004). Improvement of pCVD442, a suicide plasmid for gene allele exchange in bacteria. *Plasmid* 51, 246–255.
- Post, D.M., Mungur, R., Gibson, B.W., and Munson, R.S., Jr. (2005). Identification of a novel sialic acid transporter in *Haemophilus ducreyi*. *Infect Immun* 73, 6727–6735.
- Post, D.M.B., Yu, L., Krasity, B.C., Choudhury, B., Mandel, M.J., Brennan, C.A., Ruby, E.G., McFall-Ngai, M.J., Gibson, B.W., and Apicella, M.A. (2012). O-antigen and Core Carbohydrate of *Vibrio fischeri* Lipopolysaccharide: composition and analysis of their role in eupyrymna scolopes light organ colonization. *J Biol Chem* 287, 8515–8530.
- Le Quere, A.J., Deakin, W.J., Schmeisser, C., Carlson, R.W., Streit, W.R., Broughton, W.J., and Forsberg, L.S. (2006). Structural characterization of a K-antigen capsular polysaccharide essential for normal symbiotic infection in *Rhizobium* sp. NGR234: deletion of the *rkpMNO* locus prevents synthesis of 5,7-diacetamido-3,5,7,9-tetra-deoxy-non-2-ulose acid. *The J Biol Chem* 281, 28981–28992.
- Quirke, A.M., Reen, F.J., Claesson, M.J., and Boyd, E.F. (2006). Genomic island identification in *Vibrio vulnificus* reveals significant genome plasticity in this human pathogen. *Bioinformatics* 22, 905–910.
- Robbe, C., Capon, C., Coddeville, B., and Michalski, J.C. (2004). Structural diversity and specific distribution of O-glycans in normal human mucins along the intestinal tract. *The Biochemical Journal* 384, 307–316.
- Rosche, T.M., Yano, Y., and Oliver, J.D. (2005). A rapid and simple PCR analysis indicates there are two subgroups of *Vibrio vulnificus* which correlate with clinical or environmental isolation. *Microbiol Immunol* 49, 381–389.

- Roy, S., Douglas, C.W., and Stafford, G.P. (2010). A novel sialic acid utilization and uptake system in the periodontal pathogen *Tannerella forsythia*. *J Bacteriol* *192*, 2285–2293.
- Rutishauser, U. (2008). Polysialic acid in the plasticity of the developing and adult vertebrate nervous system. *Nature Reviews. Neuroscience* *9*, 26–35.
- Sakarya, S., Gokturk, C., Ozturk, T., and Ertugrul, M.B. (2010). Sialic acid is required for nonspecific adherence of *Salmonella enterica* ssp. *enterica* serovar Typhi on Caco-2 cells. *FEMS Immunol Med Microbiol* *58*, 330–335.
- Sanjuan, E., and Amaro, C. (2007). Multiplex PCR assay for detection of *Vibrio vulnificus* biotype 2 and simultaneous discrimination of serovar E strains. *Appl Environ Microbiol* *73*, 2029–2032.
- Sanjuan, E., Fouz, B., Oliver, J.D., and Amaro, C. (2009). Evaluation of genotypic and phenotypic methods to distinguish clinical from environmental *Vibrio vulnificus* strains. *Appl Environ Microbiol* *75*, 1604–1613.
- Sanjuan, E., Gonzalez-Candelas, F., and Amaro, C. (2010). Polyphyletic origin of *Vibrio vulnificus* biotype 2 as revealed by sequence-based analysis. *Appl Environ Microbiol* *77*, 688–695.
- Schirm, M., Soo, E.C., Aubry, A.J., Austin, J., Thibault, P., and Logan, S.M. (2003). Structural, genetic and functional characterization of the flagellin glycosylation process in *Helicobacter pylori*. *Molecular Microbiology* *48*, 1579–1592.
- Schoenhofen, I.C., Vinogradov, E., Whitfield, D.M., Brisson, J.-R., and Logan, S.M. (2009). The CMP-legionaminic acid pathway in *Campylobacter*: Biosynthesis involving novel GDP-linked precursors. *Glycobiology* *19*, 715–725.
- Scudder, P.R., and Chantler, E.N. (1982). Control of human cervical mucin glycosylation by endogenous fucosyl and sialyltransferases. *Advances in Experimental Medicine and Biology* *144*, 265–267.
- Senchenkova, S.N., Shashkov, A.S., Knirel, Y.A., Esteve, C., Alcaide, E., Merino, S., and Tomás, J.M. (2009). Structure of a polysaccharide from the lipopolysaccharide of *Vibrio vulnificus* clinical isolate YJ016 containing 2-acetimidoylamino-2-deoxy-l-galacturonic acid. *Carb Res* *344*, 1009–1013.

- Severi, E., Randle, G., Kivlin, P., Whitfield, K., Young, R., Moxon, R., Kelly, D., Hood, D., and Thomas, G.H. (2005). Sialic acid transport in *Haemophilus influenzae* is essential for lipopolysaccharide sialylation and serum resistance and is dependent on a novel tripartite ATP-independent periplasmic transporter. *Mol Microbiol* 58, 1173–1185.
- Severi, E., Hood, D.W., and Thomas, G.H. (2007). Sialic acid utilization by bacterial pathogens. *Microbiology* 153, 2817–2822.
- Severi, E., Hosie, A.H., Hawkhead, J.A., and Thomas, G.H. (2010). Characterization of a novel sialic acid transporter of the sodium solute symporter (SSS) family and in vivo comparison with known bacterial sialic acid transporters. *FEMS Microbiol Lett* 304, 47–54.
- Sharma, S.K., Moe, T.S., Srivastava, R., Chandra, D., and Srivastava, B.S. (2011). Functional characterization of VC1929 of *Vibrio cholerae* El Tor: role in mannose-sensitive haemagglutination, virulence and utilization of sialic acid. *Microbiology* 157, 3180–3186.
- Shashkov, A.S., Kocharova, N.A., Zatonksy, G.V., Blaszczyk, A., Knirel, Y.A., and Rozalski, A. (2007). Structure of the O-antigen of *Providencia stuartii* O20, a new polysaccharide containing 5,7-diacetamido-3,5,7,9-tetra-deoxy-l-glycero-d-galacto-non-2-ulosonic acid. *Carb Res* 342, 653–658.
- Simpson, L.M., White, V.K., Zane, S.F., and Oliver, J.D. (1987). Correlation between virulence and colony morphology in *Vibrio vulnificus*. *Infect Immun* 55, 269–272.
- Slomiany, B.L., Murty, V.L.N., Piotrowski, J., and Slomiany, A. (1996). Salivary mucins in oral mucosal defense. *General Pharmacology: The Vascular System* 27, 5 761–771.
- Starks, A.M., Schoeb, T.R., Tamplin, M.L., Parveen S., Doyle T.J., Bomeisl, P.E., Escudero, G.M., Gulig, P.A. (2000). Pathogenesis of infection by clinical and environmental strains of *Vibrio vulnificus* in iron-dextran-treated mice *Infect Immun* 68, 5785–5793.
- Steenbergen, S.M., Lichtensteiger, C.A., Caughlan, R., Garfinkle, J., Fuller, T.E., and Vimr, E.R. (2005). Sialic Acid metabolism and systemic pasteurellosis. *Infect Immun* 73, 1284–1294.
- Strom, M., and Paranjpye, R.N. (2000). Epidemiology and pathogenesis of *Vibrio vulnificus*. *Microbes Infect.* 2, 177–188.

- Swords, W.E., Moore, M.L., Godzicki, L., Bukofzer, G., Mitten, M.J., and VonCannon, J. (2004). Sialylation of lipooligosaccharides promotes biofilm formation by nontypeable *Haemophilus influenzae*. *Infect Immun* 72, 106–113.
- Tacket, C.O., Brenner, F., and Blake, P.A. (1984). Clinical Features and an Epidemiological Study of *Vibrio vulnificus* Infections. *Journal of Infectious Diseases* 149, 558–561.
- Tamplin, M.L., and Capers, G.M. (1992). Persistence of *Vibrio vulnificus* in tissues of Gulf Coast oysters, *Crassostrea virginica*, exposed to seawater disinfected with UV light. *Appl Environ Microbiol* 58, 1506–1510.
- Tamplin, M., Rodrick, G.E., Blake, N.J., and Cuba, T. (1982). Isolation and characterization of *Vibrio vulnificus* from two Florida estuaries. *Appl Environ Microbiol* 44, 1466–1470.
- Tamura, K., Dudley, J., Nei, M., and Kumar, S. (2007). MEGA4: Molecular Evolutionary Genetics Analysis (MEGA) software version 4.0. *Mol Biol Evol* 24, 1596–1599.
- Thiaville, P.C., Bourdage, K.L., Wright, A.C., Farrell-Evans, M., Garvan, C.W., and Gulig, P.A. (2011). Genotype is correlated with but does not predict virulence of *Vibrio vulnificus* biotype 1 in subcutaneously inoculated, iron dextran-treated mice. *Infect Immun* 79, 1194–1207.
- Thibault, P., Logan, S.M., Kelly, J.F., Brisson, J.-R., Ewing, C.P., Trust, T.J., and Guerry, P. (2001). Identification of the carbohydrate moieties and glycosylation motifs in *Campylobacter jejuni* flagellin. *J Biol Chem* 276, 34862–34870.
- Thomas, G.H., and Boyd, E.F. (2011). On sialic acid transport and utilization by *Vibrio cholerae*. *Microbiology* 157, 3253–5.
- Thornton, D.J., Carlstedt, I., Howard, M., Devine, P.L., Price, M.R., and Sheehan, J.K. (1996). Respiratory mucins: identification of core proteins and glycoforms. *The Biochemical Journal* 316 (Pt 3), 967–975.
- Tsvetkov, Y.E., Shashkov, A.S., Knirel, Y.A., Zahringer, U. (2001) Synthesis and identification in bacterial lipopolysaccharides of 5,7-diacetamido-3,5,7,9-tetradeoxy-D-glycero-D-galacto- and -D-glycero-D-talo-non-2-ulonic acids. *Carb Res* 331 3, 233-237.

- Vann, W.F., Silver, R.P., Abeijon, C., Chang, K., Aaronson, W., Sutton, A., Finn, C.W., Lindner, W., and Kotsatos, M. (1987). Purification, properties, and genetic location of *Escherichia coli* cytidine 5'-monophosphate *N*-acetylneuraminic acid synthetase. *J Biol Chem* 262, 17556–17562.
- Vann, W.F., Tavarez, J.J., Crowley, J., Vimr, E., and Silver, R.P. (1997). Purification and characterization of the *Escherichia coli* K1 neuB gene product *N*-acetylneuraminic acid synthetase. *Glycobiology* 7, 697–701.
- Vann, W.F., Daines, D.A., Murkin, A.S., Tanner, M.E., Chaffin, D.O., Rubens, C.E., Vionnet, J., and Silver, R.P. (2004). The NeuC protein of *Escherichia coli* K1 is a UDP *N*-acetylglucosamine 2-epimerase. *J Bacteriol* 186, 706–712.
- Varki, A. (1992). Diversity in the sialic acids. *Glycobiology* 2, 25–40.
- Varki, A. (2001). Loss of *N*-glycolylneuraminic acid in humans: Mechanisms, consequences, and implications for hominid evolution. *American Journal of Physical Anthropology Suppl* 33, 54–69.
- Varki, A. (2007). Glycan-based interactions involving vertebrate sialic-acid-recognizing proteins. *Nature* 446, 1023–1029.
- Varki, A. (2008). Sialic acids in human health and disease. *Trends Mol Med* 14, 351–360.
- Varki, A., and Schauer, R. (2009). Sialic acids. In essentials of glycobiology, A. Varki, R.D. Cummings, J.D. Esko, H.H. Freeze, P. Stanley, C.R. Bertozzi, G.W. Hart, and M.E. Etzler, eds. (Cold Spring Harbor (NY)),.
- Vickery, M., Nilsson, W., Strom, M., Nordstrom, J., and DePaola, A. (2007). A real-time PCR assay for the rapid determination of 16S rRNA genotype in *Vibrio vulnificus*. *J Microbiol Methods*. 68, 376–384.
- Vimr, E., and Lichtensteiger, C. (2002). To sialylate, or not to sialylate: that is the question. *Trends Microbiol* 10, 254–257.
- Vimr, E.R., and Troy, F.A. (1985). Identification of an inducible catabolic system for sialic acids (nan) in *Escherichia coli*. *J Bacteriol* 164, 845–853.
- Vimr, E.R., Kalivoda, K.A., Deszo, E.L., and Steenbergen, S.M. (2004). Diversity of microbial sialic acid metabolism. *Microbiol. Mol. Biol. Rev.* 68, 132–153.

- Vinogradov, E., Wilde, C., Anderson, E.M., Nakhamchik, A., Lam, J.S., and Rowe-Magnus, D.A. (2009). Structure of the lipopolysaccharide core of *Vibrio vulnificus* type strain 27562. *Carb Res* 344, 484–490.
- Vogel, U., Weinberger, A., Frank, R., Muller, A., Kohl, J., Atkinson, J.P., and Frosch, M. (1997). Complement factor C3 deposition and serum resistance in isogenic capsule and lipooligosaccharide sialic acid mutants of serogroup B *Neisseria meningitidis*. *Infect Immun* 65, 4022–4029.
- Wang, B. (2012). Molecular mechanism underlying sialic acid as an essential nutrient for brain development and cognition. *Advances in Nutrition* (Bethesda, Md.) 3, 465S–72S.
- Warner, E., and Oliver, J.D. (2008a). Population Structures of Two Genotypes of *Vibrio vulnificus* in Oysters (*Crassostrea virginica*) and Seawater. *Appl Environ Microbiol* 74, 80–85.
- Warner, E.B., and Oliver, J.D. (2008b). Multiplex PCR assay for detection and simultaneous differentiation of genotypes of *Vibrio vulnificus* biotype 1. *Foodborne Pathog Dis* 5, 691–693.
- Warner, J.M., and Oliver, J.D. (1999). Randomly amplified polymorphic DNA analysis of clinical and environmental isolates of *Vibrio vulnificus* and other *Vibrio* species. *Appl Environ Microbiol* 65, 1141–1144.
- Warren, L. (1959). The thiobarbituric acid assay of sialic acids. *J Biol Chem* 234, 1971–1975.
- Warren, L. (1963). The distribution of sialic acids in nature. *Comparative Biochemistry and Physiology* 10, 153–171.
- Wessels, M.R., Rubens, C.E., Benedi, V.J., and Kasper, D.L. (1989). Definition of a bacterial virulence factor: sialylation of the group B streptococcal capsule. *Proc Natl Acad Sci U S A* 86, 8983–8987.
- Wortman, A.T., Somerville, C.C., and Colwell, R.R. (1986). Chitinase determinants of *Vibrio vulnificus*: gene cloning and applications of a chitinase probe. *Appl Environ Microbiol* 52, 142–145.
- Wright, A.C., Simpson, L.M., Oliver, J.D., and Morris, J.G. (1990). Phenotypic evaluation of acapsular transposon mutants of *Vibrio vulnificus*. *Infect Immun* 58, 1769–1773.

- Wright, A.C., Hill, R.T., Johnson, J.A., Roghman, M.C., Colwell, R.R., and Morris, J.G., Jr. (1996). Distribution of *Vibrio vulnificus* in the Chesapeake Bay. *Appl Environ Microbiol* 62, 717–724.
- Wu, H., and Jerse, A.E. (2006). Alpha-2,3-sialyltransferase enhances *Neisseria gonorrhoeae* survival during experimental murine genital tract infection. *Infect Immun* 74, 4094–4103.
- Yildiz, F.H., and Visick, K.L. (2009). *Vibrio* biofilms: so much the same yet so different. *Trends in Microbiol* 17, 109–118.
- Zelmer, A., Bowen, M., Jokilampi, A., Finne, J., Luzio, J.P., and Taylor, P.W. (2008). Differential expression of the polysialyl capsule during blood-to-brain transit of neuropathogenic *Escherichia coli* K1. *Microbiology* 154, 2522–2532.

Appendix A

IACUC PROTOCOL APPROVAL



Animal Welfare Assurance # A-3381-01
August 30, 2013

To: Amanda Lewis, Ph.D. Campus Box 8230
From: Dana R. Abendschein, Ph.D., Chairman
Subject: Approval of Protocol for Experiments Utilizing Animals

Agency/Title: DEPARTMENT FUNDS
Startup #93191
Glycobiology of Host-Microbe Interactions During Colonization and
Infection

The Animal Studies Committee of Washington University has reviewed this protocol for the use of animals in conjunction with the research project named above. Federal laws and guidelines require that institutional animal care and use committees review ongoing projects annually. For the first two years after initial approval of this protocol, you will be asked to submit an annual progress report describing any changes in this protocol.

Approval Date: 07/29/2011 **Approval No. 20110149**
Expiration Date: 07/29/2014
Amendment (#1, Year 3) approved with addendum 08/30/2013
SPECIES:
Mouse

It is your responsibility to see that all persons who use animals under your direction understand and follow the approved protocol. Should it become necessary to make substantial changes in this protocol, you must submit a new protocol. **Failure to comply with these provisions can result in suspension of the research.**

Campus Box 8025, 660 South Euclid Avenue, St. Louis, Missouri 63110-1093,
(314)362-3229, Fax (314)454-6617, <http://asc.wustl.edu>

Appendix B

Strains and plasmids used in *V. vulnificus nab1* studies

| Strain or plasmid | Genotype or description | Reference or source |
|-----------------------------|--|---------------------|
| Vibrio vulnificus strains | | |
| CMCP6 | clinical isolate | |
| YJ016 | clinical isolate | (45) |
| CMCP6 $\Delta nab1$ | CMCP6 $\Delta nab1$ (VV1_0803) | This study |
| CMCP6 $\Delta nab1 + pnab1$ | CMCP6 $\Delta nab1$ +pBBR1MCSnab1 | This study |
| YJ016 $\Delta nab1$ | YJ016 $\Delta nab2$ (VV0316) | This study |
| YJ016 $\Delta nab1 + pnab1$ | YJ016 $\Delta nab1$ +pBBR1MCSnab1 | This study |
| Escherichia coli | | |
| DH5 α λ -pir | pir80dlacZ Δ M15 δ (lacZYA- argF)U169 recA1 hsdR17 deoR thi-1 supE44 gyrA96 relA1 Donor for bacterial conjugation; | |
| β 2155 DAP | thr1004 pro thi strA hsdS lacZ Δ M15 (F lacZ Δ M15 lacTRQJ36proAB) dapA Erm ^r pirRP4 (Km ^r from SM10) | |
| Plasmids | | |
| pJet1.2/blunt | High copy cloning vector | |
| pJet1.2-0803SOE | <i>V. vulnificus</i> VV1_0808 SOE product | This study |
| pJet1.2-0316SOE | <i>V. vulnificus</i> VV0316 SOE product | This study |
| pDS132 | Suicide plasmid; Cm ^r ; SacB | (42) |
| pDS0803 | <i>V. vulnificus</i> VV1_0808 SOE product | This study |
| pDS0316 | <i>V. vulnificus</i> VV0312 SOE product | This study |

Appendix B continued

| Strain or plasmid | Genotype or description | Reference or source |
|-------------------|-------------------------------------|---------------------|
| pBBR1MCS | Expression plasmid; Cm ^r | (46) |
| pBBR1MCS0803c | Expression plasmid (VV1_0803) | This study |
| pBBR1MCS03016c | Expression plasmid (VV0316) | |

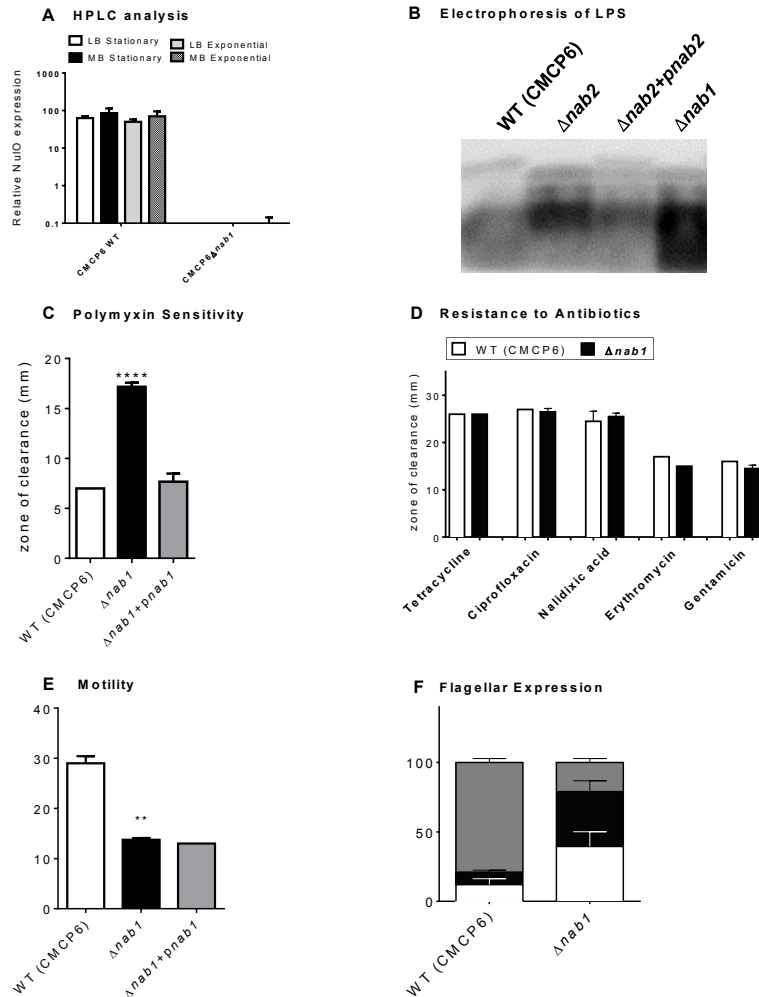
Appendix C

Primers used in *V. vulnificus nab1* studies

| Primer name | Sequence (5'–3') | T _m (°C) | Product size (bp) |
|--------------------|--|---------------------|-------------------|
| SOEVV1_0803A | TCTAGAAAGCGTGCACAAGTGGATATTCTCA | 60 | |
| SOEVV1_0803B | AACGGCACCTCTGCCCCCGCT | 60 | 241 |
| SOEVV1_0803C | AGCGGGGGCAGAGGTGCCGTTAAGCTCGGTTGATATTGACCA TGAG | 56 | |
| SOEVV1_0803D | GAGCTCGCCCCACTCCACTTGCTGA | 56 | 227 |
| SOEVV1_0803FL F | GATTACTTCGGTGGCGAAAG | | |
| SOEVV1_0803FL R | GAATCAGGTAACGTGGTGCT | 60 | 1,063 |
| SOEVV0316A | TCTAGAACGGCGCTTTCCAATCACATCGG | 60 | |
| SOEVV0316B | CACTATCGCGCCCGATGCAC | 60 | 251 |
| SOEVV0316C | GTGCATCGGGCGCGATAGTGCCAAAAGAGCGAGCGGTGGAT A | 58 | |
| SOEVV0316D | GAGCTCAGAAAGGCGTTCACGCATCGC | 58 | 224 |
| SOEVV0316FLF | GCCCAAATGGGATAAAAACC | 60 | |
| SOEVV0316LR | AGCTCGCAACAGCATAGCTT | 60 | 1068 |
| VV1_0807Fc | AAGCTTATAATGAAAATACTGGCGATTAC | 54 | |
| VV1_0807Rc | TCTAGACGCACCGATGATCAATAAC | 54 | 724 |
| VV0316Fc | AAGCTTAAGGTGAATAATCGAATGAAA | 51 | |
| VV0316Rc | TCTAGACGGCAACAAGAATAGTTTAA | 51 | 744 |

Appendix D

Functional analysis of CMCP6 $\Delta nab1$

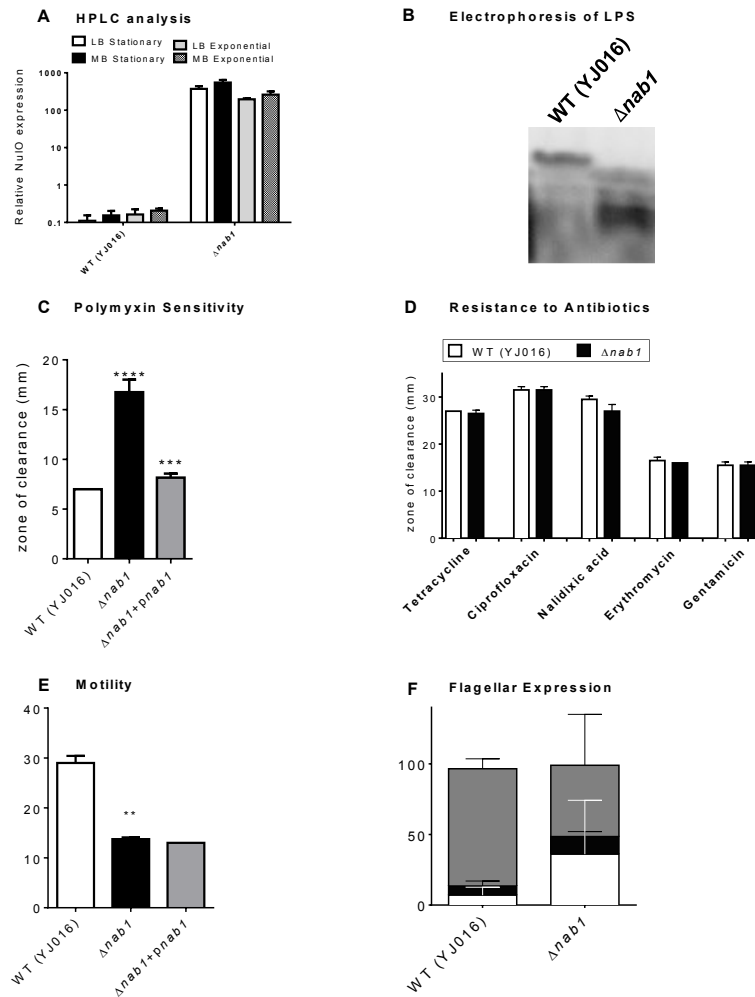


Mutation of *nab1* were found to yield identical phenotypes to $\Delta nab2$. Methods and statistically analysis performed identical to $\Delta nab2$ strain detailed in Chapter 4. (A) HPLC analysis confirms that *nab1* is essential to regulation the *V. vulnificus* NulO synthase *nab2*, no accumulation is seen when CMP-synthase mutated. (B) CMCP6 $\Delta nab1$ LPS exhibits identical molecular weight shift seen in $\Delta nab2$ strain and (C) CMCP6 $\Delta nab1$ is significantly more sensitive to the LPS-binding antibiotic

polymyxin B (100 μ g) than WT. (D) Antibiotic sensitivity is specific to polymyxin-B. (E) 16 h swim assay on MB 0.3% agarose to determined motility in CMCP6 $\Delta nab1$ significantly decreased with increased proportions of the population exhibiting shortened or missing flagella in CMCP6 $\Delta nab1$ (F). $N \geq 2$. **** = $p < 0.0001$, *** = $p < 0.001$ ** = $p < 0.01$, * = $p < 0.05$

Appendix E

Functional analysis of YJ016 $\Delta nab1$

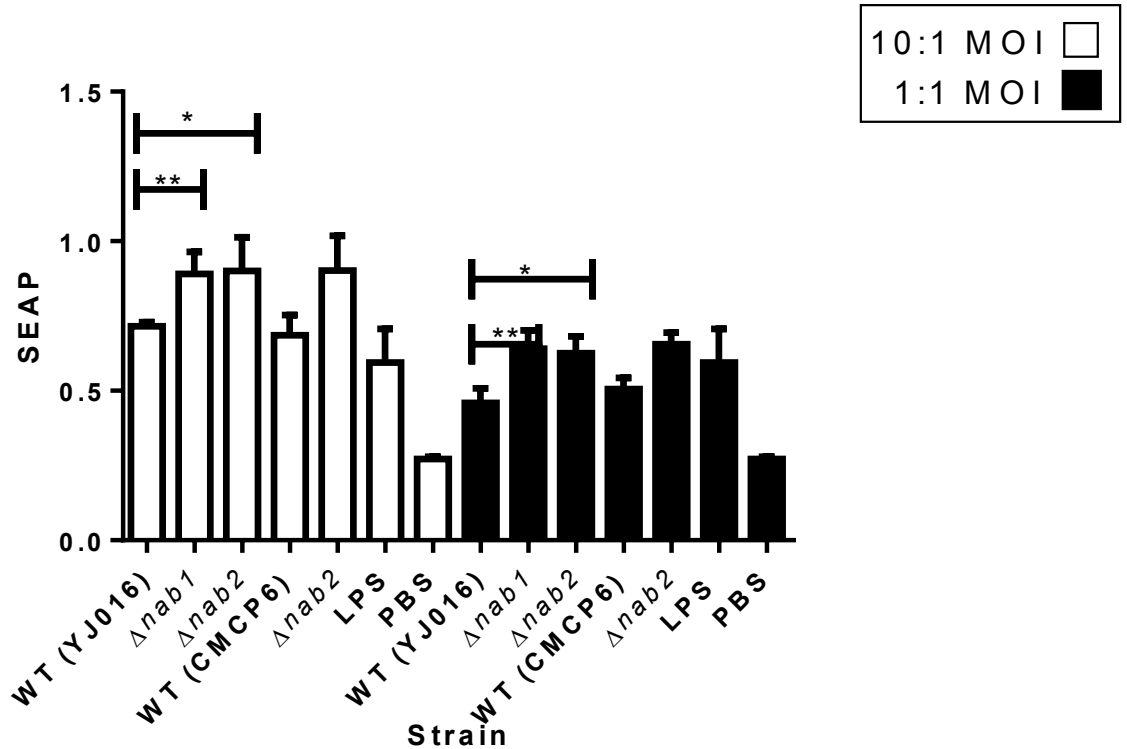


Mutation of *nab1* was found to yield similar phenotypes to $\Delta nab2$. Notable exception would be the dramatic increase in sialic acid production found in YJ06 $\Delta nab1$, compared to wild-type parent (A). Methods and statistically analysis performed identical to $\Delta nab2$ strain detailed in Chapter 4. . (A) HPLC analysis confirms that *nab1* is essential to regulation the YJ016 NulO synthase *nab2*, higher than WT levels of NulO accumulation is seen when CMP-synthase mutated. (B) YJ016 $\Delta nab1$ LPS

exhibits identical molecular weight shift seen in $\Delta nab2$ strain and (C) YJ016 $\Delta nab1$ is significantly more sensitive to the LPS-binding antibiotic polymyxin B (100 μ g) than WT. (D) Antibiotic sensitivity is specific to polymyxin-B. (E) 16 h swim assay on MB 0.3% agarose to determined motility in YJ016 $\Delta nab1$ significantly decreased with increased proportions of the population exhibiting shortened or missing flagella in YJ016 $\Delta nab1$ (F). $N \geq 2$. **** = $p < 0.0001$, *** = $p < 0.001$ ** = $p < 0.01$, * = $p < 0.05$

Appendix F

Macrophage activation assay of *V. vulnificus nab* mutants



Representative data of *V. vulnificus* macrophage activation. Studies indicate *V. vulnificus* activate macrophages through TLR 4 upon infection. This leads to the production of the pro-inflammatory cytokines, IL-6, IL-8, and TNF- α , through the NF- κ B pathway. *Vibrio vulnificus* has also been shown to have cytotoxic effects on macrophages (reviewed in Jones and Oliver, 2009). To investigate whether the sialylation of the LPS of *V. vulnificus* affects activation of the NF- κ B pathway, RAW-Blue cells (murine RAW 264.7 macrophages with an incorporated secreted embryonic alkaline phosphatase [SEAP] reporter construct inducible by NF- κ B) (Invitrogen) were used. Multiplicities of infection (MOI) of 10:1 and 1:1 heat-killed *V. vulnificus* were incubated with the macrophages at 37°C for 6 h and SEAP levels were determined by spectroscopy at 640 nm. N=3, ** = p < 0.01, * = p < 0.05

Appendix G

Acknowledgement of previously published chapters

Results and text in Chapter 2 previously published by American Society of Microbiology as Sialic acid catabolism and transport gene clusters are lineage specific in *Vibrio vulnificus*. Copyright © American Society for Microbiology, Applied and Environmental Microbiology, 78(9), 2012, 3407-3415, DOI: 10.1128/AEM.07395-11

Results and text in Chapter 3 previously published by American Society of Microbiology as Genomic and metabolic profiling of nonulosonic acids in Vibrionaceae reveal biochemical phenotypes of allelic divergence in *Vibrio vulnificus*. Copyright © American Society for Microbiology, Applied and Environmental Microbiology, 77(16), 2011, 5782-5793, DOI: 10.1128/AEM.00712-11